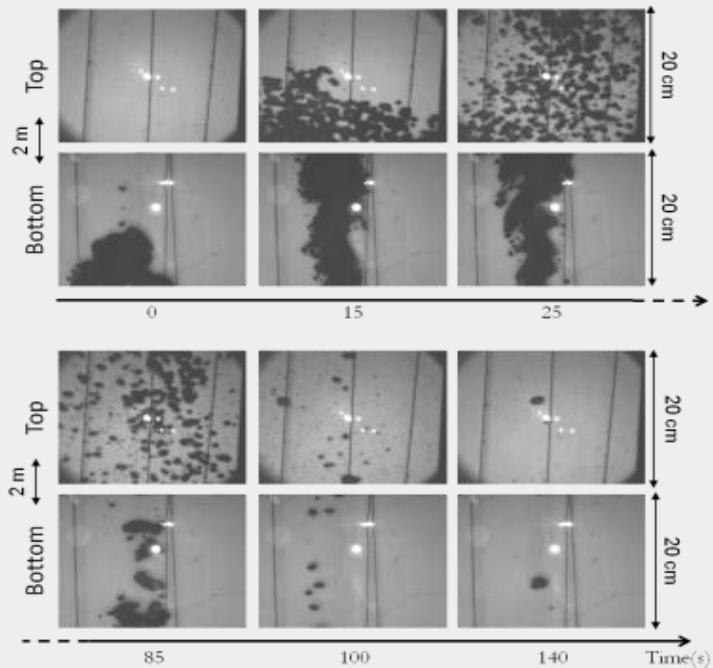




Improving Member States preparedness to face an HNS pollution of the Marine System

Understanding HNS behaviour in the marine environment

HNS-MS final report, part I



HNS-MS is a project co-funded by DG-ECHO under agreement ECHO/SUB/2014/693705. It runs from 1 January 2015 to 31 March 2017.

HNS-MS contributors

Sébastien Legrand¹, Florence Poncet², Laurent Aprin³, Valérie Parthenay⁴, Eric Donnay⁵, Gabriel Carvalho², Sophie Chataing-Pariaud², Gilles Dusserre³, Vincent Gouriou², Stéphane Le Floch², Pascale Le Guerroue², Yann-Hervé Hellouvry⁴, Frédéric Heymes³, Fabrice Ovidio¹, Samuel Orsi¹, José Ozer¹, Koen Parmentier¹, Rémi Poisvert⁴, Emmanuelle Poupon², Romain Ramel⁴, Ronny Schallier¹, Pierre Slangen³, Amélie Thomas², Vassilis Tsigourakos², Maarten Van Cappellen¹, Nabil Youdjou¹.

- (1) Royal Belgian Institute of Natural Sciences
- (2) CEDRE
- (3) ARMINES, Ecole des Mines d'Alès
- (4) Alyotech France
- (5) Belgian FPS Health, food chain safety and environment

Citation

Legrand S., F. Poncet, L. Aprin, V. Parthenay, E. Donnay, G. Carvalho, S. Chataing-Pariaud, G. Dusserre, V. Gouriou, S. Le Floch, P. Le Guerroue, Y.-H. Hellouvry, F. Heymes, F. Ovidio, S. Orsi, J.Ozer, K. Parmentier, R. Poisvert, E. Poupon, R. Ramel, R. Schallier, P. Slangen, A. Thomas, V. Tsigourakos, M. Van Cappellen and N. Youdjou (2017) "Understanding HNS behaviour in the marine environment", HNS-MS final report, part, 152 pp.

About HNS-MS

The European project HNS-MS aimed at developing a decision-support system that national maritime authorities and coastguard stations can activate to forecast the drift, fate and behaviour of acute marine pollution by Harmful Noxious Substances (HNS) accidentally or deliberately released in the marine environment. Focussing on the Greater North Sea and Bay of Biscay, this 27 months project (01/01/2015-31/03/2017) had four specific objectives:

- i. To develop a freely accessible data base documenting the most important HNS transported from or to the ports of Antwerp, Rotterdam, Hamburg, Nantes and Bordeaux;
- ii. To conduct lab experiments in order to improve the understanding of the physico-chemical behaviour of HNS spilt at sea;
- iii. To develop a 3D mathematical modelling system that can forecast the drift, fate and (SEBC) behaviours of HNS spilt at sea. Advanced processes such as chemical reactivity, explosions, fire or interaction with sediment were not considered in this first project;
- iv. To produce environmental and socioeconomic vulnerability maps dedicated to HNS that will help end-users assessing the likely impacts of HNS pollution on the marine environment, human health, marine life, coastal or offshore amenities and other legitimate uses of the sea.

All these contributions have been integrated into a web application that will help coastguard stations to evaluate the risks for maritime safety, civil protection and marine environment in case of an acute pollution at sea. HNS-MS has been co-funded by the Directorate-General of European Commission for European Civil Protection and Humanitarian Aid Operations (ECHO).

About this report

This report presents the achievements of the lab experiments carried out in the framework of tasks C and D of the project “HNS-MS – Improving Member States preparedness to face an HNS pollution of the Marine System”.

This report is part of a series of 5 technical sub-reports presenting in detail the outcome achieved by the HNS-MS consortium in the framework of this project:

- HNS-MS Layman’s report
- Sub-report I : Understanding HNS behaviour in the marine environment
- Sub-report II : Modelling drift, behaviour and fate of HNS maritime pollution
- Sub-report III : Mapping HNS environmental and socioeconomic vulnerability to HNS maritime pollution
- Sub-report IV : HNS-MS Decision-Support System User’s Guide

A copy of these reports can be obtained by downloading from the HNS-MS website <https://www.hns-ms.eu/publications/>.

Contents

1	Introduction.....	10
1.1	General context.....	11
1.2	What are HNS precisely?.....	12
1.3	How does HNS behave when spilt in the marine environment?	12
1.4	HNS-MS objectives.....	13
1.5	HNS-MS workflow.....	14
1.6	Objectives of the Lab experiments.....	16
2	The HNS-MS data base, a freely accessible HNS database.....	19
2.1	The HNS selection.....	19
2.2	The HNS-MS database.....	24
2.2.1	Design and structure.....	24
2.2.2	Access.....	26
2.2.3	Detailed information page.....	36
3	HNS laboratory characterization for non-standard conditions.....	43
3.1	Introduction.....	43
3.2	Physical properties.....	44
3.3	Evaporation kinetics.....	46
3.3.1	Evaporation of the HNS.....	46
3.3.2	Evaporation of the HNS at sea surface.....	50
3.4	Dissolution kinetics.....	54
3.4.1	Protocol.....	54
3.4.2	Results.....	56
4	Competition between evaporation and dissolution kinetics.....	65
4.1	Experimental tool.....	65
4.2	Experimental protocol.....	66
4.3	Results.....	67
4.3.1	Evaporation process.....	67

4.3.2	Dissolution process.....	69
4.3.3	Overall fate	71
5	HNS behaviour in the water column.....	85
5.1	Introduction	85
5.1.1	Behaviour of chemicals in water	85
5.1.2	Droplet size distribution at breach level.....	86
5.1.3	Dripping mode.....	88
5.1.4	Jetting mode.....	88
5.1.5	Rising velocity of chemical droplet in seawater	88
5.1.6	Spherical shape.....	89
5.1.7	Ellipsoid shape.....	89
5.1.8	Spherical cap.....	90
5.1.9	Solubilisation of chemicals droplets rising in seawater	91
5.2	Materials and methods	93
5.2.1	Droplet distribution measurements.....	94
5.2.2	Droplets velocity and solubilization measurements	97
5.3	Results.....	101
5.3.1	Release flow rate.....	101
5.3.2	Dispersion in the water column	103
5.3.3	Droplet solubilisation	107
5.4	Conclusion.....	119
6	Strength and weakness of the SEBC classification	123
7	Conclusion.....	127
	References	131
	Annex 1: Experimental data for 2-ethylhexanoic acid.....	134
	Annex 2: Experimental data for n-butyl acetate.....	137
	Annex 3: Experimental data for Butyl acrylate	139
	Annex 4: Experimental data for 2-ethylhexyl acrylate	141
	Annex 5: Experimental data for Heptane	143

Annex 6: Experimental data for n-nonanol.....	144
Annex 7: Experimental data for Pentane.....	145
Annex 8: Experimental data for Texanol®	146
Annex 9: Experimental data for Toluene.....	148
Annex 10: Experimental data for Xylenes	149

PAGE INTENTIONALLY LEFT BLANK

Introduction

PAGE INTENTIONALLY LEFT BLANK

1 Introduction

1.1 General context

“Maritime services have benefited in recent years by considerable expansion fostered by globalization.”¹ “Around 90% of world trade is carried by the international shipping industry. Without shipping the import and export of goods on the scale necessary for the modern world would not be possible. Seaborne trade continues to expand, bringing benefits for consumers across the world through competitive freight costs. Thanks to the growing efficiency of shipping as a mode of transport and increased economic liberalisation, the prospects for the industry’s further growth continue to be strong.”²

If maritime shipping is undoubtedly a key factor of the worldwide economic growth, the constantly growing fleet of tankers, bulk carriers and ever-increasing size container ships exacerbates the risk of maritime accidents, loss of cargoes and acute maritime pollution. In particular, more than 2,000 **harmful or noxious chemical substances (HNS)** are regularly shipped in bulk or package forms and can potentially give rise to significant environmental and/or public health impacts in case of spillage in the marine environment.

In recent years, huge efforts have been made by IMO, EMSA as well as other maritime authorities towards greater consideration of these risks. For instance, given the importance and complexity of the matter, the Bonn Agreement, HELCOM, Lisbon Convention, Barcelona Convention/REMPEC, Copenhagen Convention, DG ECHO and EMSA have jointly identified the urgent need of improving preparedness and response to HNS spills (10th Inter-Secretariat Meeting, Helsinki, 27.02.2014).

Until now, preparedness actions at various levels have primarily aimed at classifying the general environmental or public health hazard of an HNS (e.g. development of IBC and IMDG codes; GESAMP profiles), at developing operational datasheets collating detailed, substance-specific information for responders and covering information needs at the first stage of an incident. (MAR-CIS; MIDSIS-TROCS; CAMEO) or at performing a risk analysis of HNS transported in European marine regions (e.g. EU projects HASREP and BE-AWARE). However, contrary to oil pollution preparedness and response tools, only few decision-support systems currently used by Member States authorities (Coastguard agencies or other) integrate 3D models that are able to simulate the drift, fate and behaviour of HNS spills in the marine environment. When they do, they usually rely on black box commercial software or consider simplified or steady-state environmental conditions.

¹ World Trade Organization - https://www.wto.org/english/tratop_e/transport_e/transport_maritime_e.htm

² International Chamber of Shipping - <http://www.ics-shipping.org/shipping-facts/shipping-and-world-trade>

HNS-MS aims at developing a 'one-stop shop' integrated decision-support system that is able to predict the drift, fate and behaviour of HNS spills under realistic environmental conditions and at providing key product information - drawing upon and in complement to existing studies and databases - to improve the understanding and evaluation of a HNS spill situation in the field and the environmental and safety-related issues at stake.

The key challenge in this project is to understand the physico-chemical processes that drive the numerous behaviours and fate of HNS spilt in the marine environment.

1.2 What are HNS precisely?

HNS-MS defines **hazardous and noxious substances** or **HNS** following the OPRC-HNS Protocol 2000:

"HNS are any substances other than oil which, if introduced into the marine environment, are likely to create hazards to human health, to harm living resources and marine life, to damage amenities or to interfere with other legitimate uses of the sea".

This generic definition covers a wide range of chemicals with diverse intrinsic qualities (such as toxicity, flammability, corrosiveness, and reactivity with other substances or auto-reactivity). It includes:

- oil derivatives;
- liquid substances which are noxious or dangerous;
- liquefied gases;
- liquids with flashpoints not exceeding 60°C;
- packaged dangerous, harmful and hazardous materials; and
- solid bulk material with associated chemical hazards.

In the framework of HNS-MS, vegetal oils are also considered as HNS.

1.3 How does HNS behave when spilt in the marine environment?

The behaviour of a substance spilt at sea is the way in which it is altered during the first few hours after coming into contact with water. Predicting this behaviour is one of the most important stages in the development of a response strategy.

Since the early 1990's, the best HNS behaviours predictions were given by the Standard European Behaviour Classification (SEBC) [Bonn Agreement, 1991]. This classification determines the theoretical behaviour of a substance according to its density, vapour pressure and solubility. Five main behaviour classes are considered: **gas**, **evaporator**, **floaters**, **dissolver** and

sinker. However, most of the time, a substance does not have one single behaviour but rather several behaviours due to its nature and the environmental conditions (wind, waves, current). This is the reason why the SEBC considers a total of 12 mixed behaviours classes (Figure 1). For example, ethyl acrylate is classified as FED as it floats, evaporates and dissolves.

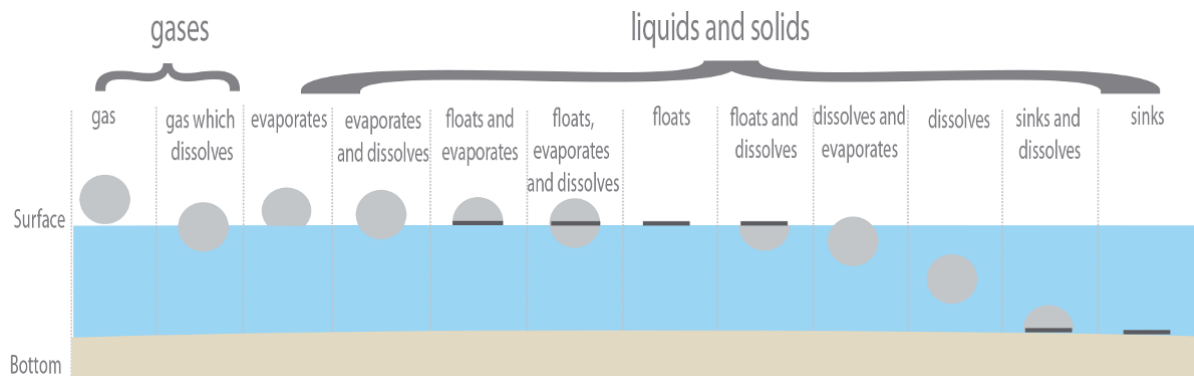


Figure 1: According the Standard European Behaviour Classification (SEBC), a substance spilt at sea will behave following one of these 12 theoretical behaviour classes.

The SEBC code has its limits. It is based on experiments conducted in the laboratory on pure products at a temperature of 20°C in fresh water. These controlled conditions are quite different from those encountered in case of a real incident at sea. In addition, the SEBC also fails to provide any information on the physico-chemical processes explaining the observed mixed behaviour, their kinetics and their eventual competitions. As a consequence, further experimental characterization of chemicals behaviour at different scales (ranging from laboratory to the field) is needed in order to gain a better understanding of the physico-chemical processes at stake, to develop more reliable mathematical models of these processes (taking into account the actual environmental conditions) and eventually to provide more accurate answers to decision makers when they plan response efforts and pollution control.

1.4 HNS-MS objectives

The project HNS-MS aimed at developing a decision-support system that national maritime authorities and coastguard stations can activate to forecast the drift, fate and behaviour of acute marine pollution by Harmful Noxious Substances (HNS) accidentally released in the marine environment.

Focussing on the Greater North Sea and Bay of Biscay, this 2 year project (01/01/2015-31/03/2016) had four specific objectives:

- i. To develop a freely accessible data base documenting the most important HNS transported from or to the ports of Antwerp, Rotterdam, Hamburg, Nantes and Bordeaux;
- ii. To conduct lab experiments in order to improve the understanding of the physico-chemical behaviour of HNS spilt at sea;
- iii. To develop a 3D mathematical modelling system that can forecast the drift, fate and (SEBC) behaviours of HNS spilt at sea. Advanced processes such chemical reactivity, explosions, fire or interaction with sediment were not considered in this first project;
- iv. To produce environmental and socioeconomic vulnerability maps dedicated to HNS that will help end-users assessing the likely impacts of HNS pollution on the marine environment, human health, marine life, coastal or offshore amenities and other legitimate uses of the sea.

All these contributions have been integrated into a web application that will help coastguard stations to evaluate the risks for maritime safety, civil protection and marine environment in case of acute pollution at sea.

1.5 HNS-MS workflow

To meet HNS-Ms objectives, the workflow has been subdivided into 10 tasks articulated around 4 main axes (Figure 2):

1. **Lab experiments:** The first axis aims at collating or producing data and information to support the development of the HNS drift and fate model. First a selection of 100+ important HNS transported in the Bonn Agreement area has been performed from a literature and database review. Then, keeping in mind that only processes fully understood can accurately be simulated; several laboratory experiments have been carried out in order to improve our understanding of HNS behaviour both in the water column and at the sea surface. For instance, for the first time, a Lab experiment has been conducted in order to quantify the competition between the evaporation and dissolution kinetics of chemical floating at the sea surface. Finally, two field campaigns have been organised.

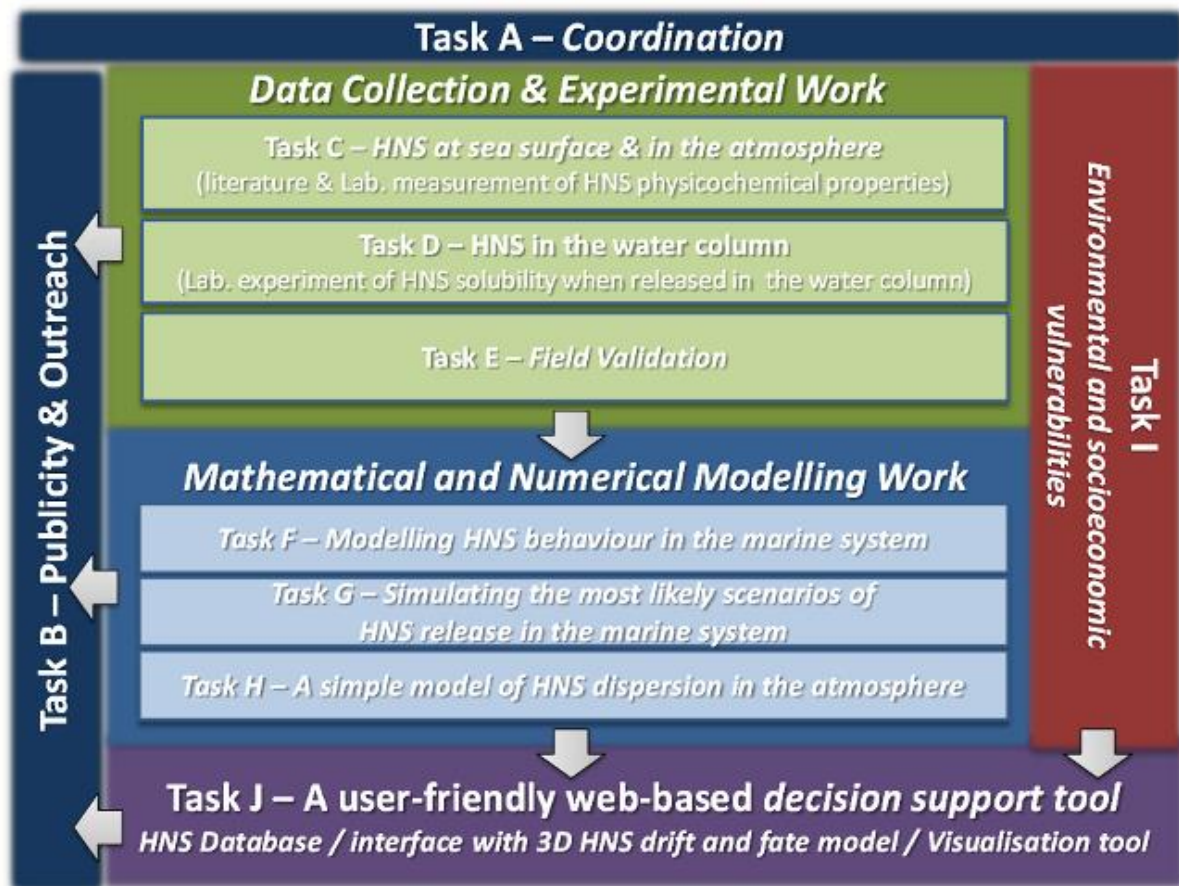


Figure 2: HNS-MS workflow is articulated around 4 main axes: Lab experiments, model development, environmental and socio-economic vulnerabilities mapping and development of a Decision Support System. (Figure from the project proposal submitted to DG-ECHO call to projects 2014)

- Mathematical modelling:** The second axis aims at developing a 3D HNS drift and fate modelling software. In order to handle (i) the large variety of HNS physico-chemical properties, (ii) the large variety of possible spillage scenarios and (iii) the large variety of the involved time and space scales, three different models have been developed, namely
 - ChemSPELL, HNS-MS near-field model
 - ChemDRIFT, HNS-MS far-field model
 - ChemADEL, HNS-MS atmospheric dispersion model
- Environmental and socio-economic vulnerabilities:** The third axis aims at developing a series of regional and local vulnerability for HNS-sensitive environmental and socioeconomic features. The HNS-MS vulnerability ranking methodology is mainly an extension of methodology developed in the framework of the BE-AWARE projects, also funded by DG-ECHO.

4. **Decision support System:** Finally, the fourth axis aims at integrating all the previously obtained results in an intuitive, easy-to-use operational web-based HNS decision-support system for the Bonn Agreement area and the Bay of Biscay.

1.6 Objectives of the Lab experiments

The objectives of the lab experiments are manifolds.

The first objective is to identify 100+ important HNS transported in the Bonn Agreement area. For each of the selected HNS, a review of the available literature and databases has to be performed in order to (i) collate the physico-chemical properties needed to execute model simulations of the drift, behaviour and fate of HNS spills but also (ii) to collate other elements of information that can help the HNS-MS end-users correctly interpreting the model simulation results.

Most of the physico-chemical properties available in the literature have been measured for standard conditions (20°C and in fresh water), that are different from the field conditions. The second objective of the lab experiments was therefore to assess the reliability of the available data by measuring the physico-chemical properties of 19 HNS for non-standard conditions, typical of the open-sea and of the estuaries in the Bonn Agreement area for summer and winter.

Very few experiments that simultaneously observe and quantify the kinetics of the SEBC behaviours are reported in the literature. However, these observations are of the upper most importance to better understand the physico-chemical processes involved, to develop better parametrisations of these processes (i.e. a mathematical representation of the process that can be implemented in a model) and finally to assess the model quality to simulate all the processes together. The third and fourth objectives of the lab experiments were therefore to develop experimental set-ups to measure the kinetics involved in the competition between the HNS slick evaporation and dissolution at the sea surface and the kinetics between HNS droplets dissolution and resurfacing in the water column, respectively. Of course, in the latter case, HNS jet characteristics and droplet distributions at the HNS tank breach must be fully understood.

A freely accessible HNS-MS database

PAGE INTENTIONALLY LEFT BLANK

2 The HNS-MS data base, a freely accessible HNS database

This action aimed to identify 100+ relevant HNS based on various criteria in order to establish a database containing physico-chemical properties needed for modelling purpose. Because several stakeholders reported us their difficulties to access to trustful HNS information, the database was quickly re-designed and extended in order to include 90+ elements of information spanning the following 6 themes: names and regulation, physical and chemical properties, behaviour, eco-toxicity and hazards.

2.1 The HNS selection

A total of **123 relevant HNS** -760 HNS with all synonyms- have been selected taken into account criteria such as

- Frequency of appearance in existing HNS lists/databases³,
- transported volumes from and to the Bonn Agreement area,
- potential toxicity for the marine environment,
- risk (threat for human lives),
- representation of different SEBC behaviour classes,
- product data availability and reliability.

This list of the selected HNS is given in **Table 1**. The list mainly includes pure chemical substances but also some blended substances and covers about 90% of the HNS volume shipped in the Bonn Agreement area. This selection is rather balanced in terms of SEBC. It includes 40 dissolvers, 18 floaters and persistent floaters, 11 evaporators, 11 sinkers, 11 dissolver-evaporators, 9 floater-evaporators, 9 sinker-dissolvers, 4 floater-dissolvers, 4 evaporator-dissolvers, 3 gases and 3 floater-evaporator-dissolvers.

Depending on the availability and reliability of information found in the literature, in existing datasets or measured in the framework of the HNS-MS project (cf. chapter 3), each selected HNS has been described by 90+ elements of information spanning the following 6 themes: names and regulation, physical and chemical properties, behaviour, eco-toxicity and hazards. The exact list of documented properties is given in **Table 2: Structure of the database developed in HNS-MS project**; some properties being described by more than one element of information. Altogether, the collated dataset forms the core of the HNS-MS database.

³ Namely the BE-AWARE Top-100 products list, the ARCOPOL top-20, the HASREP top-100, the GESAMP top-100 lists; the MARCIS +200, CLARA's MAIA 70 products and Finland HNS list.

Table 1: List of 123 HNS selected for the HNS-MS project

Substance name	CAS Number	SEBC
1,2,3-Trichlorobenzene (molten)	87-61-6	S
1,2,4-Trimethylbenzene	95-63-6	ED
1,2-Dichloroethane	107-06-2	SD
1,2-Dichloropropane	78-87-5	SD
1,3-Cyclopentadiene dimer (molten)	77-73-6	Fp
1,5,9-cyclododecatriene	4904-61-4	F
1-Hexene	592-41-6	E
2,2,4-Trimethyl-1,3-Pentanediol-1-Isobutyrate	25265-77-4	F
2-Ethylhexanoic acid	149-57-5	FD
2-Ethylhexyl acrylate	103-11-7	F
Acetic acid	64-19-7	D
Acetic anhydride	108-24-7	D
Acetone	67-64-1	DE
Acetone cyanohydrin	75-86-5	D
Acrylic acid	79-10-7	D
Acrylonitrile	107-13-1	DE
Adiponitrile	111-69-3	FD
Ammonia anhydrous	7664-41-7	DE
Ammonia aqueous (28% or less)	1336-21-6	D
Ammonium nitrate solution (93% or less)	6484-52-2	D
Aniline	62-53-3	FD
Benzene and mixtures >10% benzene	71-43-2	E
Benzene, C10-C13 Alkyl derivs	67774-74-7	E
Benzyl chloride	100-44-7	S
Bis(2-ethylhexyl) phthalate DEHP	117-81-7	F
Butane	106-97-8	G
Butyl acrylate	141-32-2	FED
Butylene glycol	110-63-4	D
Calcium lignosulphonate solutions	8061-52-7	D
Calcium nitrate solutions (50% or less)	10124-37-5	D
Carbon disulphide	75-15-0	SD
Chloroacetic acid	79-11-8	SD
Chloroform	67-66-3	SD
Cyclohexane	110-82-7	E
Cyclohexanone	108-94-1	D
Decene	872-05-9	F
Di-(2-ethylhexyl) adipate DEHA	103-23-1	F
Dichloromethane	75-09-2	SD
Diethylene glycol	111-46-6	D
Diisononyl phthalate	28553-12-0	F
Dimethylamine solution	124-40-3	DE

Dimethylformamide	68-12-2	D
Diphenylmethane diisocyanate	101-68-8	S
Dodecene (all isomers)	6842-15-5	F
Dodecyl alcohol	112-53-8	F
Dodecylbenzene	123-01-3	F
Epichlorohydrin	106-89-8	D
Ethanolamine	141-43-5	D
Ethyl acetate	141-78-6	DE
Ethyl acrylate	140-88-5	ED
Ethyl alcohol	64-17-5	D
Ethyl tert-butyl ether	637-92-3	E
Ethylbenzene	100-41-4	FED
Ethylene glycol	107-21-1	D
Ethylene glycol butyl ether	111-76-2	D
Ethylene glycol methyl butyl ether	13343-98-1	D
Ethylene glycol monomethyl ether	109-86-4	D
Ethylenediamine	107-15-3	D
FAME (Fatty Acid Metyl Ester)		Fp
Formaldehyde solutions (45% or less)	50-00-0	D
Formic acid	64-18-6	D
Heptane (all isomers)	142-82-5	E
Hexamethylenediamine	124-09-4	D
Hexamethylenetetramine solutions	100-97-0	D
Hydrochloric acid	7647-01-0	DE
Hydrogen peroxide	7722-84-1	D
Isobutyl alcohol	78-83-1	D
Isopropyl alcohol	67-63-0	DE
Isopropylbenzene	98-82-8	E
Lauric acid	143-07-7	Fp
Maleic anhydride	108-31-6	SD
Marine Diesel Oil MDO		
Methane	72-82-8	G
Methacrylic acid	79-41-4	D
Methanol (Methyl alcohol)	67-56-1	DE
Methyl acrylate	96-33-3	D
Methyl ethyl ketone	78-93-3	D
Methyl isobutyl ketone	108-10-1	FED
Methyl methacrylate	80-62-6	FED
Methyl tert-butyl ether	1634-04-4	DE
Naphtha (petroleum), hydrodesulfurized heavy	64742-82-1	FE
Naphthalene	91-20-3	S
n-Butyl acetate	123-86-4	FED
n-Butyl alcohol	71-36-3	FED
n-Hexane	110-54-3	E
Nitric acid	7697-37-2	D
Nitrobenzene	98-95-3	SD

Nonene	27215-95-8	FE
Nonyl alcohol (all isomers)	2430-22-0	F
Nonylphenol	25154-52-3	FD
Nonylphenol poly (4+)ethoxylate	9016-45-9	D
Octane (all isomers)	111-65-9	FE
Palm Oil	8002-75-3	Fp
Pentane (all isomers)	109-66-0	E
Perchloroethylene	127-18-4	S
Phenol	108-95-2	SD
Phosphoric acid	7664-38-2	D
Polymethylene polyphenyl isocyanate	9016-87-9	S
Potassium hydroxide	1310-58-3	D
Propane	74-98-6	G
Propionic acid	79-09-4	D
Propylbenzene	103-65-1	FE
Propylene glycol	57-55-6	D
Propylene glycol methyl ether	107-98-2	D
Propylene glycol methyl ether acetate	108-65-6	D
Propylene oxide	75-56-9	DE
Sodium hydroxide solution	1310-73-2	D
Styrene monomer	100-42-5	FE
Sulphur (commercially formed, solid)	7704-34-9	S
Sulphur (molten)	7704-34-9	S
Sulphuric acid	7664-93-9	D
Tall Oil (crude)	8002-26-4	
Tallow	61789-97-7	F
tert-Amyl methyl ether	994-05-8	SD
tert-Butyl alcohol	75-65-0	D
Tetrahydrofuran	109-99-9	DE
Toluene	108-88-3	E
Toluene diisocyanate	584-84-9	S
Trichloroethylene	79-01-6	S
Urea solution	57-13-6	D
Vinyl acetate	108-05-4	ED
Vinyl ethyl ether	109-92-2	E
Xylenes	1330-20-7	FE

Table 2: Structure of the database developed in HNS-MS project

Theme	Properties
Names and Regulation	English name, French name, synonyms
	CAS and UN numbers
	MARPOL classification
	Accidentology
Physical and chemical properties	Formula, Molar mass, Abilities
	State at 25°C, Melting point, Boiling Point
	Critical molar volume, temperature and pressure
	Liquid density, Surface tension, Interfacial tension, Viscosity, Hydrosolubility
	Vapour pressure, Vapour density
	Flash point, Explosion limits
	Heat of vaporization, Heat of combustion, Specific heat
	Combustion characteristics
Behaviour	Henry's law constant
	Log Kow, Log Koc
	Hydrolysis, photolysis
	Biodegradation
	SEBC classification
Ecotoxicity data	Bio concentration factor
	CL50, NOEC, PNEC
Hazard	Assessment factor
	IDLH
	GESAMP profile
	CLP pictograms
	Hazard statements, precautionary statements

2.2 The HNS-MS database

The purpose of the HNS-MS database is to give users one central point of access to all necessary HNS parameters and eventually use them in a simulation without having to compare multiple sources.

2.2.1 Design and structure

The database design is based on simple principles:

- Minimize redundancy
 - o Nothing is stored twice in the database.
 - o This allows perfect accuracy and consistency without risk of incoherence in the information targeted.
- Facilitate maintenance
 - o Backups, restorations, editions and any other operations are done with well-documented and reliable tools. (SQL)
- Standardized response
 - o The response is easily interpretable without risk of misunderstanding.
 - o No need of external tools to interpret data.
- Easily accessible
 - o User friendly search tool.
 - o Only a modern web browser supporting HTML5 and CSS3 is required to view the summary.
 - o Only an internet connection is required to use the HNS MS data directly on a remote system (simulation system, ...)

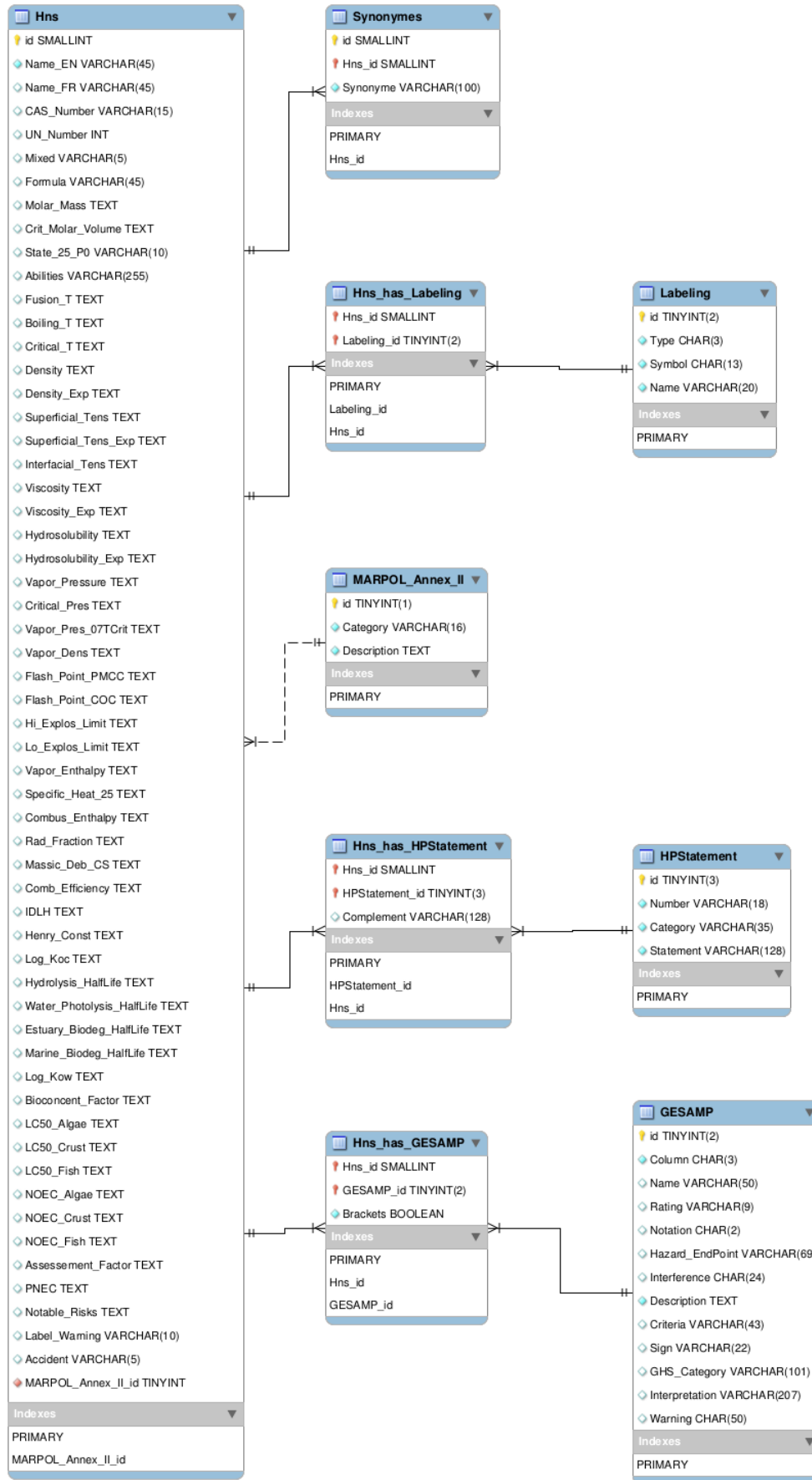


Figure 3 The HNS-MS Database structure

2.2.2 Access

The content of the database could be obtained in different ways:

- via web-site (by all visitors)
- via web-app (by registered users)
- via JSON REST API (machine to machine)

To facilitate access to normal users, scientists or not, an easy to use search tool is provided on the web site and web app.

This tool allow research by 4 parameters:

- Name
- SEBC Behaviour (floater, dissolver, ...)
- CAS Number
- UN Number

Assuming some chemicals could have complex names; the search tool is able to work with a part of it and guide the users to the right substance.

In case of unsuccessful search, the tool invites the users to go to other websites.

· SEARCH HNS ·

How to use

You can search by :

- Name
- SEBC Behaviour
- CAS Number
- UN Number

No result found.

You can found other chemical's data on the following websites :

- [CAMEO](#)
- [European Chemical Agency](#)
- [NIST's webbook of chemistry](#)
- [MIDSIS - TROCS](#)

Access by web site

Targeted audience	Everyone
Requirement	Internet connection Modern web-browser
Search tool URL	https://www.hns-ms.eu/hnsdb/

The HNS database is accessible through the search tool.

The screenshot shows the HNS-MS website in a browser. The URL bar shows 'https://www.hns-ms.eu/'. The page title is 'Improving Member States preparedness to face an HNS pollution of the Marine System (HNS-MS)'. The navigation menu includes 'Home', 'What are HNS?', 'Background and objectives', 'Actors and beneficiaries', 'Tasks and methods', 'Publications', 'Tools', 'Meeting', and 'Contact us'. The 'Tools' menu is expanded, showing 'HNS Database' and 'Sensitivity maps'. The 'HNS Database' link is highlighted with a red circle and the number '3'. The 'Background and objectives' link is highlighted with a red circle and the number '1'. The 'Final stakeholder meeting' section is also visible.

Figure 4 Where to find the search tool ?

Example of typical usage:

Let us search information about the chemical called “2-Hydroxy-2-Methylpropanenitrile” also called “Acetone Cyanohydrin”.

1. Go to the search tool

- a. By direct URL : <https://www.hns-ms.eu/hnsdb/>
- b. Or via the menu bar (see Figure 4)

HNS-MS is funded by DG-ECHO under agreement ECHO/SUB/2014/693705
 hns-ms@naturalsciences.be

Improving Member States preparedness to face an HNS pollution of the Marine System (HNS-MS)

Home What are HNS? Background and objectives Actors and beneficiaries Tasks and methods Publications Tools Meeting Contact us

SEARCH HNS

How to use

You can search by :

- Name
- SEBC Behaviour
- CAS Number
- UN Number

Search

About the project
 We aim to develop a decision-support tool that national maritime authorities and coastguard stations will activate in order to forecast the drift, fate and behavior of acute marine pollution by Harmful Noxious Substances (HNS) accidentally released in the marine system.

Consortium

- > OD Nature, Royal Belgian Institute of Natural Sciences
- > Cedre
- > Ecole des Mines d'Alès
- > Alyotech Technologies
- > DG Environment, FPS Health, Food Chain Safety & Environment

Contact us

- Web: <http://hns-ms.eu/>
- Tel : +32 (0)2 773-2102
- Mail : hns-ms@naturalsciences.be

Copyright © 2015–2017 HNS-MS Consortium

HNS-MS is funded by DG-ECHO under agreement ECHO/SUB/2014/693705 and runs from 1 January 2015 to 31 March 2017.

Web development by: SWAP • webmaster@odnature.be

What are HNS? Background and objectives Actors and beneficiaries Tasks and methods Publications Contact us

Figure 5 The search tool on the web site

2. In the “Search” field type a part of the name (e.g. “propane”)

SEARCH HNS

How to use

You can search by :

- Name
- SEBC Behaviour
- CAS Number
- UN Number

propane

Search

3. By clicking on the search button, a list of available HNS is displayed.

By default, the results are not sorted. The user can change the sorting by clicking on the column name he wants to sort.

· SEARCH HNS ·

How to use

You can search by :

- Name
- SEBC Behaviour
- CAS Number
- UN Number

Search

Search



◆ Name	◆ SEBC	◆ CAS Number	◆ UN Number	◆ Details
2-Ethoxy-2-Methylpropane	E	637-92-3	1993	Details
Methyl-2-Ethoxypropane	E	637-92-3	1993	Details
2-Methyl-2-Ethoxypropane	E	637-92-3	1993	Details
2-Methoxy-2-Methyl Propane	ED	1634-04-4	2398	Details
2-Methyl-2-Methoxypropane	ED	1634-04-4	2398	Details
2-Phenylpropane	FE	98-82-8	1918	Details
1,2-Dihydroxypropane	D	57-55-6		Details
1,2-Propanediol	D	57-55-6		Details
Propane-1,2-Diol	D	57-55-6		Details
Propanediol	D	57-55-6		Details
2-Hydroxypropane	D	67-63-0	1219	Details
2-Hydroxy-2-Methylpropanenitrile	D	75-86-5	1541	Details
1,2-Epoxy-3-Chloropropane	D	106-89-8	2023	Details
1-Chloro-2,3-Epoxypropane	D	106-89-8	2023	Details
3-Chloro-1,2-Epoxypropane	D	106-89-8	2023	Details
1-Hydroxymethylpropane	D	78-83-1	1212	Details
2-Acetoxy-1-Methoxypropane	D	108-65-6	3271	Details
Ketone Propane	DE	67-64-1	1090	Details
Beta-Ketopropane	DE	67-64-1	1090	Details
1,2-Epoxypropane	DE	75-56-9	1280	Details
Epoxypropane	DE	75-56-9	1280	Details
1,2-Dichloropropane	SD	78-87-5	1279	Details

4. We have found our targeted chemical in the list.

By clicking on the blue label “Details”, the user will access to the detailed information about the HNS.

Access by web-app

Targeted audience	Registered users
Requirement	Internet connection Modern web-browser
Search tool URL	https://www.hns-ms.eu/app/#/hns/list

Remark: the web app is only accessible for registered users. A login is required to access the search tool.



Figure 6 Where to find the search tool ?

Example of typical usage:

Let us search information about the chemical having the CAS number “75-86-5” also called “2-Hydroxy-2-Methylpropanenitrile”.

1. Go to the search tool
 - a. By direct URL (if already logged in): <https://www.hns-ms.eu/app/#/hns/list>
 - b. Or via the menu bar (see Figure 6) of the web app:
<https://www.hns-ms.eu/app/>

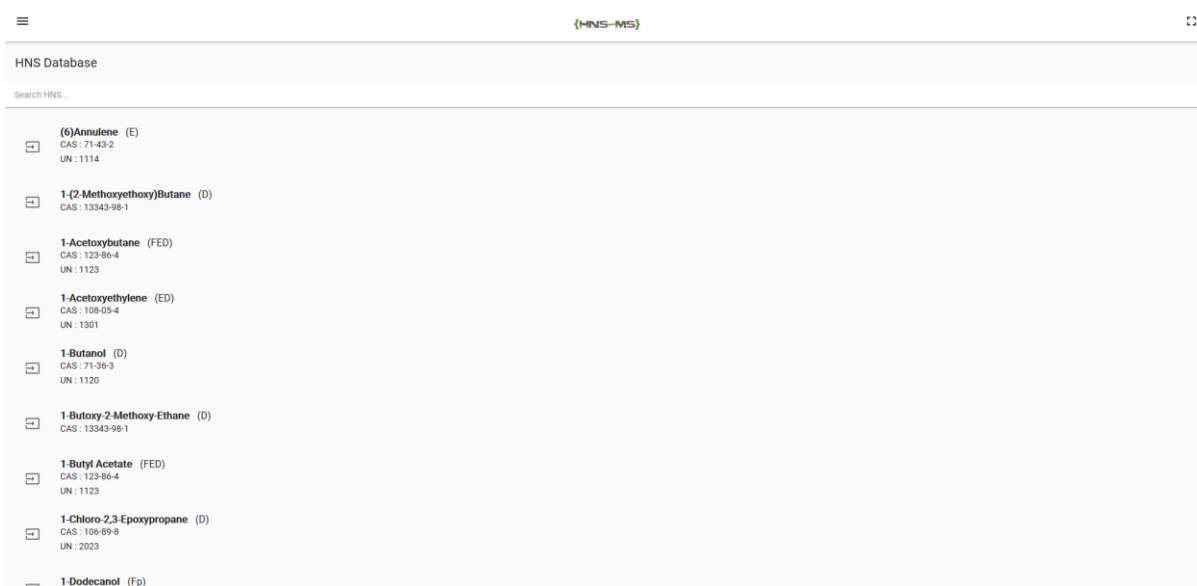


Figure 7 The search tool on the web app

On web app, the search tool displays a complete list of available HNS sorted alphabetically by name. The user can navigate through this list of synonyms to find the targeted chemical. Or use the integrated search tool.

- In the “Search HNS...” field begin to type “75-86-5”.

As the user begins to type, a drop down list of 5 HNS appears. More the user will type; more the list will become accurate. The result are sorted by name in alphabetical order.

HNS Database

75-86

2-Cyano-2-Propanol


2-Hydroxy-2-Methylpropanenitrile

2-Hydroxy-2-Methylpropionitrile

2-Hydroxyisobutyronitrile

2-Methylacetonitrile

UN : 1123

 **1-Acetoxyethylene (ED)**
CAS : 108-05-4
UN : 1301


 **1-Butanol (D)**
CAS : 71-36-3
UN : 1120

Figure 8 The drop down list under the search field

- By clicking on one of the chemical listed, the user will access to the detailed information about the HNS.

Access by JSON REST API

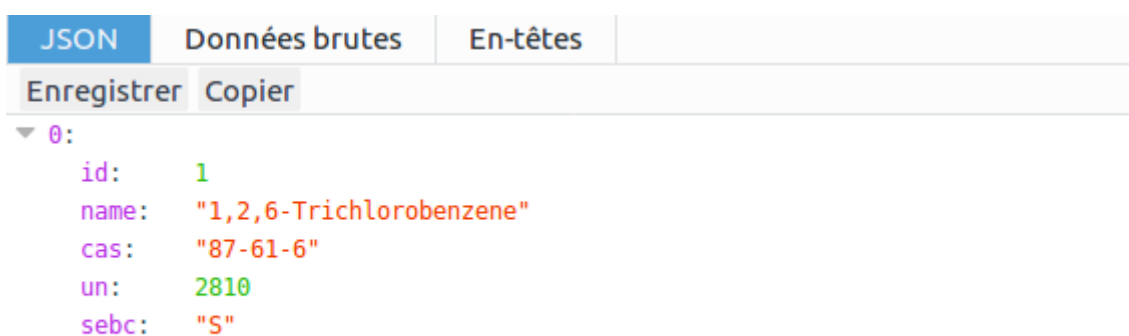
Targeted audience	Machines
URL	https://www.hns-ms.eu/api/hns/

The JSON REST API has the same capabilities as the web site and web app search tool, but without user interface and with more advanced search capabilities. It is not dedicated to be used by humans, but by machine. It allow external users to implement their version of the search tool or directly inject HNS parameters in external application (simulation systems, comparison systems, ...).

The output format is JSON (JavaScript Object Notation), more information on this format can be found on <http://www.json.org/>

Example of output : (<https://www.hns-ms.eu/api/hns/?limit=1>)

```
[
  {
    "id": 1,
    "name": "1,2,6-Trichlorobenzene",
    "cas": "87-61-6",
    "un": 2810,
    "sebc": "S"
  }
]
```



The screenshot shows a web browser interface with a tab labeled 'JSON'. Below the tab are buttons for 'Données brutes', 'En-têtes', 'Enregistrer', and 'Copier'. The main content area displays a JSON array with one object. The object contains the following fields: 'id' (1), 'name' ('1,2,6-Trichlorobenzene'), 'cas' ('87-61-6'), 'un' (2810), and 'sebc' ('S').

```
▼ 0:
  id: 1
  name: "1,2,6-Trichlorobenzene"
  cas: "87-61-6"
  un: 2810
  sebc: "S"
```

Figure 9 Example of output in a modern web browser

How to use

By default the API return list of the first 20 HNS stored in the database. This output is modified by adding parameters to the URL.

Two type of output are available :

- A list of HNS
- Detailed information about one HNS (only if the "id" parameter is set)

Remarks:

- The first parameter begins with a question mark "?" and the parameters are separated by "&".
- The order in witch the parameters are added is not important.
- All parameters are optional.

Available parameters:

limit=	<i>Integer</i> Sets the maximal number of returned items
offset=	<i>Integer</i> Sets the distance from the beginning of the list
order_by=	<i>[id, name, cas, un, sebc]</i> Sets the column to order by.
sort=	<i>[ASC, DESC]</i> Sets ascending or descending order.
text_search=	<i>Text</i> The text field to search. It could be a name a CAS number, UN number or SEBC (space are permitted without quotes)
id=	<i>Integer</i> The id of the HNS to get detailed information. If set, all other parameters are ignored.

Examples of usage:

To get the full list of HNS available:

<https://www.hns-ms.eu/api/hns/?limit=3000>

To get the full list of HNS available sorted by name:

https://www.hns-ms.eu/api/hns/?limit=3000&order_by=name

or

https://www.hns-ms.eu/api/hns/?order_by=name&limit=3000

To get a list of the 2 first HNS containing the word “propane”:

https://www.hns-ms.eu/api/hns/?text_search=propane&limit=2

To get detailed information about the HNS with id=19:

<https://www.hns-ms.eu/api/hns/?id=19>

Detailed information are only available when the “id” parameter is set. The correspondences between HNS and id are listed in the full list of HNS.

2.2.3 Detailed information page

The detailed information page is identical on the web site and web app and is divided in 7 sections:

1. Description

Summary of chemical classifications and synonyms.

2. GHS Security Information

Labelling of the HNS according to the Globally Harmonised System of Classification and Labelling of Chemicals (GHS)

· SEARCH RESULT ·

Acrylonitrile

Description Physico-chemical Behaviour Ecotoxicity Hazards GESAMP profile

Description

Top ^

CAS number	107-13-1
UN number	1093
Chemical formula	C ₃ H ₃ N
Accident occurred	Yes
Standard European Behaviour Classification (SEBC)	Dissolver that evaporates (DE)
Notable risks	Oxidizer. Polymerization.

GHS Security Information



Danger

GESAMP Hazard profile

A1	A2	B1	B2	C1	C2	C3	D1	D2	D3	E1	E2	E3
2	NR	3	0	2	3	3	2	2	CMSs	NT	DE	3

Marine pollution Classification (MARPOL Annex II)

Category	Description
Y	Noxious Liquid Substances which, if discharged into the sea from tank cleaning or deballasting operations, are deemed to present a hazard to either marine resources or human health or cause harm to amenities or other legitimate uses of the sea and therefore justify a limitation on the quality and quantity of the discharge into the marine environment.

Alternate names for this chemical

Acrylonitrile Monomer
Cianoethylene
2-Propenenitrile
Propenoic Acid Nitrile
Vinyl Cyanide
Cyanure De Vinyle
Nitrile Acrylique
Acrylonitrile

3. Physico-chemical properties

List of physical and chemical parameters.

Physico-chemical properties		Top ^
Chemical formula	C ₃ H ₃ N	
Molar mass	53.06 [g/mol]	
Critical molar volume	0.000173 [m ³ /mol]	
State	Liquid at 25°C and 1 atm	
Fusion temperature	-83 [°C]	
Boiling temperature	77.4 [°C]	
Critical temperature	540 [°C]	
Density	810 [Kg/m ³] at a temperature of 20°C	
Surface tension	27.22 [mN/m] at a temperature of 20°C	
	26.63 [mN/m] at a temperature of 25°C	
Kinematic viscosity	0.43 [cSt] at a temperature of 20°C	
	0.42 [cSt] at a temperature of 25°C	
Hydrosolubility	79000 [mg/l] at a temperature of 20°C and salinity of 0‰	
Vapour pressure	11500 [Pa] at a temperature of 20°C	
	14470 [Pa] at a temperature of 25°C	
Critical pressure	4660000 [Pa]	
Vapour density	1.9	
Flash point (Pensky-Martens closed cup)	-1 [°C]	
Lower explosivity limit (LEL)	3 [%]	
Upper explosivity limit (UEL)	17 [%]	
Vaporization enthalpy	616000 [J/Kg] at a temperature of 77.4°C	
Combustion enthalpy	31900000 [J/Kg]	
Specific heat capacity	2050 [J/(Kg·K)]	
Combustion efficiency	98 [%]	
Mass flow rate of the combustion surface	0.05 [Kg/(m ² ·s)]	
Radiative fraction	26 [%]	
Henry's constant	8.7 [mol/(m ³ ·Pa)]	

4. Behaviour

Information about the behaviour in aquatic environment.

Behaviour		Top ^
Log Kow	-0.92	
Log Koc	-0.07	
Hydrolysis (Half-life)	Not hydrolysable	
Aqueous photolysis (Half-life)	Not photolysable	
Biodegradation in estuary environment (Half-life)	Not biodegradable	
Biodegradation in marine environment (Half-life)	Not biodegradable	
Standard European Behaviour Classification (SEBC)	Dissolver that evaporates (DE)	
Bioconcentration factor (BCF)	1	

5. Ecotoxicity

Information about toxicity in aquatic environment.

Ecotoxicity		Top ^
Lowest median lethal concentration (LC ₅₀) on algae	1.63 [mg/l]	
Lowest median lethal concentration (LC ₅₀) on crustacean	6 [mg/l]	
Lowest median lethal concentration (LC ₅₀) on fishes	5.16 [mg/l]	
Highest no observed effect concentration (NOEC) on algae	0.8 [mg/l]	
Highest no observed effect concentration (NOEC) on crustacean	0.5 [mg/l]	
Highest no observed effect concentration (NOEC) on fishes	0.17 [mg/l]	
Assessment factor (AF)	100 on the short-term	
	100 on the long-term	
Predicted No Effect Concentration (PNEC)	16.3 [µg/l] on the short-term	
	1.7 [µg/l] on the long-term	

6. Hazards

Labelling, hazards (H) and prevention (P)statement according to the Globally Harmonised System of Classification and Labelling of Chemicals (GHS)

Hazards

[Top ^](#)



Danger

IDLH	85 [ppm]
-------------	----------

Hazards statements

Physical

H225 Highly flammable liquid and vapour.

Health

- H301 Toxic if swallowed.
- H311 Toxic in contact with skin.
- H317 May cause an allergic skin reaction.
- H318 Causes serious eye damage.
- H331 Toxic if inhaled.
- H335 May cause respiratory irritation.
- H350 May cause cancer.

Environmental

H411 Toxic to aquatic life with long lasting effects.

Precautionary statements

Prevention

- P201 Obtain special instructions before use.
- P202 Do not handle until all safety precautions have been read and understood.
- P210 Keep away from heat/sparks/open flames/hot surfaces. No smoking.
- P231 Handle under inert gas.
- P242 Use only non-sparking tools.
- P243 Take precautionary measures against static discharge.
- P260 Do not breathe dust/fume/gas/mist/vapours/spray.
- P262 Do not get in eyes, on skin, or on clothing.
- P270 Do no eat, drink or smoke when using this product.
- P272 Contaminated work clothing should not be allowed out of the workplace.
- P273 Avoid release to the environment.
- P280 Wear protective gloves/protective clothing/eye protection/face protection.
- P284 Wear respiratory protection.

Response

- P331 Do NOT induce vomiting.
- P301 + P310 IF SWALLOWED: Immediately call a POISON CENTER or doctor/physician.
- P302 + P352 IF ON SKIN: Wash with plenty of soap and water.
- P304 + P340 IF INHALED: Remove victim to fresh air and keep at rest in a position comfortable for breathing.
- P305 + P351 + P338 IF IN EYES: Rinse cautiously with water for several minutes. Remove contact lenses, if present and easy to do. Continue rinsing.
- P370 + P378 In case of fire: Use ... for extinction.

Storage

- P405 Store locked up.
- P403 + P233 Store in a well-ventilated place. Keep container tightly closed.

Disposal

- P501 Dispose of contents/container to ...

7. GESAMP

Detailed GESAMP profile.

GESAMP													Top
GESAMP Hazard profile													
A1	A2	B1	B2	C1	C2	C3	D1	D2	D3	E1	E2	E3	
2	NR	3	0	2	3	3	2	2	CMSs	NT	DE	3	
A1: Bioaccumulation													
Rating	Description												
2	Low potential to bioaccumulate												
A1a:													
Rating	Description	Criteria [mg/l]											
0	No potential to bioaccumulate	Log Kow < 1											
A1b:													
Rating	Description	Criteria											
2	Low potential to bioaccumulate	10 ≤ BCF < 100											
A2: Biodegradation													
Rating	Description												
NR	Not readily biodegradable												
B1: Acute aquatic toxicity													
Rating	Description	Criteria [mg/l]											
3	Moderately toxic	1 < LC/EC/C50 ≤ 10											
B2: Chronic aquatic toxicity													
Rating	Description	Criteria [mg/l]											
0	Negligible	NOEC > 1											
C1: Acute oral toxicity													
Rating	Description	Criteria [mg/Kg]											
2	Moderate	50 < AOTE ≤ 300											
C2: Acute dermal toxicity (skin contact)													
Rating	Description	Criteria [mg/Kg]											
3	Moderately high	50 < ADTE ≤ 200											
C3: Acute inhalation toxicity													
Rating	Description	Criteria [mg/l] (4 hours exposure)											
3	Moderately high	0.5 < AITE ≤ 2											
D1: Skin irritation or corrosion													
Rating	Description	Sign	GHS category										
2	Irritating	Marked erythema, Obvio	Irritant Category 2										
D2: Eye irritation													
Rating	Description	Sign	GHS category										
2	Irritating	Marked conjunctival hy	Irritant Category 2A										
D3: Long-term health effects													
Notation	Hazard endpoint	Description	GHS category										
C	Carcinogenicity	Chemicals which have been shown to induce or increase the incidence of cancer	Category 1 for Carcinogens										
M	Mutagenicity	Cause a permanent change in the amount or structure of genetic material in cells	Categories 1 and 2 for Germ Cell Mutagens										
Ss	Skin Sensitization	Cause specific skin hypersensitivity or allergy following skin contact	Category 1 for Skin Sensitizers										
E1: Tainting of seafood													
Rating	Description												
NT	The substance has been tested for tainting and found not to taint following exposure of the fish for 24h to 1mg/l.												
E2: Behaviour of chemicals in the marine environment													
Rating	Description												
DE	Dissolver that evaporates												
E3: Interference with the use of coastal amenities													
Rating	Interference	Description	Interpretation	Warning									
3	Highly objectionable	1 is highly acutely toxic; and/or 2 is severely irritant or corrosive to skin or eyes; and/or 3 is carcinogenic, mutagenic or reprotoxic; and/or 4 is a floater or persistent floater with associated health effects	1 C1 and/or C2 and/or C3 = 4; and/or 2 D1 or D2 = 3, 3A, 3B, or 3C; and/or 3 D3 contains C, M or R; and/or 4 E2 = F or Fp and D3 contains Ss, Sr, T, A, N, or I	Warning issued leading to the closure of amenities									

Further lab characterisation of HNS

PAGE INTENTIONALLY LEFT BLANK

3 HNS laboratory characterization for non-standard conditions

3.1 Introduction

Most of the physico-chemical properties available in the literature have been measured for standard conditions (20°C and in fresh water), that are different from the field conditions. The second objective of the lab experiments was therefore to assess the reliability of the available data by measuring the physico-chemical properties of 19 HNS for non-standard conditions, typical of the open-sea and of the estuaries in the Bonn Agreement area for summer and winter.

Because the tested HNS must also be used for quantifying the competition at the sea surface between evaporation and dissolution (chapter 4), these 19 HNS have been selected as a subset of Floaters, Dissolvers and/or Evaporators from the HNS-MS database. Other selection criteria were the availability of the data (one objective is also to test undocumented HNS) and toxicity (in order to preserve Cedre's staff health).

Table 3 presents the list of the 19 selected HNS for which laboratory tests have been realized to perform their characterization.

Table 3: List of HNS for laboratory characterization

HNS	CAS number	SEBC
1-Nonanol	2430-22-0	F
2,2,4-Trimethyl-1,3-Pentanediol-1-Isobutyrate (Texanol®)	25265-77-4	F
2-Ethylhexanoic acid	149-57-5	FD
2-Ethylhexyl acrylate	103-11-7	F
2-propanol	67-63-0	D
Acetone	67-64-1	DE
Butyl acrylate	141-32-2	FED
Ethyl acetate	141-78-6	DE
Heptane	142-82-5	E
Methanol	67-56-1	DE
Methyl isobutyl ketone	108-10-1	FED
Methyl methacrylate	80-62-6	FED
Methyl tert-butyl ether	1634-04-4	ED
n-Butyl acetate	123-86-4	FED
n-Butyl alcohol	71-36-3	D
n-Hexane	110-54-3	E
Pentane	109-66-0	E
Toluene	108-88-3	E
Xylenes	1330-20-7	FE

The characterization of these products concerns the following properties:

- Their specific gravity, viscosity and surface tension at 5, 10 and 20 °C (paragraph 3.1);
- The evaporation kinetics of the HNS alone and at the surface of water (paragraph 3.2);
- The dissolution kinetics of HNS at 20 °C and various salinities (0, 5 and 35 ‰) (paragraph 3.3).

The interfacial tension between HNS and seawater was initially planned to be measured. The methodology used has been re-evaluated following preliminary tests. In fact, the pendant drop method (based on the optical measurement of the geometry of a drop) has been applied. The data are still being processed.

3.2 Physical properties

The results for specific gravities, viscosities and surface tensions are given in Table 4, Table 5 and Table 6. In Table 5, the exact temperatures during the measurements are indicated in addition to the expected temperatures (5, 10 and 20 °C).

Table 4: Specific gravities at 5, 10 and 20 °C

HNS	Specific gravity at given temperature		
	5 °C	10 °C	20 °C
2,2,4-Trimethyl-1,3-Pentanediol-1-Isobutyrate	0,9577	0,9542	0,9477
2-Ethylhexanoic acid	0,9173	0,9142	0,9061
2-Ethylhexyl acrylate	0,897	0,8918	0,8861
Methyl isobutyl ketone	0,8145	0,8102	0,8031
Methyl methacrylate	0,9574	0,9534	0,9438
n-Butyl acetate	0,896	0,8916	0,881
n-Butyl alcohol	0,8213	0,8179	0,8116
1-Nonanol	0,8383	0,8348	0,8291
Xylenes	0,879	0,8743	0,8677
Butyl acrylate	0,9131	0,9085	0,9001
Ethyl acetate	0,9181	0,9119	0,902
Methyl tert-butyl ether	0,7574	0,7527	0,7531
Toluene	0,8809	0,8757	0,8683
Pentane	0,6429	0,6384	0,6278
n-Hexane	0,6753	0,6696	0,6613
Heptane	0,6971	0,6938	0,6853
Methanol	0,8055	0,8013	0,7932
Acetone	0,807	0,8018	0,7918
2-Propanol	0,7875	0,7946	0,7946

The experimental data of specific gravity at 20°C are in accordance with literature data with gaps smaller than 2%. A decrease in temperature results in an increase of specific gravity: the difference is of 1 to 2% between 5 and 20°C. In the Bonn Agreement area, annual water temperature variations are more or less in this temperature range and as 2%-gaps are acceptable for modelling purposes, it seems unnecessary to pursue experimental measurements on this parameter.

Table 5: Viscosities at 5, 10 and 20 °C

HNS	Viscosity (mPa.s)		
	5°C	10°C	20°C
2,2,4-Trimethyl-1,3-Pentenediol-1-Isobutyrate	45,52	33,37	18,95
2-Ethylhexanoic acid	16,43	12,83	8,41
2-Ethylhexyl acrylate	3,99	3,73	5,55
Methyl isobutyl ketone	1,90	2,31	1,78
Methyl methacrylate	2,11	2,03	1,82
n-Butyl acetate	2,42	2,25	2,06
n-Butyl alcohol	4,78	9,79	3,88
1-Nonanol	15,25	18,77	12,39
Xylenes	2,10	2,03	1,91
Butyl acrylate	2,58	2,50	2,36
Ethyl acetate	1,63	1,63	1,59
Methyl tert-butyl ether	1,33	1,32	1,14
Toluene	1,98	1,81	1,81
Pentane	0,86	0,85	0,62
n-Hexane	1,21	1,04	1,12
Heptane	1,42	1,38	1,33
Methanol	1,95	1,79	1,60
Acetone	1,28	1,16	1,36
2-Propanol	4,44	3,63	3,51

The experimental results for viscosity at 20°C are in accordance with literature data for HNS with a viscosity above 3mPa.s. Difficulties have been encountered for measurements of HNS with low viscosity and the experimental protocol has to be modified. Usually, a decrease in temperature results in an increase of viscosity. For viscosity above 8mPa.s at 20°C, the viscosity at 5°C increases at least by a factor of 2. As viscosity is linked to the capacity of spreading and is greatly impacted by temperature, efforts need to be maintained on this parameter. Globally, experimental data at 20°C are in accordance with literature data. A decrease in temperature results in an increase of surface tension: the difference is of 3 to 10% between 5 and 20°C.

Table 6: Surface tensions at 5, 10 and 20 °C

HNS	Surface tension γ (mN/m)	Temperature (5°C)	Surface tension γ (mN/m)	Temperature (10°C)	Surface tension γ (mN/m)	Temperature (20°C)
2,2,4-Trimethyl-1,3-Pentanediol-1-Isobutyrate	29,46	6,2	28,73	12,4	28,12	19,5
2-Ethylhexyl acrylate	27,91	5,4	27,68	11,3	26,82	19,3
n-Butyl acetate	25,8	5,7	25,02	10,6	24,83	18,4
n-Butyl alcohol	25,71	3,8	24,90	11,1	24,25	18,4
1-Nonanol	28,91	5,7	28,02	11,2	27,8	18,8
Butyl acrylate	26,77	6,1	26,56	11,3	25,63	19,1
2-Ethylhexanoic acid	28,42	6,9	27,62	11,2	26,86	19,5
Ethyl acetate	25,08	5,6	24,39	10,4	23,82	18,6
Pentane	17,55	5,1	16,77	10,2	16,43	15,3
Methyl tert-butyl ether	20,04	5	19,07	10,1	18,06	18,5
n-Hexane	19,92	5	19,09	10	18,6	17,7
Heptane	21,6	6	21,08	10,1	20,32	18,1
Acetone	24,9	5,1	24,14	9,8	23,44	18
Methyl methacrylate	27,77	5,1	27,10	10,9	25,99	19,8
Methanol	23,88	4,1	23,06	10,1	22,67	18,1
Methyl isobutyl ketone	24,47	5,1	23,73	11,8	23,61	18,2
Xylenes	29,04	5,3	27,88	10	26,96	17,9
Toluene	29,8	5,6	28,66	11,6	28,01	18,1
2-Propanol	21,44	6,9	21,00	12,5	20,79	20,2

3.3 Evaporation kinetics

The evaporation kinetics of the HNS listed in Table 2 have been studied. The tests included two phases for each HNS: the evaporation of the product alone and the evaporation when the product forms a slick at the surface of seawater.

3.3.1 Evaporation of the HNS

Protocol

7 mL of HNS were spilled in a beaker with small edges (2 cm) to avoid side effects and the accumulation of vapors at the surface of the HNS. The beaker was placed on a scale (precision: 1mg) and the weight was recorded at regular time intervals.

An evaporation rate was then calculated: the mass was transformed in percent to be able to compare all the HNS. The evaporation rate ($\% \cdot h^{-1}$) is the opposite of the slope of the percentage of HNS remaining by time.

Evaporation rates

The evaporation rates of the 19 HNS are shown in Table 7.

Table 7: Evaporation rates of the HNS

HNS	Evaporation Rate (%.h ⁻¹)
Pentane	233.67
Methyl tert-butyl ether	83.54
Acetone	71.59
n-Hexane	64.1
Heptane	34.64
Methanol	32.92
Ethyl acetate	25.94
Methyl methacrylate	21.09
Toluene	20.93
2-Propanol	14.94
Methyl isobutyl ketone	14.12
n-Butyl acetate	14.12
Xylenes	6.03
Butyl acrylate	5.57
n-Butyl alcohol	4.45
2-Ethylhexyl acrylate	0.33
2,2,4-Trimethyl-1,3-Pentanediol-1-Isobutyrate	0.12
2-Ethylhexanoic acid	0.02
1-Nonanol	-0.04

The 19 HNS are ordered by evaporation rate and classified in groups:

- Group 1: evaporation rate above 200%.h⁻¹ ;
- Group 2: evaporation rate between 60 and 90%.h⁻¹ ;
- Group 3: evaporation rate between 20 and 40%.h⁻¹ ;
- Group 4: evaporation rate between 14 and 15%.h⁻¹ ;
- Group 5: evaporation rate between 4 and 7%.h⁻¹ ;
- Group 6: evaporation rate between 0.1 and 0.5%.h⁻¹ ;
- Group 7: evaporation rate below 0.05%.h⁻¹.

1-Nonanol has a negative evaporation rate (group 7). The evaporation is so low that a movement of the scale could have changed the initial weight. Moreover, the weigh is fluctuating

around 100.5% so the evaporation is not linear. Since the evaporation rate is calculated with the slope of the evaporation, the evaporation rate for 1-nonanol is not precise. This negative value can be replaced by 0. Even if the evaporation rate of 2-ethylhexanoic acid is positive, the same observations can be made.

Texanol® and 2-ethylhexyl acrylate have a very low evaporation rate: less than 1% per hour (group 6).

Butyl acetate, xylenes, butyl acrylate and butyl alcohol have a low evaporation rate: between 4 and 7% are evaporated in one hour (group 5).

Heptane, methanol, ethyl acetate, methyl methacrylate, toluene, 2-propanol and methyl isobutyl ketone have a mean evaporation: between 14 and 35% of the 7 mL is evaporated in one hour (groups 5-4-3).

Methyl tert-butyl ether, acetone and n-hexane have a high evaporation: between 64 and 86% of the 7mL is evaporated in one hour (group 2).

Pentane evaporates the fastest, before half an hour; it is fully evaporated (group 1).

Evaporation kinetics

The evaporation kinetics of some HNS are shown in Figure 10. The HNS on the graph have been selected to represent all the behaviour of the 19 HNS.

Most of the HNS have a linear evaporation except methanol and butyl acrylate that present two linear sections.

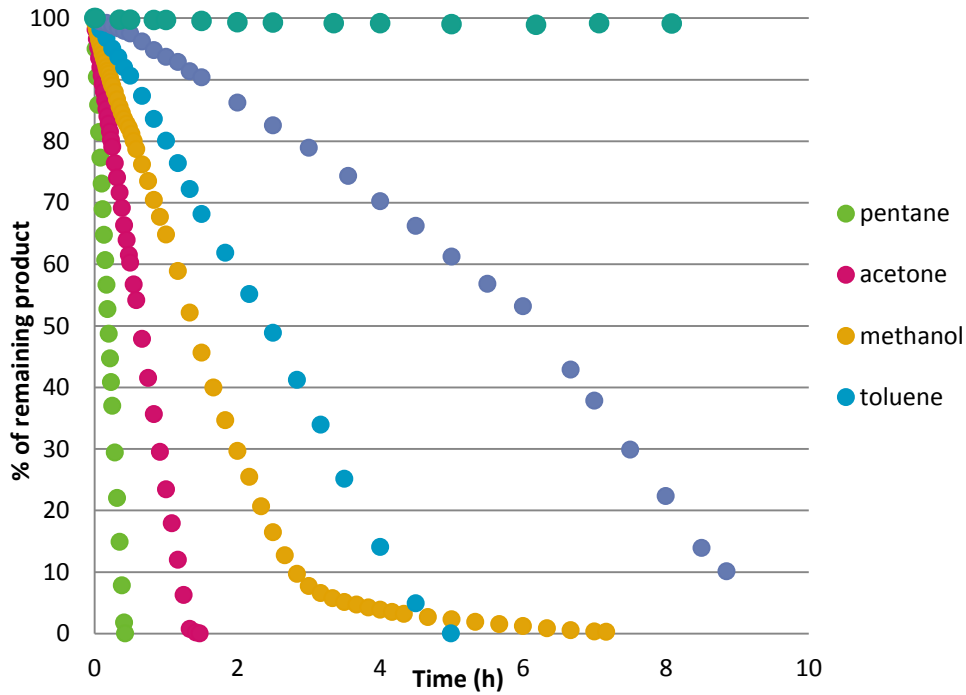


Figure 10: Evaporation kinetics of some HNS

Correlation with vapour pressure

A positive correlation exists between the evaporation rate and the vapour pressure of the HNS (except for heptane and 2-propanol). The evaporation of those two HNS is not truly linear so the calculation of the evaporation rate (based on the slope of the evaporation line) is less precise than for the other HNS which are linear. The evaporation of methyl methacrylate, methyl isobutyl ketone and butyl acetate are also not strictly linear. The correlation between evaporation rate and vapour pressure is given in Figure 11.

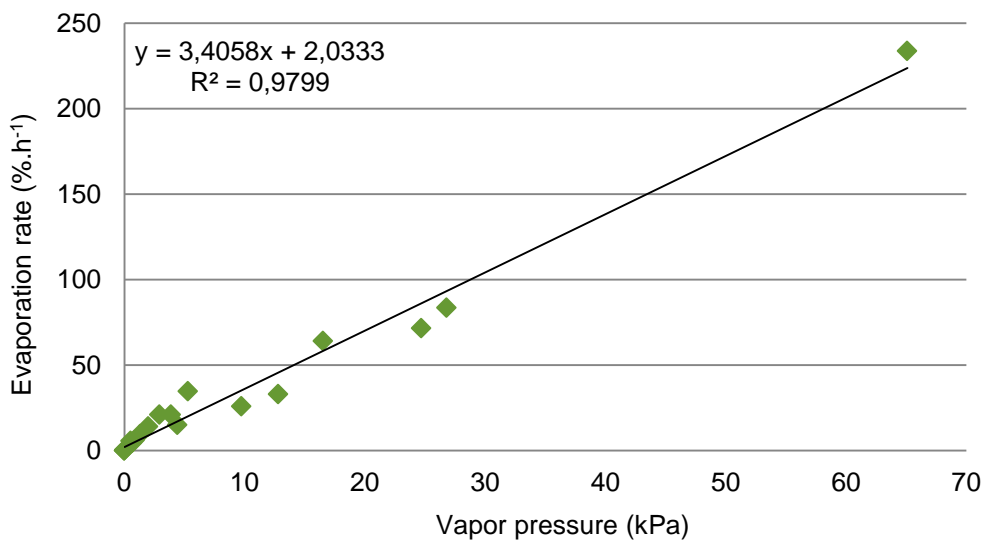


Figure 11: Correlation between evaporation rates and vapour pressures

The coefficient of correlation between the evaporation rate and vapour pressure is 0.9799 when all the HNS are represented. However, the evaporation rate of pentane is so high compared to all the other HNS that it has a strong influence on the global correlation. The same graph without 1-nonanol and pentane is given in Figure 12. Pentane has been removed because of its influence and 1-nonanol has been removed because the only value of the vapour pressure found was at 25 °C. The correlation is still good: the coefficient of correlation is 0.9377.

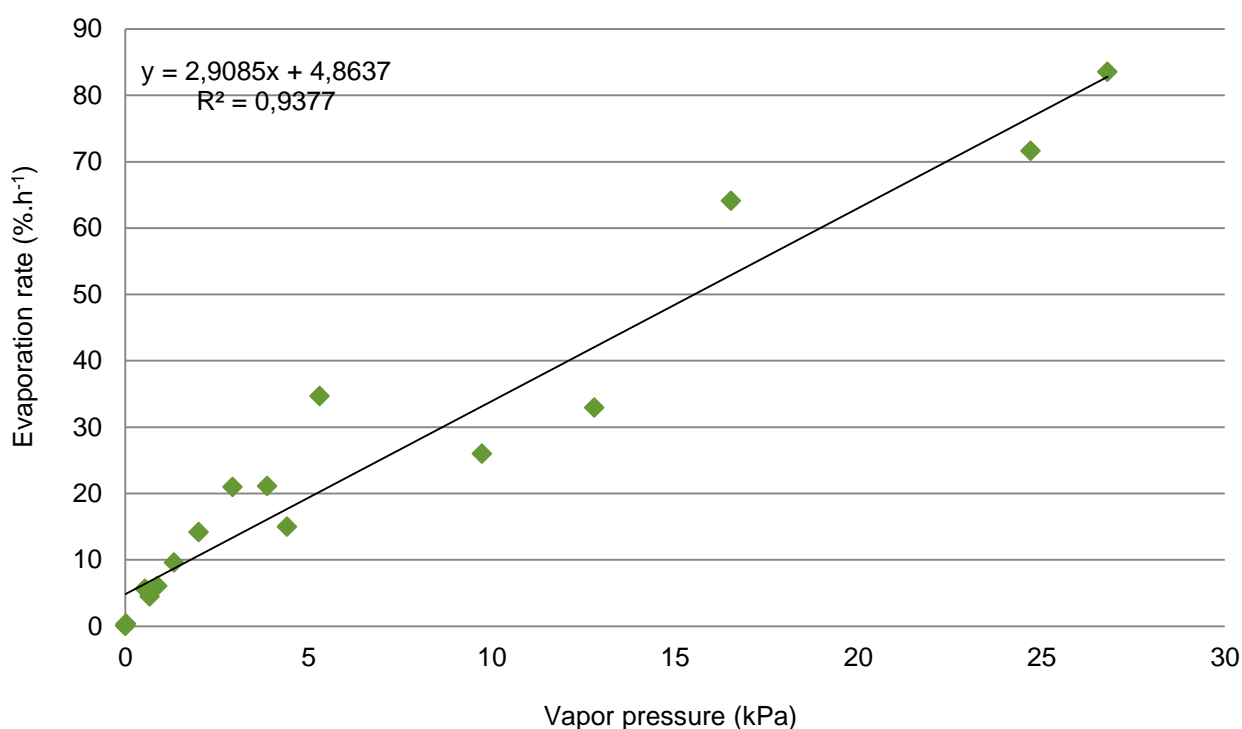


Figure 12: Correlation between evaporation rate and vapour pressure without pentane and 1-nonanol

3.3.2 Evaporation of the HNS at sea surface

Protocol

The HNS were spilled in a beaker filled with seawater (35 ‰). The sea water was made from osmosis water and aquarium salt. The same volume of HNS as in the first experiment was spilled.

The volume of water was calculated based on the solubility of the HNS. To study the competition between dissolution and evaporation, the water should not be saturated. If the water is saturated, the evaporation is favoured. The slick covered the whole surface and so water evaporation was negligible. The mass evaporated was found by removing the initial weight of water to the mass weighted and the evaporation rate was calculated as before.

For some products, the volume of water needed to be under the solubility was so high that it could not be weighted precisely. That's why the amount of product spilled was reduced. The volumes of HNS spilled at the surface of water are given in Table 8.

Table 8 : Volumes of HNS spilled

HNS	HNS volume (mL)	Water volume (L)
Pentane	3	0.5
Acetone	7	0.3
n-Hexane	Not tested	-
Methanol	7	0.3
Ethyl acetate	7	0.3
Methyl tert-butyl ether	7	0.3
Heptane	Not tested	-
Methyl methacrylate	7	0.5
Toluene	0.5	1
2-Propanol	7	0.3
Methyl isobutyl ketone	7	0.3
n-Butyl acetate	7	1
Xylenes	0.15	1
n-Butyl alcohol	7	0.3
Butyl acrylate	2	1
2-Ethylhexyl acrylate	Not tested	-
2-Ethylhexanoic acid	2	1
1-Nonanol	0.15	1
2,2,4-Trimethyl-1,3-Pentanediol-1-Isobutyrate	0.5	0.5

9 HNS were tested with a volume of 7 mL. We can compare the evaporation of these products alone and the evaporation of them at the surface of seawater.

For the evaporation of xylenes and 1-nonanol, a volume of 0.15 mL was spilled. The slick did not cover the whole surface so the evaporation of water could append. The weight lost every period of time was the addition of the mass of xylene or 1-nonanol evaporated and the mass of water evaporated. The same observations can be made for Texanol® and toluene. That's why the results were not considered. The volumes calculated for hexane, heptane and 2-ethylhexyl acrylate were also too small to be tested.

For pentane and butyl acrylate, another evaporation of the product alone has been done with the volume of product tested (respectively 3mL, 0.5mL, 2 mL).

Even if 2 mL of 2-ethylhexanoic acid spilled, the evaporation of 2 mL alone was not tested because its evaporation rate was too low.

Results

The evaporation rates of the HNS alone and at the surface are given in Table 9.

Table 9 : Evaporation rates of the HNS alone and at the surface of water

HNS	Evaporation rate alone (%.h ⁻¹)	Evaporation rate at the surface (%.h ⁻¹)
Pentane*	628.37	1648.17
Methyl tert-butyl ether	83.54	58.23
Acetone	71.59	23.89
n-Hexane	64.10	Not tested
Heptane	34.64	Not tested
Methanol	32.92	12.54
Ethyl acetate	25.94	21.72
Methyl methacrylate	21.09	101.91
Toluene*	20.93	X
2-Propanol	14.94	15.36
Methyl isobutyl ketone	14.12	7.71
Xylenes*	6.03	X
n-Butyl acetate	9.54	37.70
Butyl acrylate*	13.32	37.05
n-Butyl alcohol	4.45	7.49
2-Ethylhexyl acrylate	0.33	Not tested
2,2,4-Trimethyl-1,3-Pentanediol-1-Isobutyrate*	0.12	X
2-Ethylhexanoic acid*	0.02	X
1-Nonanol*	-0.04	X

*: different volume spilled

X: results not considered

Yellow: Evaporation rate at the surface is higher than for the HNS alone.

Green: Evaporation rate at the surface is lower than for the HNS alone.

Pentane, methyl methacrylate, butyl acetate, butyl acrylate and n-butyl alcohol have a much higher evaporation rate when they are at the surface of water than when they are alone (yellow coloration in Table 9). When these HNS are spilled, the surface of water seems to boil and the agitation of the surface could help the evaporation. The example of butyl acetate is shown in Figure 13.

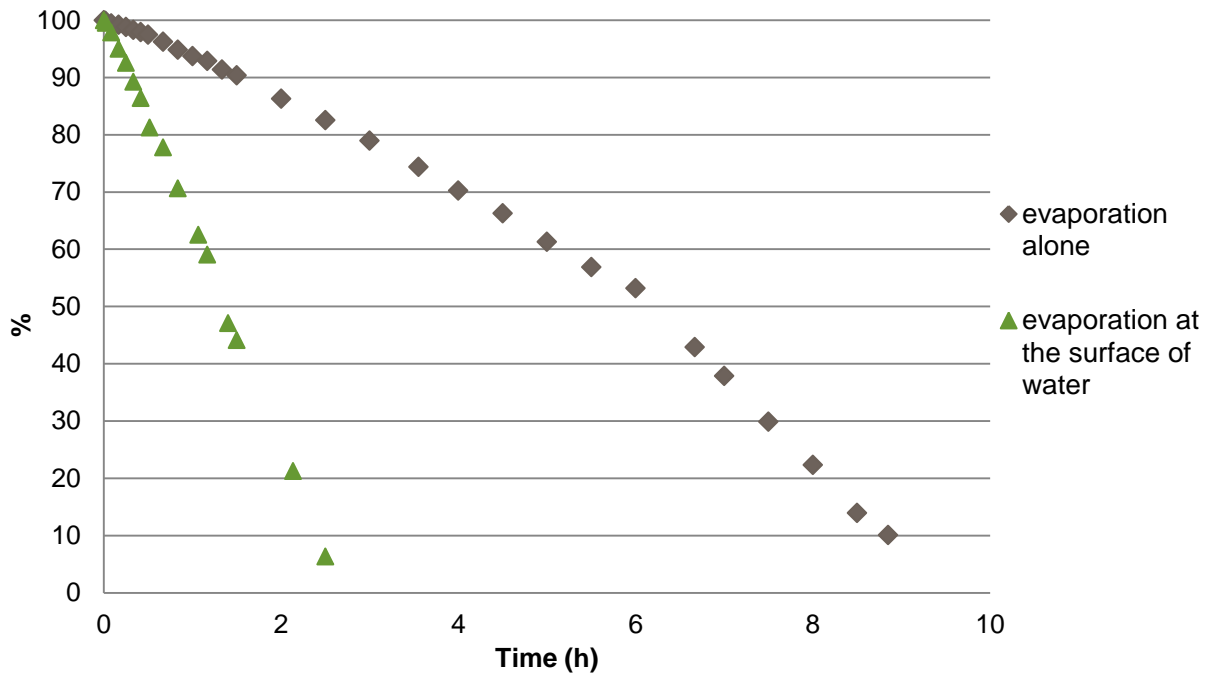


Figure 13: Comparison of the evaporation of butyl acetate alone and at the surface of water

Methyl tert-butyl ether, acetone, methanol, methyl isobutyl ketone and ethyl acetate have a lower evaporation rate at the surface than alone (green coloration in Table 9). This could be explained by their high solubility in water. The example of methyl tert-butyl ether is shown in Figure 14.

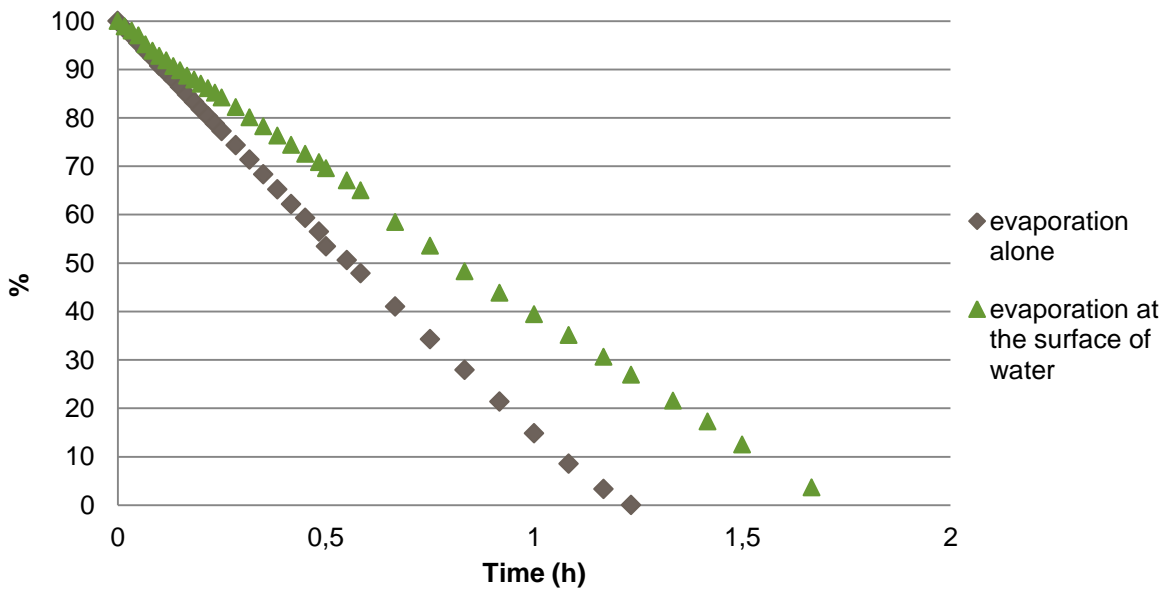


Figure 14: Comparison of the evaporation of methyl tert-butyl ether alone and at the surface of water

No correlations have been found between the evaporation and the evaporation at the surface of the water and between the evaporation at the surface of the water and vapour pressure, density, solubility, surface tension and viscosity. The values used for correlation were the ones found by previous tests on HNS.

3.4 Dissolution kinetics

3.4.1 Protocol

The dissolution of the HNS has been tested with three different salinities: freshwater, 5‰ and 35‰ (average salinity of seawater around the world). Osmosis water was used for freshwater. 5‰ and 35‰ were made from aquarium salts and osmosis water.

Considering the list of HNS in Table 3, all HNS have been tested except methanol, acetone and 2-propanol due to their miscibility with water.

2L of water (either freshwater, 5 ‰ or 35‰) were put in glass bottles with a draining tap at the bottom and a magnetic bar inside (Figure 15). The amount of product spilled at the surface was calculated to be in large excess (compared to the value of solubility found in literature). Three replicates were performed for each salinity at the same time to have a reproducible measure. The flasks were put on a magnetic stirrer with a low agitation (100 rpm) so that there would not be a vortex inside the bottle. The experiment took place in a room kept at 20°C.

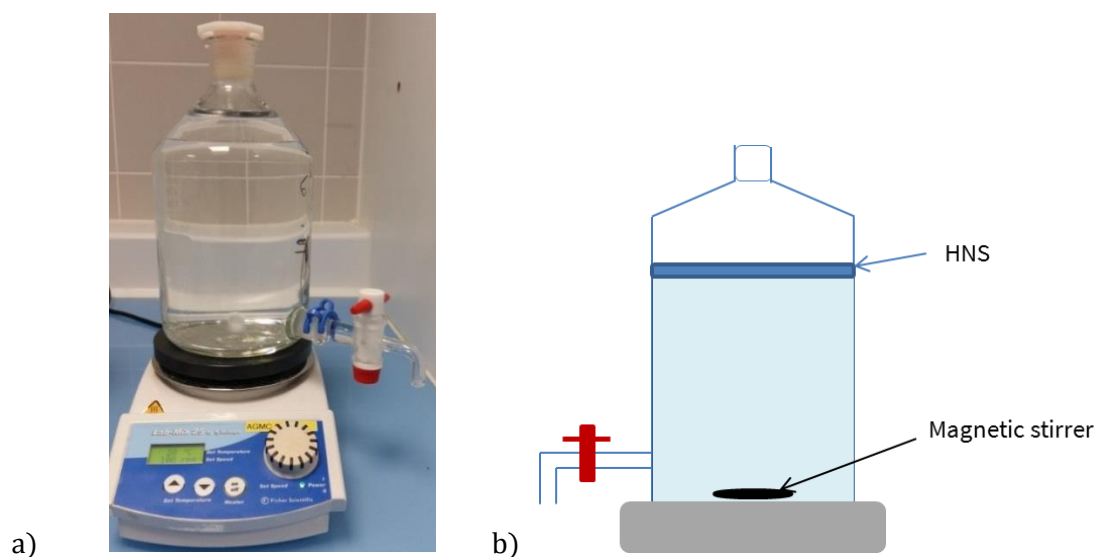


Figure 15: Picture (a) and scheme (b) of the experimental protocol

Three samples of 10 mL of each flask were taken the first day after 1 hour, 5 hours and 8 hours and then two samples a day were taken at 24 and 29 hours. The sampling continued until the concentration of the triplicates was stable during four samplings times.

The 10mL-samples were analysed with different analytical methods:

- the HNS with a high solubility and a high boiling point were analysed by GC-FID with a liquid-liquid extraction by hexane;
- the HNS with a low solubility and a high boiling point were analysed by GC-MS with a liquid extraction by hexane;
- the HNS with a low boiling point or a high vapour pressure were analysed by GC-MS with headspace (HS) extraction.

In every sample, an internal standard was added before the extraction to prevent injection differences between the samples during the extraction and the variations of injection in GC. The analytical methods and the internal standard for each HNS are given in Table 10.

Table 10 : Analytical methods and internal standards of the HNS

HNS	Analytical method	Internal standard
2,2,4-Trimethyl-1,3-Pentanediol-1-Isobutyrate	GC-FID	1-nonanol
2-Ethylhexanoic acid	GC-FID	Octanoic acid
2-Ethylhexyl acrylate	GC-FID	Hexyl acrylate
Methyl isobutyl ketone	HS-GC-MS	Diisobutyl ketone
Methyl methacrylate	HS-GC-MS	Hexyl acrylate
n-Butyl acetate	GC-FID	Pentyl acetate
n-Butyl alcohol	HS-GC-MS	Pentanol
1-Nonanol	GC-FID	Texanol®
Xylenes	LIQUIDE-GC-MS	Toluene D8
Butyl acrylate	LIQUIDE-GC-MS	Hexyl acrylate
Ethyl acetate	HS-GC-MS	Methyl acetate
Methyl tert-butyl ether	HS-GC-MS	Tert-amyl-methyl ether
Toluene	LIQUIDE-GC-MS	Toluene D8
Pentane	HS-GC-MS	Octane
n-Hexane	HS-GC-MS	Octane
Heptane	HS-GC-MS	Octane

When four concentrations had been measured at the same level, the average concentration of the four sampling times with the standard deviation was considered as the solubility limit.

3.4.2 Results

Solubility

The protocol has been performed on all HNS and the results are given in Table 11.

Table 11 : Limit concentrations measured experimentally

HNS	Limit concentration in fresh water (g.L ⁻¹)	Limit concentration in 5‰ water (g.L ⁻¹)	Limit concentration in 35‰ water (g.L ⁻¹)
Texanol [®]	0.97 ± 0.03	0.87 ± 0.05	0.66 ± 0.03
2-Ethylhexanoic acid	1.64 ± 0.12	1.68 ± 0.16	0.96 ± 0.04
2-Ethylhexyl acrylate	0.036 ± 0.003	0.035 ± 0.004	0.021 ± 0.001
Methyl isobutyl ketone	6.42 ± 1.11	6.32 ± 0.69	4.60 ± 0.82
Methyl methacrylate	13.64 ± 0.80	13.00 ± 0.47	10.37 ± 0.88
n-Butyl acetate	7.24 ± 0.35	6.97 ± 0.54	5.67 ± 0.35
n-Butyl alcohol	72.67 ± 6.75	66.73 ± 3.52	54.26 ± 5.56
1-Nonanol	0.13 ± 0.006	0.12 ± 0.007	0.094 ± 0.004
Xylenes	0.13 ± 0.01	0.12 ± 0.01	0.10 ± 0.01
Butyl acrylate	1.61 ± 0.26	1.34 ± 0.18	1.44 ± 0.24
Ethyl acetate	54.39 ± 4.98	38.86 ± 5.51	36.81 ± 10.20
Methyl tert-butyl ether	31.78 ± 1.30	26.87 ± 2.11	20.55 ± 1.68
Toluene	0.16 ± 0.01	0.15 ± 0.01	0.11 ± 0.01
Pentane	0.037 ± 0.0018	0.038 ± 0.0025	0.027 ± 0.0022
n-Hexane	0.0088 ± 0.0007	0.0071 ± 0.0009	0.0066 ± 0.0016
Heptane	0.0032 ± 0.0005	0.0028 ± 0.0003	0.00048 ± 0.00003

Because of the differences of solubility of the HNS, the results are presented in Figure 16 to Figure 19. The solubility in seawater has been found in the literature and added on the graphs for 4 HNS (Xylene, Toluene, Pentane and Hexane). Comparisons between results in freshwater and seawater, results in freshwater and 5‰ water, theoretical solubility and solubility measured in freshwater and theoretical solubility and solubility measured in seawater are shown in Figure 20.

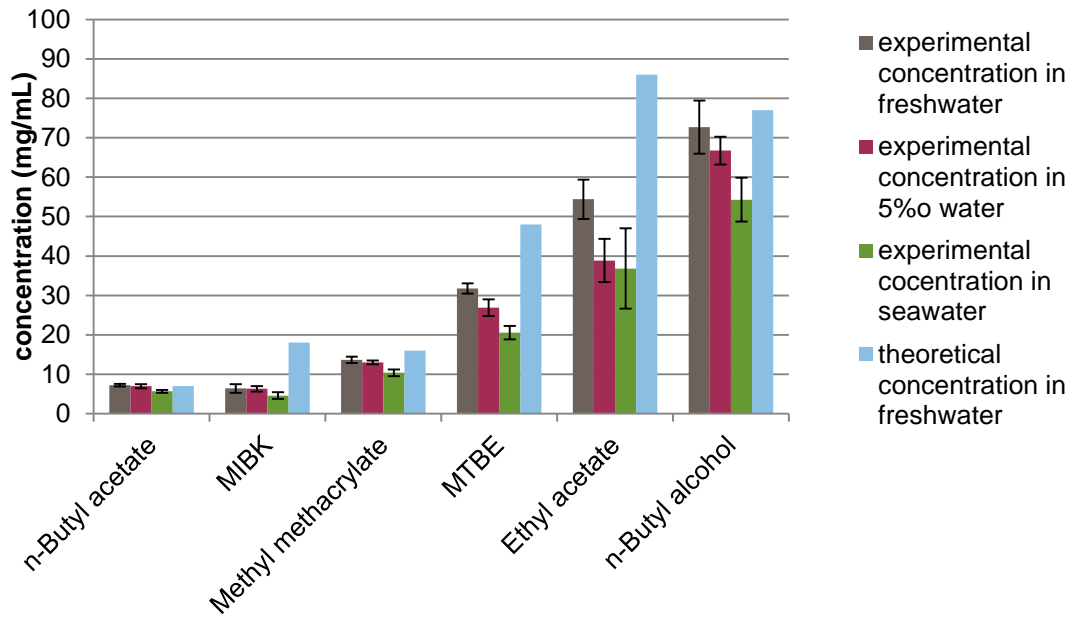


Figure 16: Solubility of n-Butyl acetate, MIBK, Methyl methacrylate, MTBE, Ethyl acetate, n-Butyl alcohol

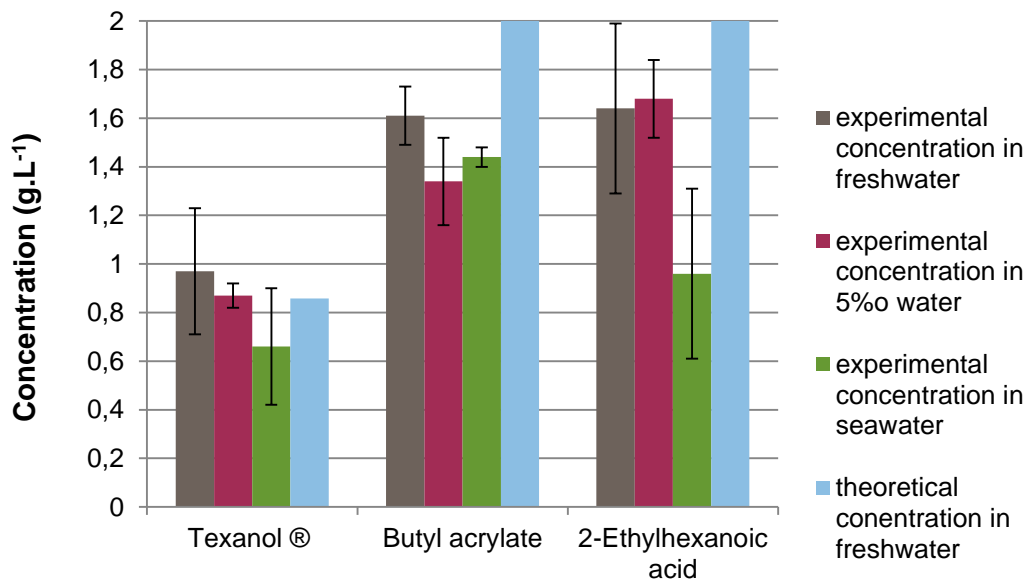


Figure 17: Solubility of Texanol®, Butyl Acrylate and 2-Ethylhexanoic acid

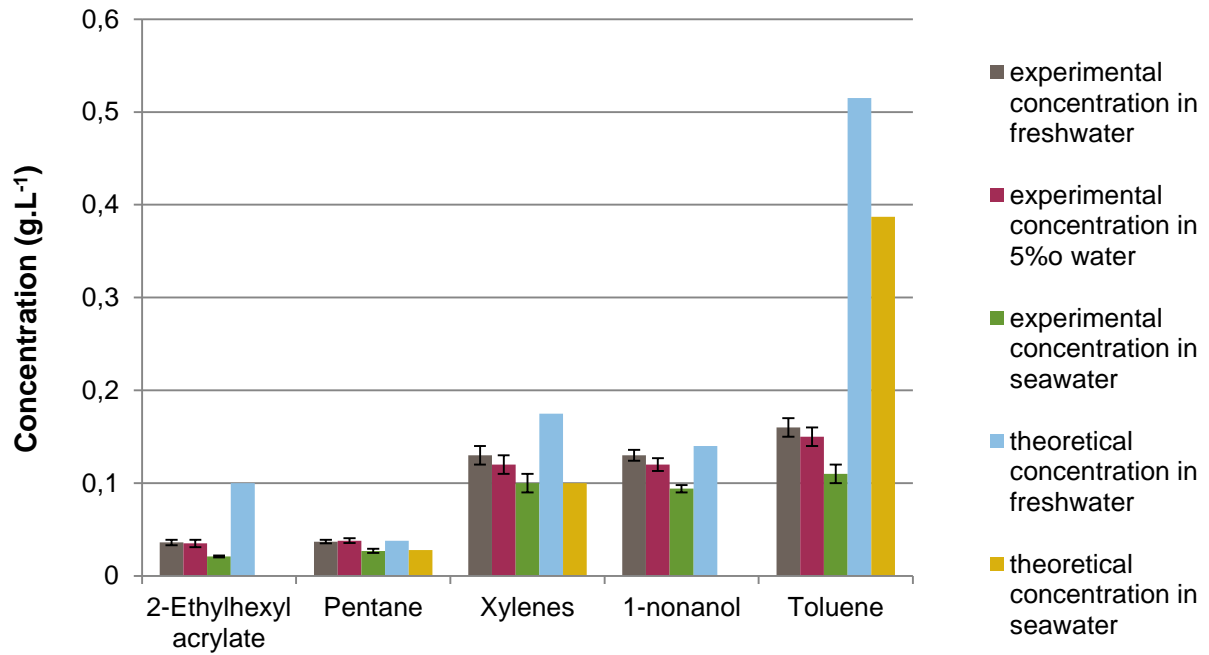


Figure 18: Solubility of 2-Ethylhexyl acrylate, Pentane, Xylenes, 1-Nonanol, Toluene

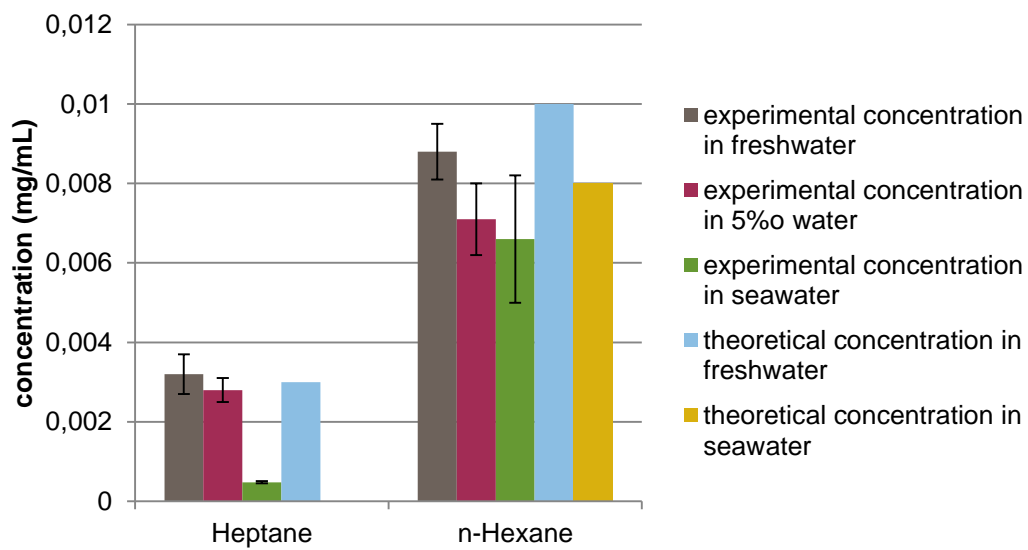


Figure 19: Solubility of Heptane and Hexane

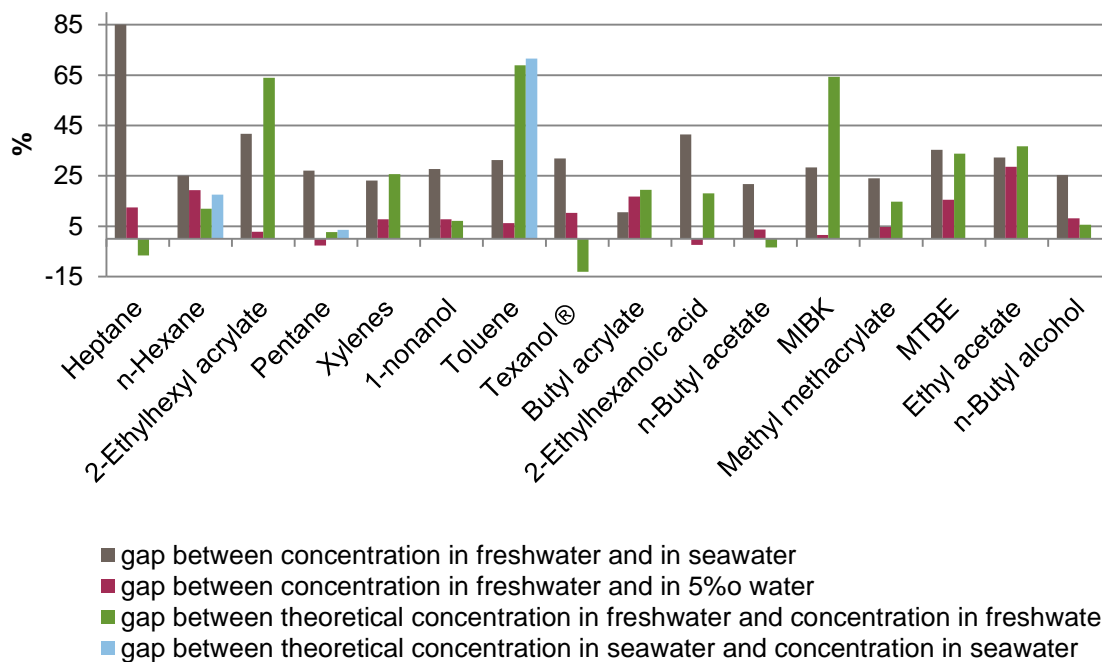


Figure 20: Comparison of results in freshwater, seawater, 5‰ water and literature data

For all HNS, the solubility measured in freshwater is higher than in seawater. The solubility measured in freshwater is 21 to 41% higher than in seawater, except for butyl acrylate (10 %) and heptane (85 %).

Except for pentane and 2-ethylhexanoic acid, the solubility measured in freshwater is 1.5 to 28.5% higher than in 5‰ water. Solubilities for pentane and 2-ethylhexanoic are slightly higher in 5‰ water than in freshwater (2 to 3%).

These results are in adequacy with the “salting out effect” establishing that, for most of the chemicals, solubility is lower at high salt concentrations.

The results of the solubility tests have been compared to the data found in literature. The correlation is given in Figure 21.

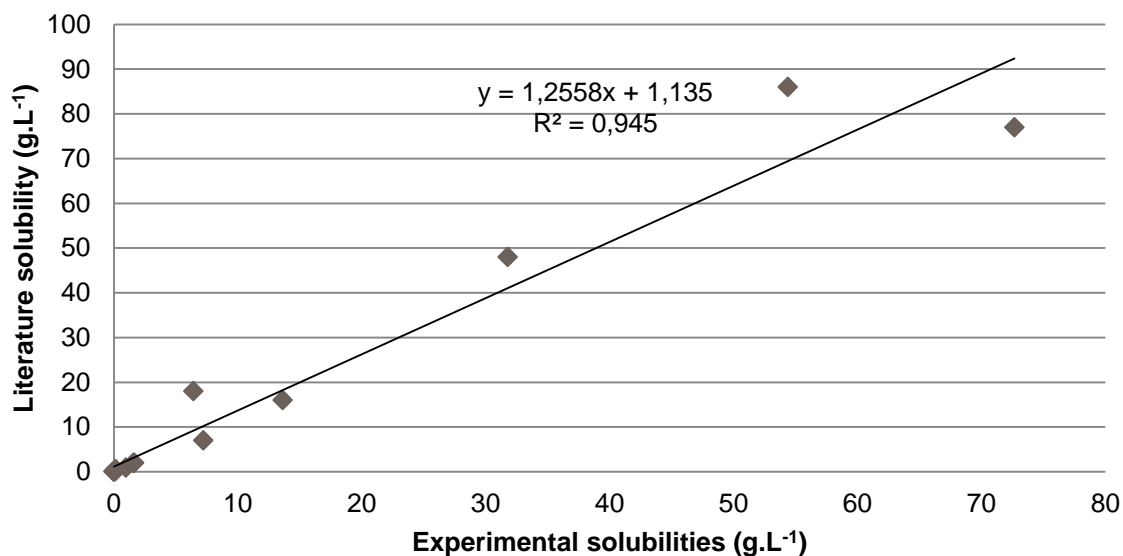


Figure 21 : Correlation between the solubility given in the literature and the solubility measured in freshwater

The solubility measured for Texanol® is 13% higher than the theoretical solubility. The solubilities measured for heptane, butyl acetate, pentane, butyl alcohol and 1-nonanol are 7% lower to 7% higher than theoretical concentrations. The solubilities measured for hexane, methyl methacrylate, 2-ethylhexanoic acid, butyl acrylate, xylenes, methyl tert-butyl ether and ethyl acetate are 12 to 35% lower than the theoretical concentration. For ethylhexyl acrylate, methyl isobutyl ketone and toluene, the solubilities found in the literature are much lower than the one measured with the tests (64 to 69%).

However, solubilities measured at 20°C are in adequacy with the literature data as show in Figure 21. A linear correlation exists between experimental and theoretical solubilities (coefficient of correlation of 0.94).

The data usually found in literature are given for 20 °C in freshwater but for 4 HNS, the data have also been found at 20°C in seawater. Except for Toluene, the theoretical and experimental measures in seawater are close. There is no difference for xylene, theoretical concentration is 3% higher for pentane and 17.5% higher for hexane. Theoretical concentration for toluene in seawater is 72% higher than the solubility measured.

Dissolution kinetics

For all the HNS, the stable concentration is reached between 23 and 48 hours after the beginning of the test and the plot is always following the same trend. There is a fast and strong augmentation the first day and then the concentration stabilizes. The example of methyl methacrylate is given in Figure 22.

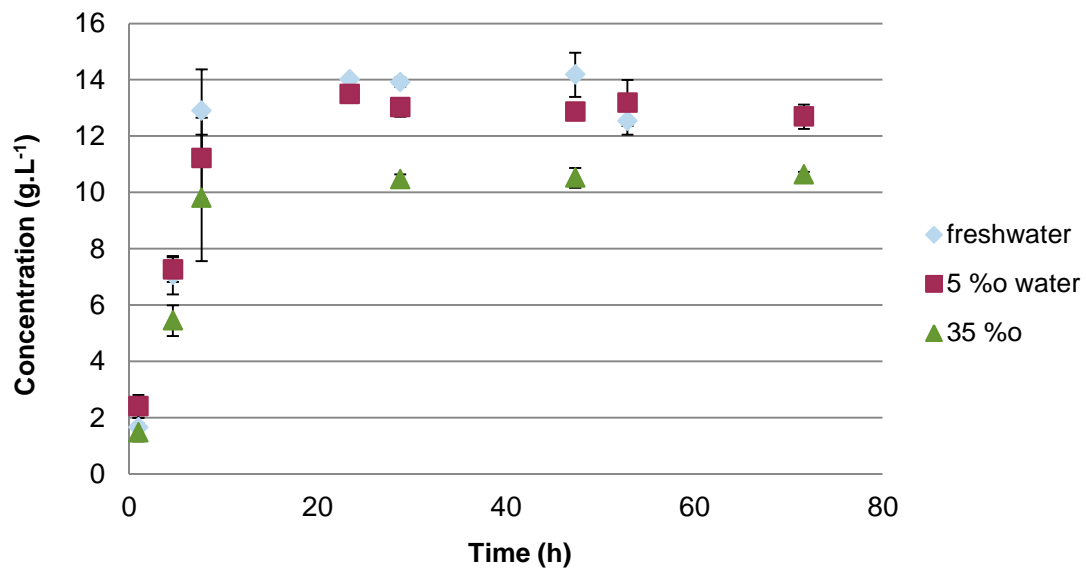


Figure 22 : Concentration of methyl methacrylate by time

PAGE INTENTIONALLY LEFT BLANK

Competition between evaporation and dissolution

PAGE INTENTIONALLY LEFT BLANK

4 Competition between evaporation and dissolution kinetics

This action aims to evaluate experimentally the overall fate of chemicals at the water surface under controlled environmental conditions through the determination of evaporation and dissolution kinetics occurring simultaneously.

4.1 Experimental tool

The “chemical test bench” is the Cedre’s facility used for this part of the project. This tool is made with a cylindrical stainless steel reactor with an internal diameter of 50 cm. As shown on Figure 23, the stainless steel is partially replaced by a curved hardened glass window to visualize the slick of the HNS during experimentations.

The volume of water (fresh or seawater) introduced in the reactor is 80 L. A constant seawater temperature is fixed with the help of a SIEBEC M15 pump connected to a TECO TR20 thermoregulated batch. The set point temperature is adjusted in order to obtain an efficient temperature of 10 ± 1 °C or $20 \text{ °C} \pm 1$ °C, measured with a thermocouple in the reactor.

A constant velocity of wind is applied with the help of a ventilation unit and an Atlantic IP.65 regulator. The actual velocity of wind is recorded with a multisensory anemometer MiniAir20 (Schiltknecht), the sensitive part being placed at about 5 cm above water surface. Air temperature is regulated with the help of a mobile reversible air-conditioning unit CoolMobile E25. A SOL500 lamp from HONLE society, reproducing radiations of sunshine and able to shine the surface of water, is fixed above the reactor but was not used for this study.

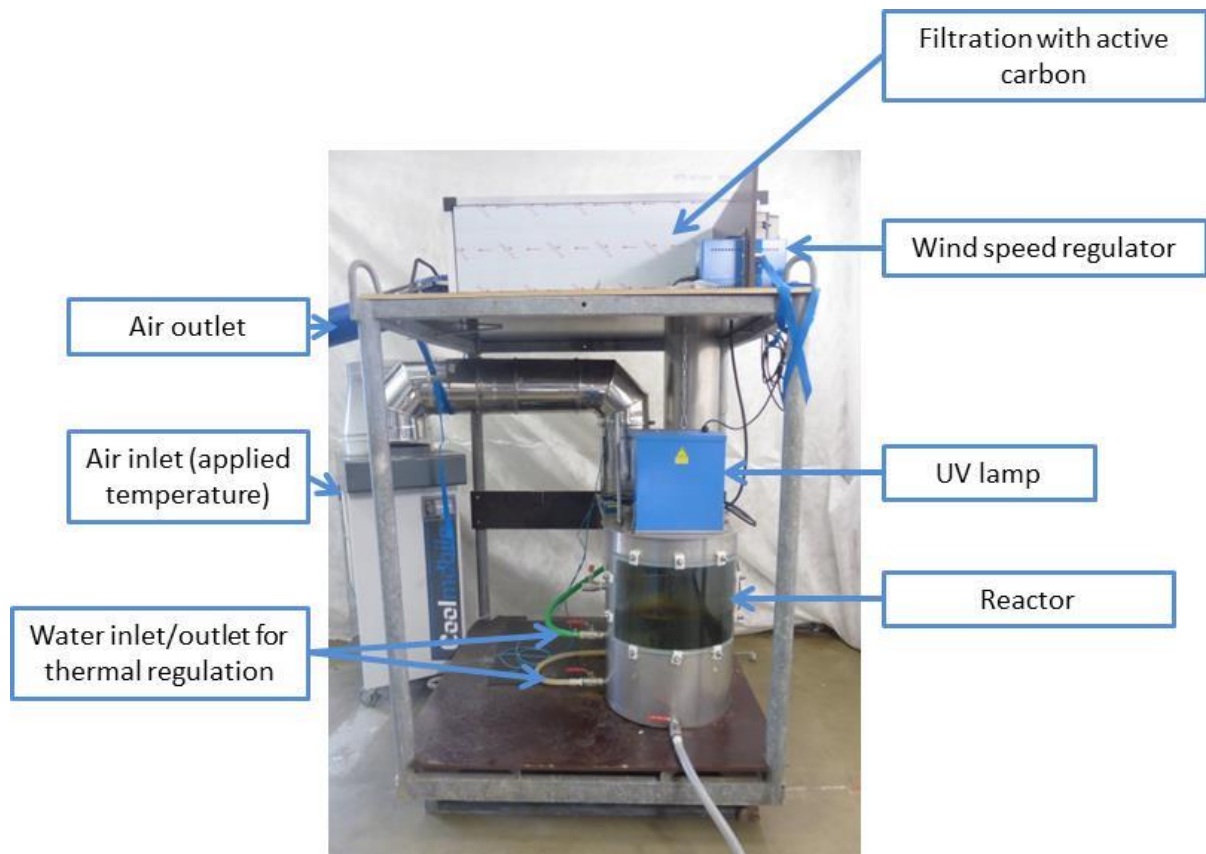


Figure 23: Chemical test bench

4.2 Experimental protocol

The chemical test bench is filled with 80L of natural seawater. Six environmental conditions are tested, 3 wind velocities and 2 temperatures defined as follow:

- Three levels were chosen: $0.40 \pm 0.1 \text{ m.s}^{-1}$, $3.0 \pm 0.07 \text{ m.s}^{-1}$ and $6.9 \pm 0.10 \text{ m.s}^{-1}$. It is not possible to obtain 0 m.s^{-1} because of the evacuation of the vapors emanating from the slick. The second wind velocity corresponds to 2 on the Beaufort scale which means a light breeze. The last wind velocity corresponds to 4 on the Beaufort scale which means moderate breeze.
- The temperatures tested are $20 \pm 1^\circ\text{C}$ and $10 \pm 1^\circ\text{C}$.

When the temperature is stabilized in the tank, 150mL of HNS are gently spilled at the surface to form a slick. The fate processes are evaluated by:

- Continuous measurements of the concentration of HNS in the atmosphere above water thanks to a Photo Ionization Detector (PID) MiniRAE 3000 equipped with a lamp of 10.6eV. The calibration is performed with isobutylene and a factor of correction is

applied, correlated with HNS studied. The air admission tip is placed 10cm above surface water and an average measure is recorded every 10s. In first approximation, we consider that HNS slick has disappeared when the signal of PID tends to 0.

- Water sampling 1 hour, 3 hours, 5 hours, 7 hours and 8.5 hours after the release of HNS. A volume of 10mL is sampled always at the same depth (around 22cm below the surface). The samples are then analysed following the same methods as the water samples of the solubilisation tests (paragraph 3.2).
- Slick sampling at the end of the test (if a slick is still remaining). Before the spillage, an internal standard is added to the HNS and its concentrations, analysed in GC-FID, at the beginning and the end of the test are compared to evaluate the persistence of the slick.

The protocol has been performed on 10 HNS listed in Table 12.

Table 12 : List of the HNS tested in the chemical test bench

HNS	CAS number	SEBC
1-nonanol	2430-22-0	F
2,2,4-Trimethyl-1,3-pentanediol-1-isobutyrate (Texanol®)	25265-77-4	F
2-ethylhexanoic acid	149-57-5	FD
2-ethylhexyl acrylate	103-11-7	F
Butyl acetate	123-86-4	FED
Butyl acrylate	141-32-2	FED
Heptane	142-82-5	E
Pentane	109-66-0	E
Toluene	108-88-3	E
Xylene	1330-20-7	FE

4.3 Results

First, the evaporation and dissolution processes are discussed separately even if they are occurring simultaneously. Then, a global presentation of the fate of HNS is proposed.

The experimental data are given in Annexes (1 to 10).

4.3.1 Evaporation process

Impact of the wind velocity

The evaluation of the impact of the wind velocity on the evaporation process is presented through the example of butyl acetate (FED in the SEBC classification). The concentrations of butyl acrylate in the atmosphere for the tests realized at 20 °C and the 3 wind conditions are presented in Figure 24.

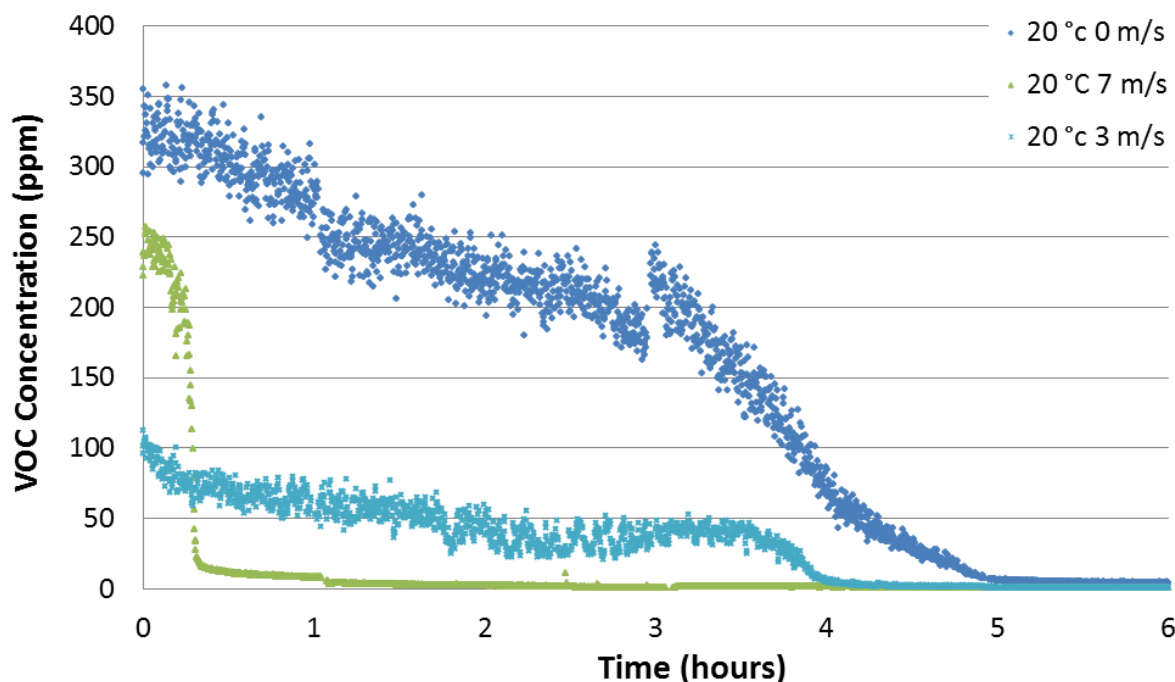


Figure 24: Atmospheric concentrations of butyl acrylate at 20°C for three wind conditions

Without wind, the vapours of butyl acrylate are remaining above the slick (higher density than air) and so the concentration of VOC is higher than for the other wind conditions. This result is of major importance for first responders in case of an accident in low ventilated places (interior of a ship for example).

The evaporation is faster with stronger wind conditions. Without wind, the slick disappears 5 hours after the spillage. The persistence of the slick lasts 4 hours with a wind velocity of 3 m.s⁻¹ and only 1 hour with a wind velocity of 7 m.s⁻¹. In fact, the wind induces a renewal of the air that favors the evaporation process.

Moreover, the concentrations in butyl acrylate are 2.5 times higher at the beginning of the test with a wind velocity of 7 m.s⁻¹ than with a wind velocity of 3 m.s⁻¹. To conclude, the evaporation is faster and more intense for high wind velocities.

Impact of the temperature

The evaluation of the impact of the temperature on the evaporation process is presented through the example of xylenes (FE in the SEBC classification). The concentrations of xylenes in the atmosphere for the tests realized at a wind velocity of 3 m.s⁻¹ at 10 and 20 °C are presented in Figure 25.

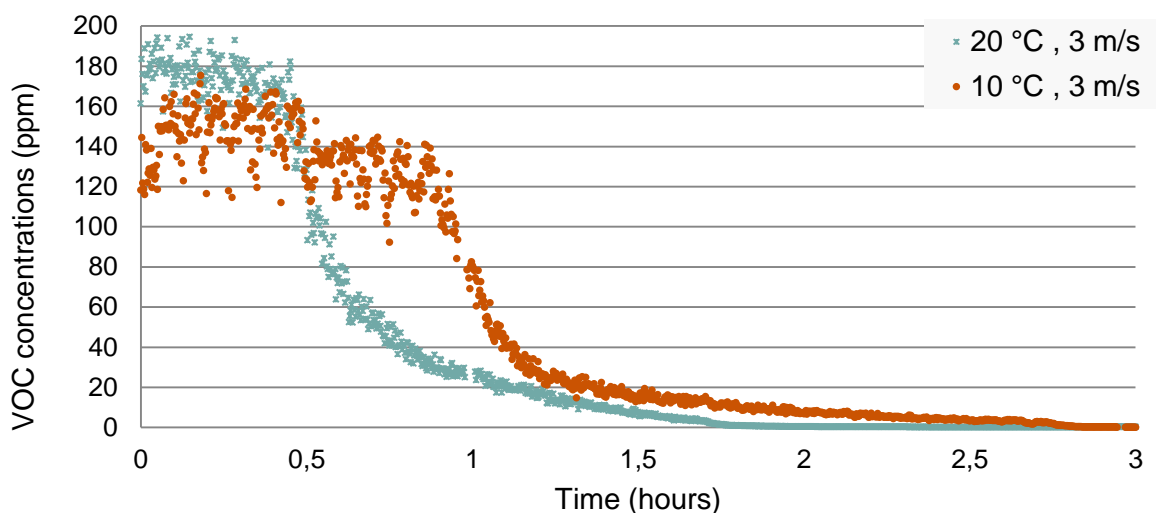


Figure 25: Atmospheric concentrations of xylenes at 10 and 20°C for a wind velocity of 3m.s⁻¹

For an intermediate wind velocity (3m.s⁻¹), the measured concentrations of xylenes in the atmosphere are higher at 20°C than at 10 °C. Moreover, the evaporation is faster for the highest temperature regarding the persistence of the slick. To conclude, the evaporation is favoured by an increase in temperature.

4.3.2 Dissolution process

Impact of the wind velocity

The wind velocity directly impacts the surface agitation in the chemical test bench. To evaluate the influence of it on the dissolution process, the example of 2-ethylhexanoic acid (FD in the SEBC classification) is presented. The concentrations in the water of this acid at 10°C and for the three wind velocities are shown in Figure 26.

The dissolution is much higher with a wind velocity of 7 m.s⁻¹ than for the other conditions. In fact, the maximum concentration reached is around 1.4g.L⁻¹ compared to 0.4g.L⁻¹ reached with the other wind velocities. Also, the maximum concentration is reached much faster with the stronger wind: the maximum is reached 3 hours after the spillage for 7 m.s⁻¹ whereas the maximum does not seem to be reached yet at the end of the test for the lower wind velocities.

These results could be explained by the surface agitation induced by the wind velocity. In fact, a stronger wind implies a much more agitated surface and so a more important contact between the water and the HNS which clearly favour the dissolution process. To conclude, the dissolution is favoured by an increase in wind velocity.

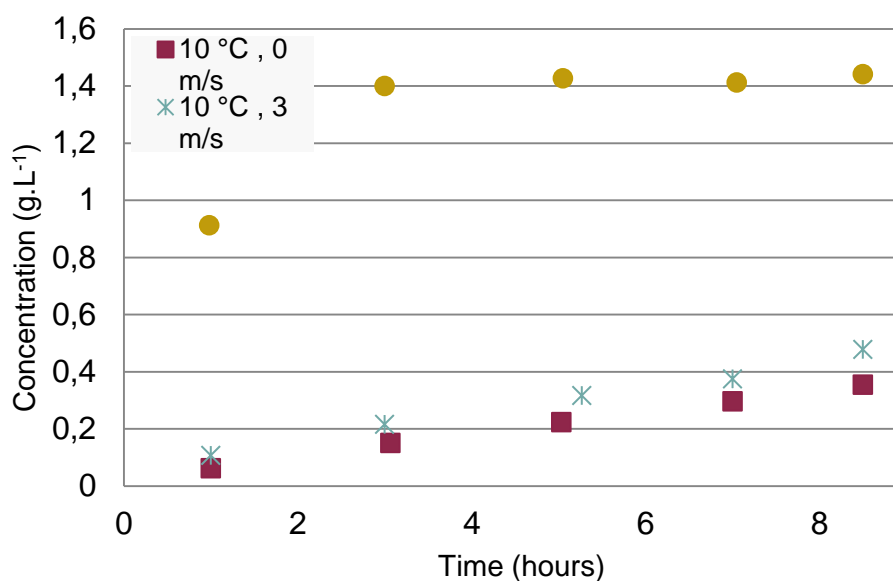


Figure 26: Water concentrations of 2-ethylhexanoic acid at 10°C for three wind velocities

Impact of the temperature

The temperature can have two kinds of influence on the dissolution process: direct and indirect.

To evaluate the direct effect of the temperature on the dissolution process, the 2-ethylhexanoic acid (FD) is taken as an example (Figure 27). The concentrations in water are slightly higher at 20°C compared to 10°C (less than 3%). As this HNS does not evaporate, the slick remains during the entire test and the only process occurring is the dissolution. To conclude, the dissolution is generally more important for higher temperatures.

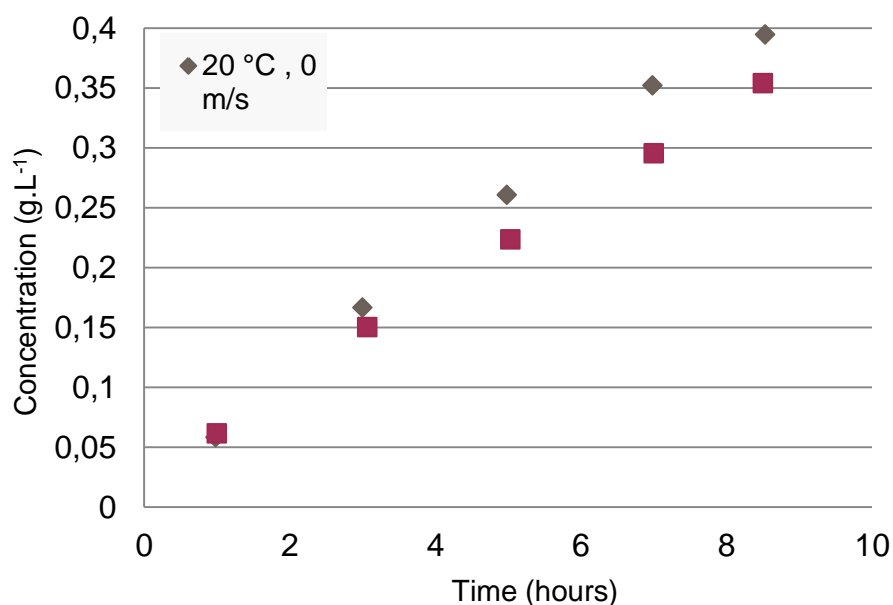


Figure 27: Water concentrations of 2-ethylhexanoic acid without wind at 10 and 20°C

To evaluate the indirect influence of the temperature on the dissolution, butyl acetate (classified as FED in the SEBC) is taken as example. The concentrations of butyl acetate in water at 10 and 20°C for an intermediate wind velocity ($3\text{m}\cdot\text{s}^{-1}$) are given in Figure 28.

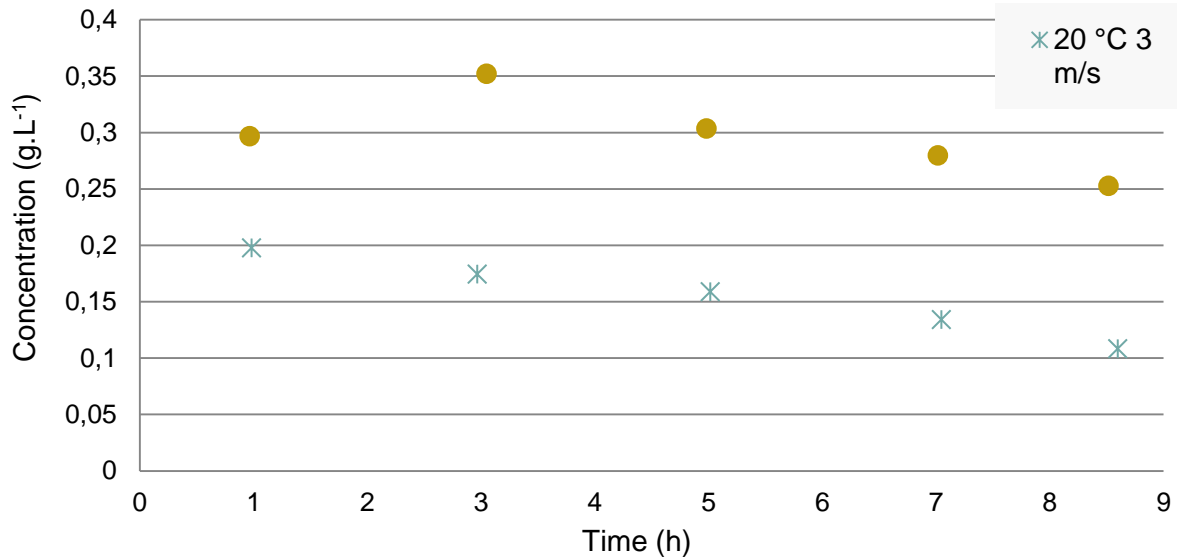


Figure 28: Water concentrations of butyl acetate at 10 and 20°C and $3\text{m}\cdot\text{s}^{-1}$

The concentrations in water are higher for the 10°C condition which can be surprising at first. In fact, as butyl acetate is FED, evaporation and dissolution of the product occur simultaneously. At 20°C, the evaporation process is favoured by the temperature and so butyl acetate evaporates faster. As the slick disappears quickly, the contact time between the HNS and water is lowered and the dissolution is less important. For colder temperature, the dissolution is favoured due to a lower evaporation of the HNS. This phenomenon is also explained by the kinetics of the two processes: evaporation is a fast process whereas dissolution has a lower kinetic.

After the disappearance of the slick, the concentration of butyl acetate decreases in the water for both temperature conditions. This can be explained by the evaporation of the HNS directly from the water column.

4.3.3 Overall fate

The overall fate of an HNS can be represented by normalized mass balance expressed versus time. An extrapolation of the plot of PID measurements, assimilated to a straight line, allows determining the time when the slick is supposed to have totally disappeared. From that point, the amount of product evaporated is deducted from the total initial amount of product minus the amount dissolved in water, the latter being calculated with the concentration of the dissolved fraction in seawater.

This graphic representation is given for butyl acetate in Figure 29 and for the other tested HNS in Figure 30 to Figure 38. On Figure 29, it can be noticed that the concentration of the dissolved part always go through a maximum. This shows that the process occurring in the reactor can be divided in two phases. At the beginning of the experimentation, the chemical is progressively and simultaneously dissolved in seawater and evaporated in the atmosphere. This part is interesting as it reflects the competition between mass transfer processes of dissolution versus evaporation. Then, when the gradient of concentration between chemical dissolved in seawater and the surface is reversed (absence of slick), the dissolved fraction can diffuse to the surface and evaporate. It can also be noticed that, at fixed temperature, the minimum amount of chemical dissolved in seawater corresponds to the 3 m.s^{-1} velocity of wind. At a higher velocity of wind, surface agitation promotes dissolution during first hours.

The results obtained also allow roughly quantifying the performance and evolution versus time of each process depending on the experimental conditions. Thus, during the first minutes or hours after HNS is spilled, temperature regulates the maximum amount of product evaporated, higher at $20 \text{ }^{\circ}\text{C}$, while the velocity of wind promotes directly the kinetic of evaporation.

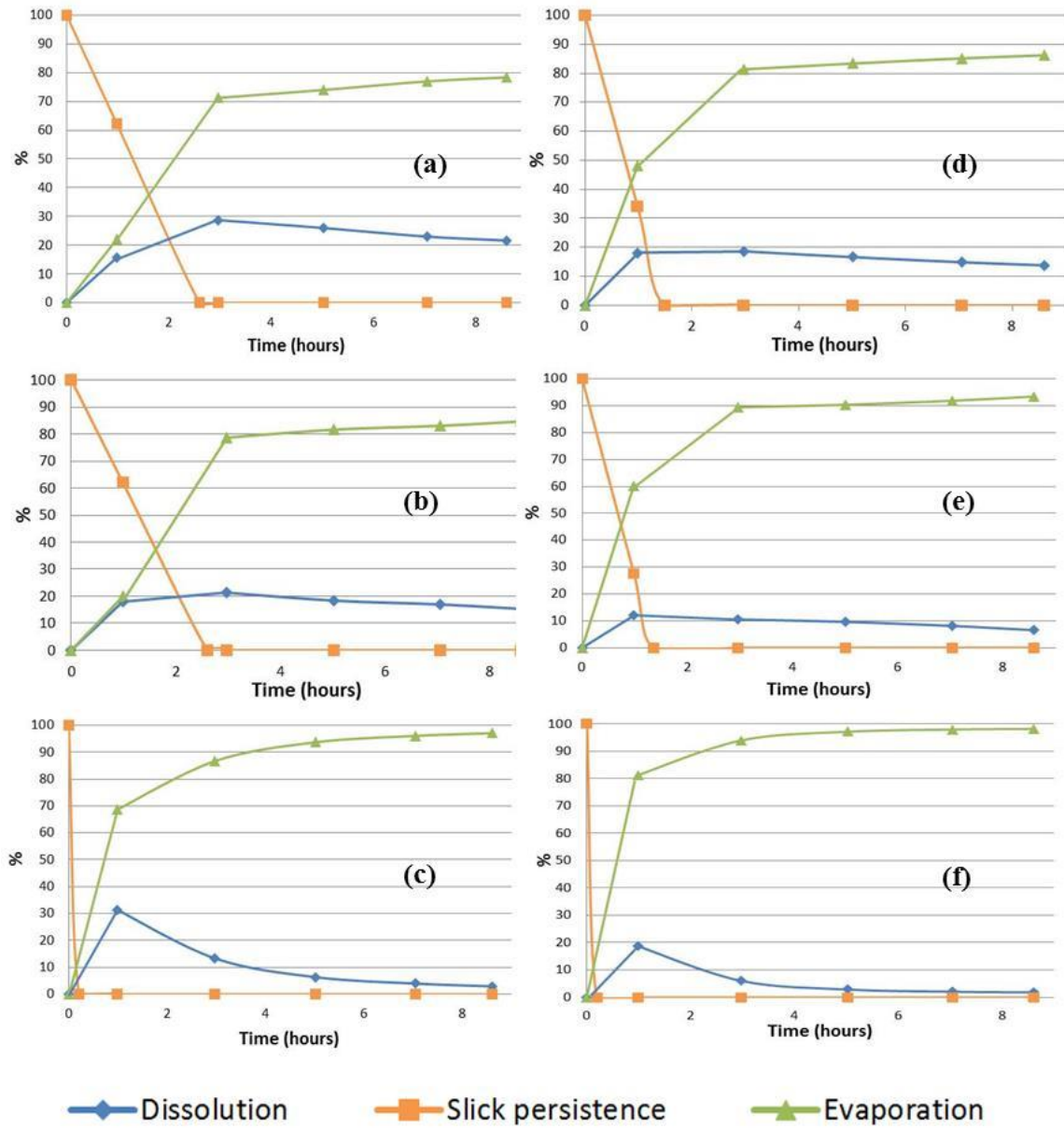


Figure 29: Normalized material balance of Butyl acetate dissolved in seawater, remaining as a slick or evaporated at wind velocities of 0; 3 and 7 m.s⁻¹ at 10°C (a, b, c) and 20°C (d,e,f)

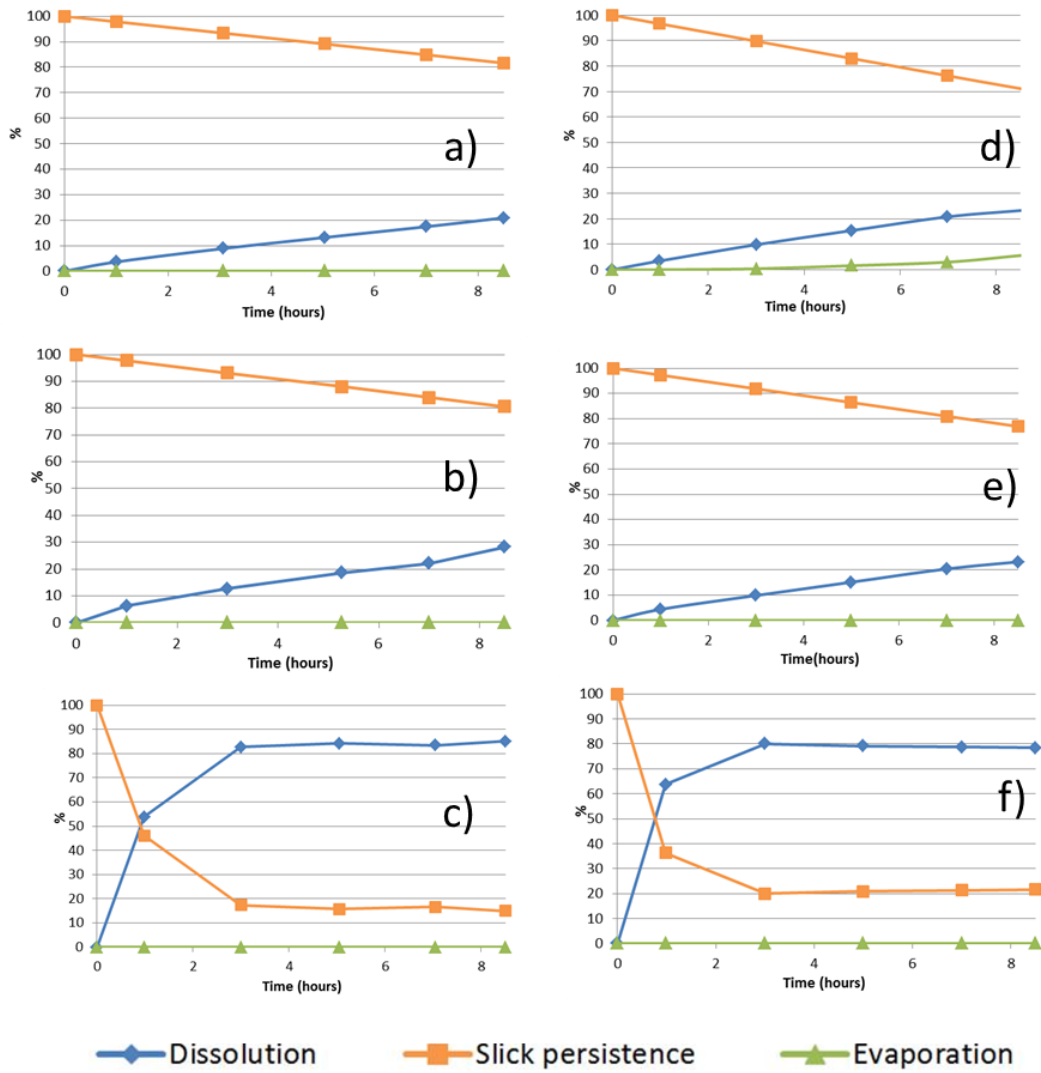


Figure 30: Normalized material balance of 2-ethylhexanoic acid dissolved in seawater, remaining as a slick or evaporated at wind velocities of 0; 3 and 7 m.s⁻¹ at 10°C (a, b, c) and 20°C (d,e,f)

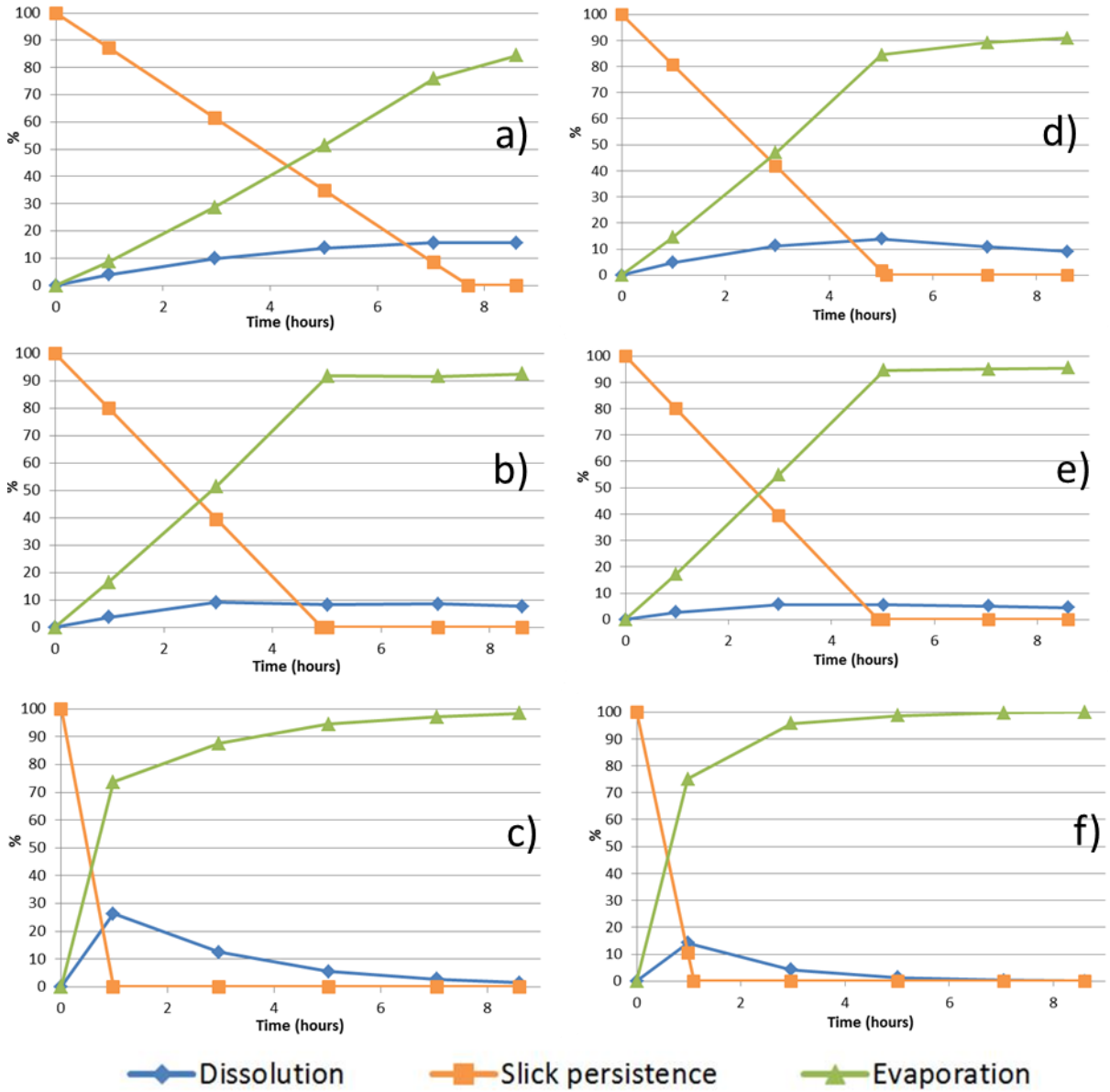


Figure 31: Normalized material balance of Butyl acrylate dissolved in seawater, remaining as a slick or evaporated at wind velocities of 0; 3 and 7 m.s⁻¹ at 10°C (a, b, c) and 20°C (d,e,f)

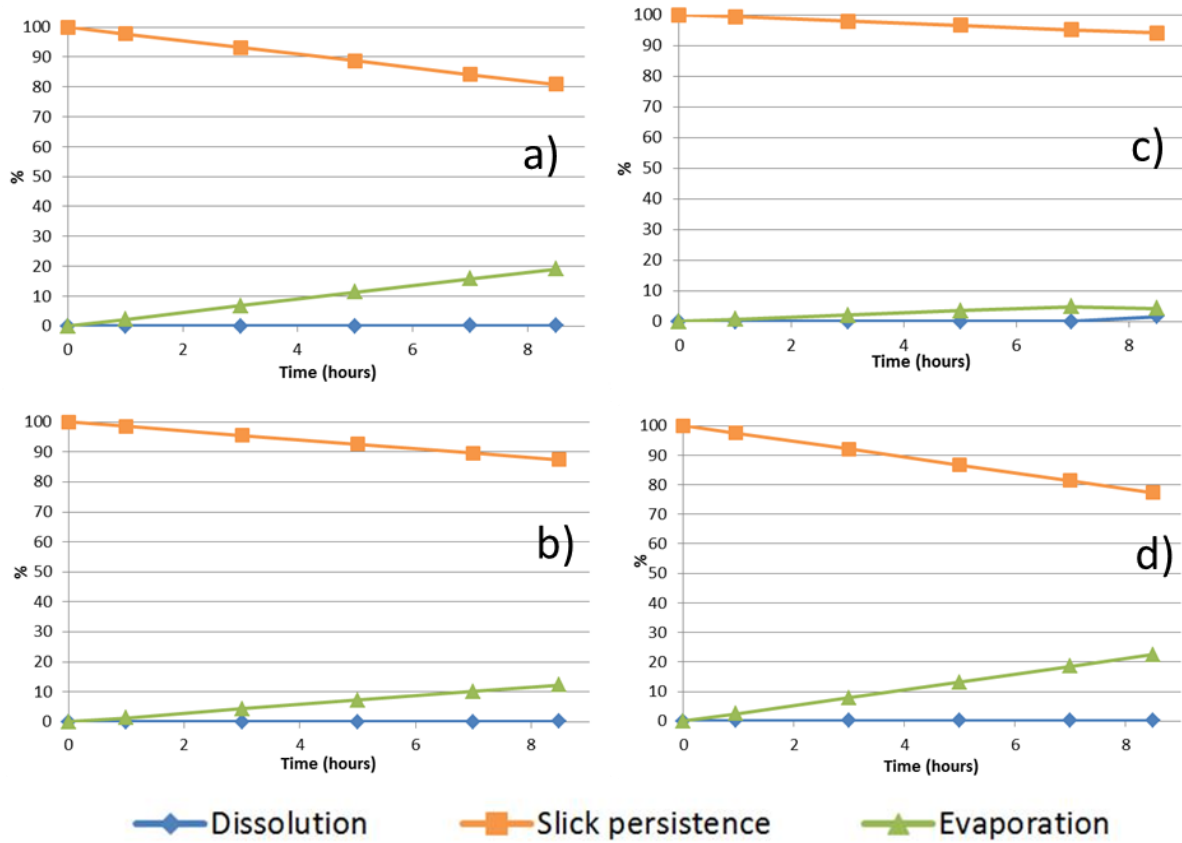


Figure 32: Normalized material balance of 2-ethylhexyl acrylate dissolved in seawater, remaining as a slick or evaporated at wind velocities of 0 and 3 m.s⁻¹ at 10°C (a, b) and 20°C (c, d)

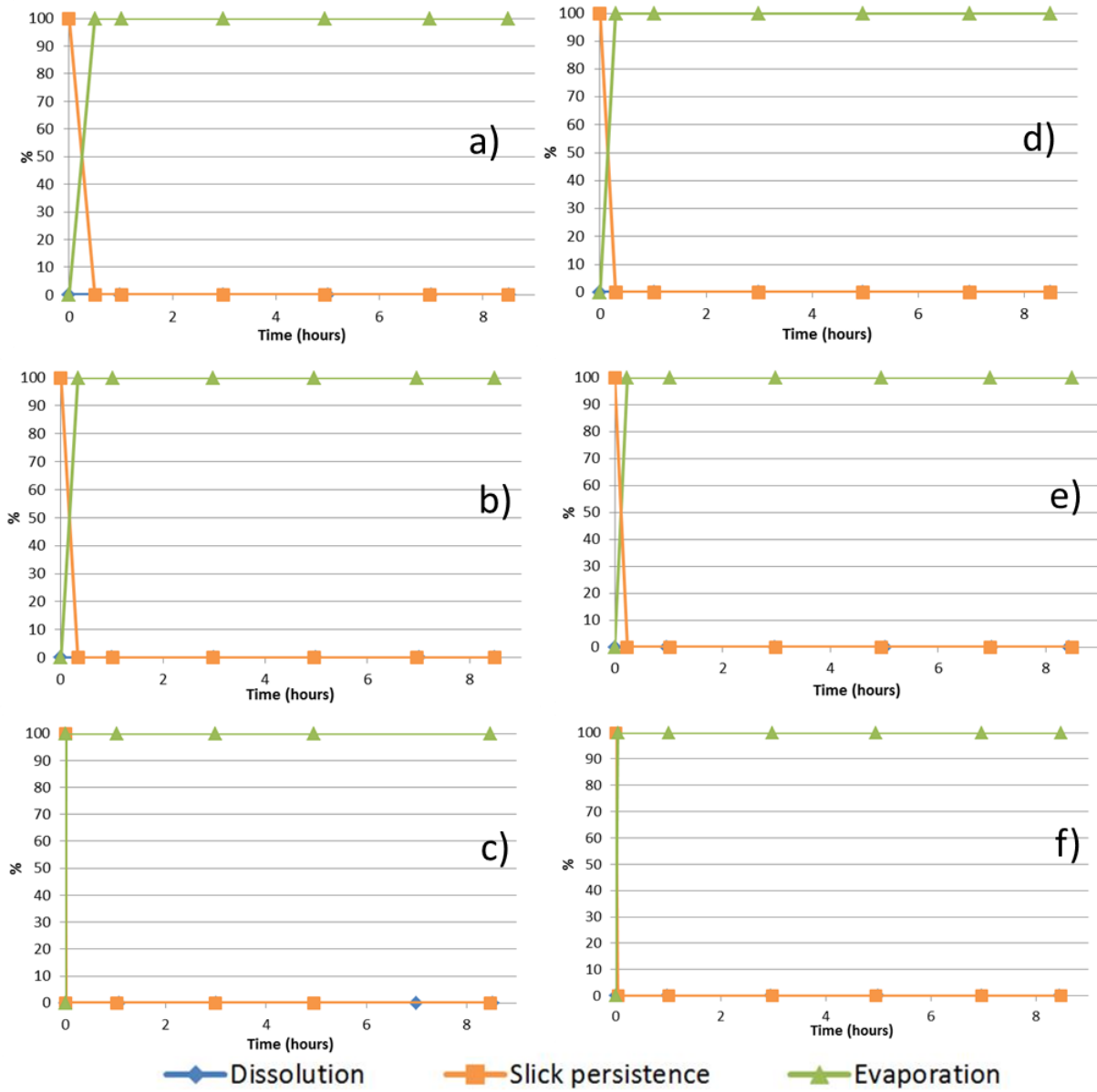


Figure 33: Normalized material balance of Heptane dissolved in seawater, remaining as a slick or evaporated at wind velocities of 0; 3 and 7 m.s⁻¹ at 10°C (a, b, c) and 20°C (d,e,f)

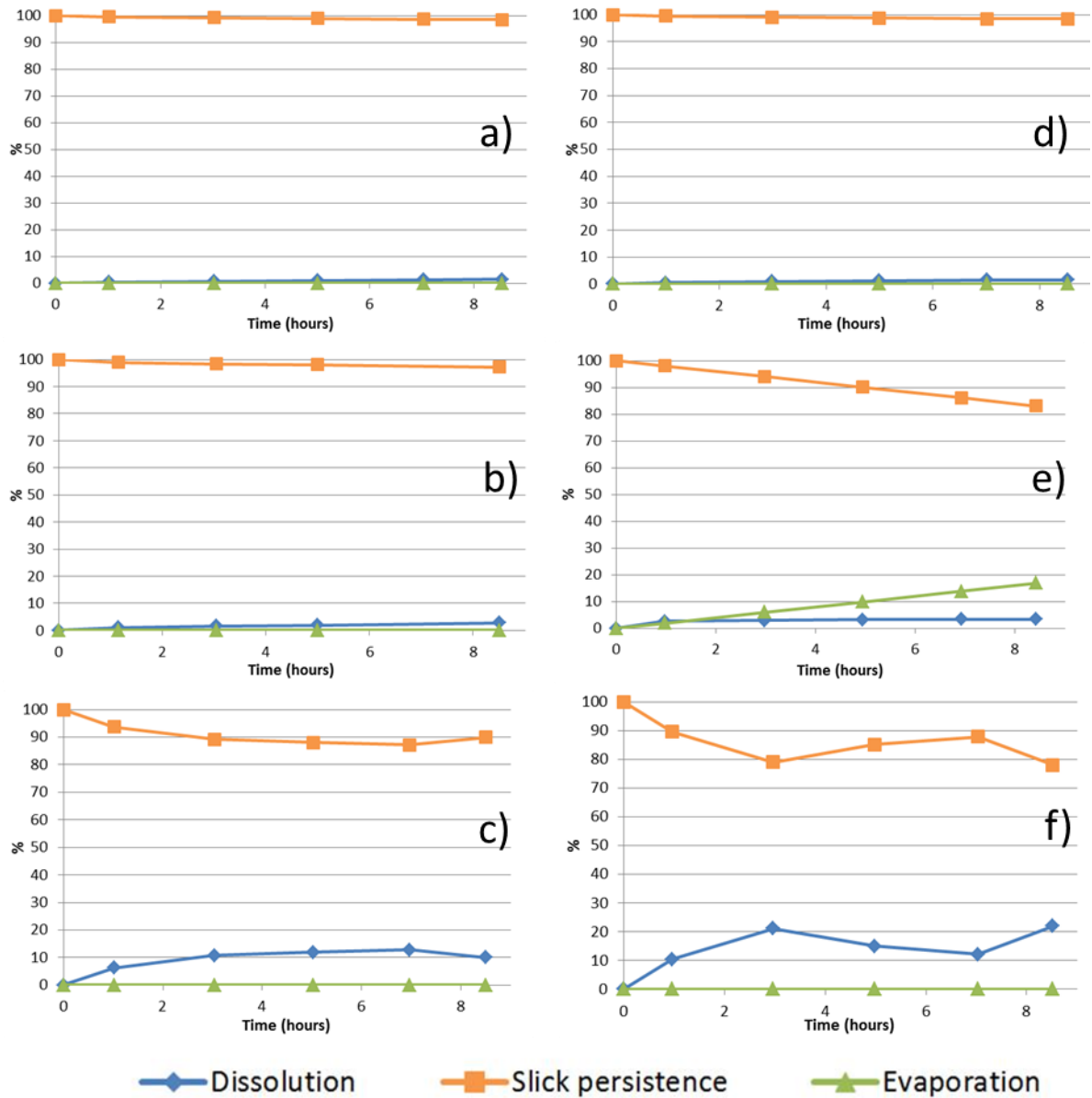


Figure 34: Normalized material balance of n-nonanol dissolved in seawater, remaining as a slick or evaporated at wind velocities of 0; 3 and 7 m.s⁻¹ at 10°C (a, b, c) and 20°C (d,e,f)

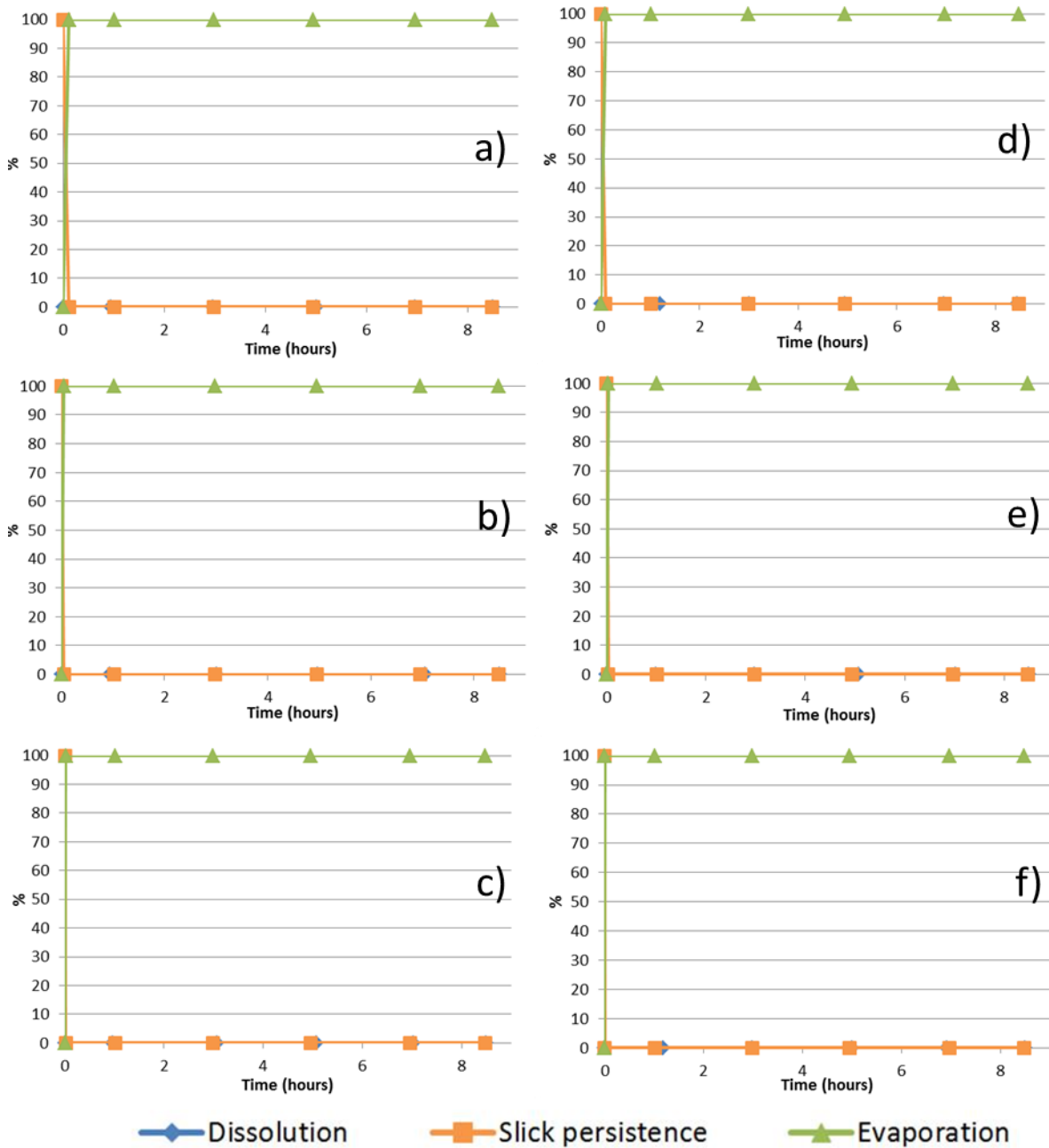


Figure 35: Normalized material balance of Pentane dissolved in seawater, remaining as a slick or evaporated at wind velocities of 0; 3 and 7 m.s⁻¹ at 10°C (a, b, c) and 20°C (d,e,f)

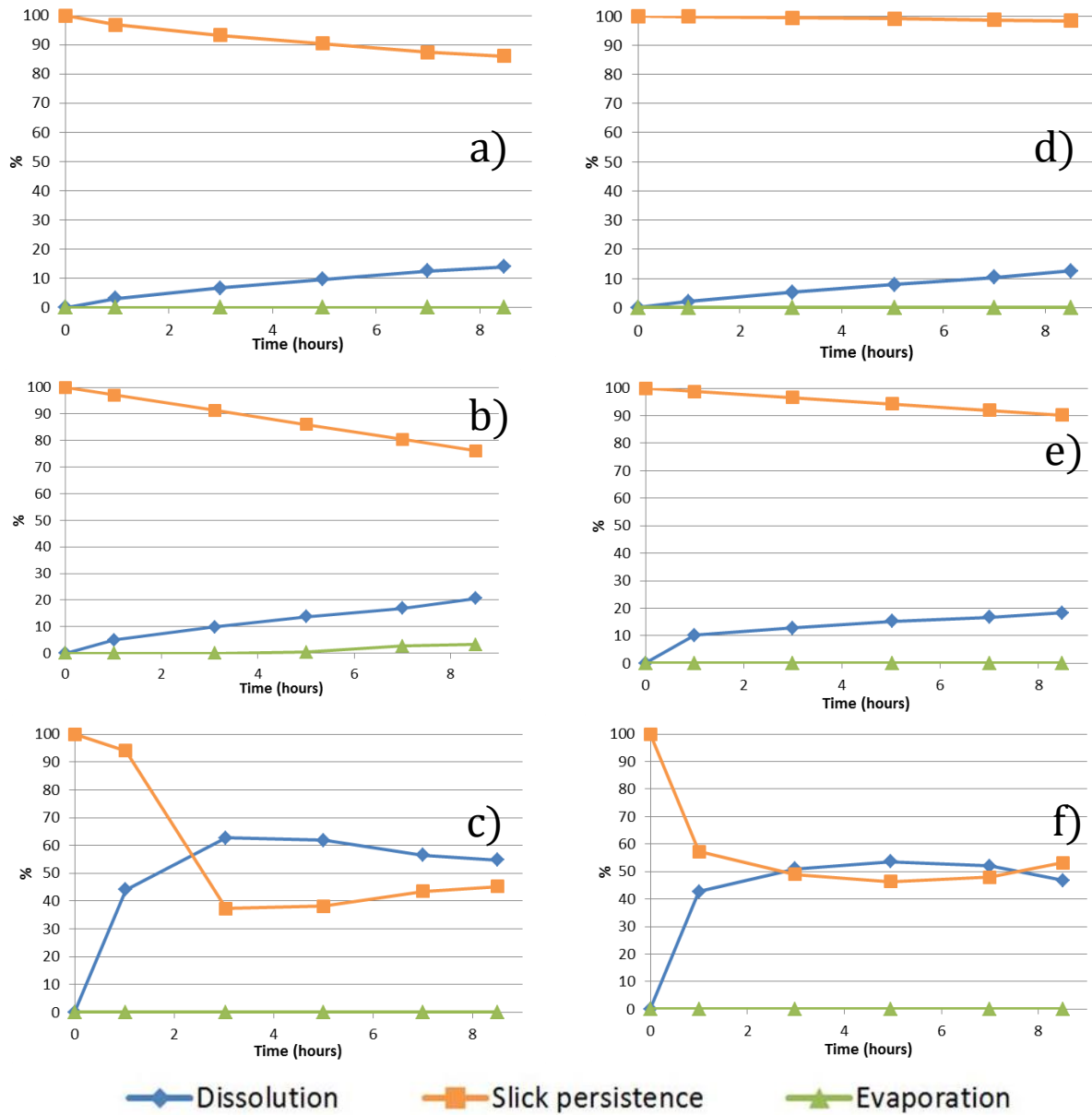


Figure 36: Normalized material balance of Texanol@ dissolved in seawater, remaining as a slick or evaporated at wind velocities of 0; 3 and 7 m.s⁻¹ at 10°C (a, b, c) and 20°C (d,e,f)

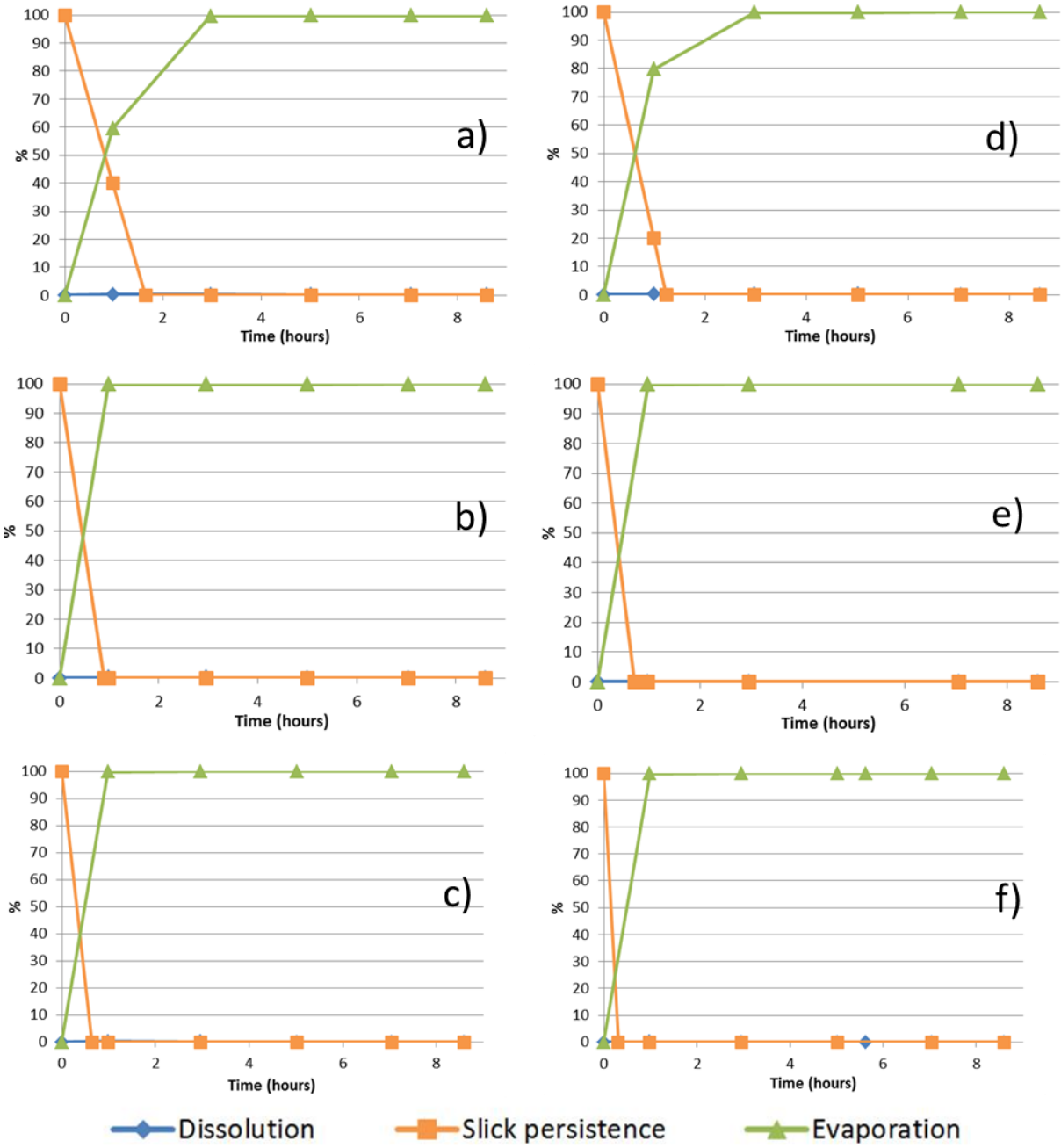


Figure 37: Normalized material balance of Toluene dissolved in seawater, remaining as a slick or evaporated at wind velocities of 0; 3 and 7 m.s⁻¹ at 10°C (a, b, c) and 20°C (d,e,f)

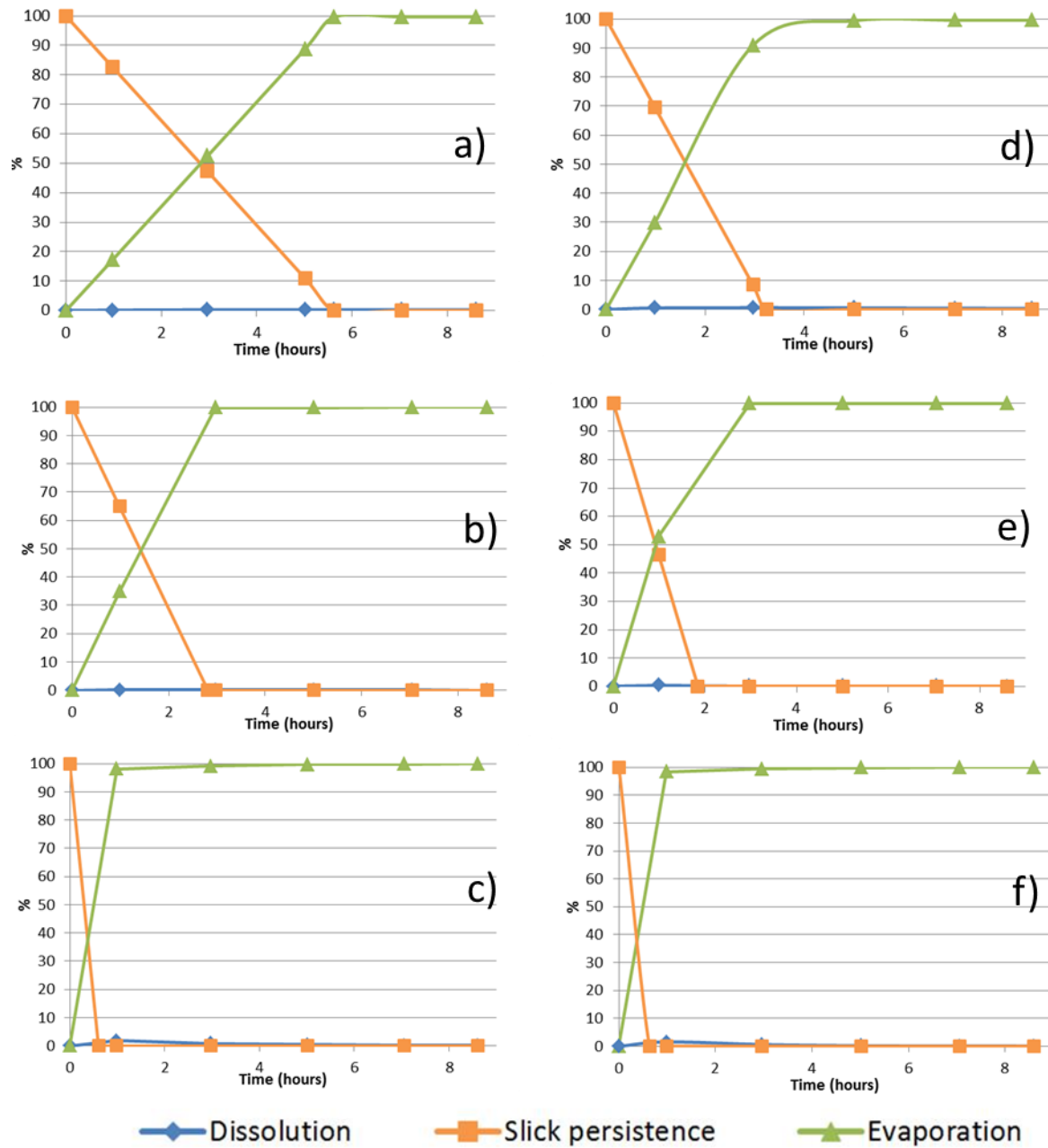


Figure 38: Normalized material balance of Xylenes dissolved in seawater, remaining as a slick or evaporated at wind velocities of 0; 3 and 7 m.s⁻¹ at 10°C (a, b, c) and 20°C (d,e,f)

HNS behaviour in the water column

PAGE INTENTIONALLY LEFT BLANK

5 HNS behaviour in the water column

5.1 Introduction

5.1.1 Behaviour of chemicals in water

Up to now, the international regulations governing the carriage of Hazardous and Noxious Substances (HNS) are based on a theoretical evaluation of the chemical behaviour, through the Standard European Behaviour Classification (SEBC) (Figure 39). SEBC categorizes chemicals on their theoretical behaviour in water, the sinking product (S), the floating products (F), dissolving product (D), the evaporating product (E) or a combination of two or three of these behaviours (Bonn Agreement, 1994). This classification contributes to define two major international regulations, as the IBC Code (IMO, 2007), which defines the type of ship that may carry a given substance; or the MARPOL classification (IMO, 2006), which assesses the impact of these substances on the marine environment in case of spillage. However, the SEBC code is based on physico-chemical properties (density, water solubility and vapour pressure) of substances to determine the typical behaviour following a spill. These properties are obtained in the laboratory using standard protocols; for example, solubilisation is characterized at saturation concentration in fresh water, it is measured at 20°C and atmospheric pressure. This definition does not take into account the time factor and meteorological conditions, which are the critical parameters during shipwreck (Le Floch et al. 2010). According to Xie et al. (1997) solubilisation in salt water is about two times slower than in fresh water. Thus the parameters used to classify chemicals in the SEBC are far from those encountered at sea during a marine accident. If the SEBC may provide an initial answer, operational in charge of the accident can criticize its reading to assess whether the specific environment of the accident will change or not the result.

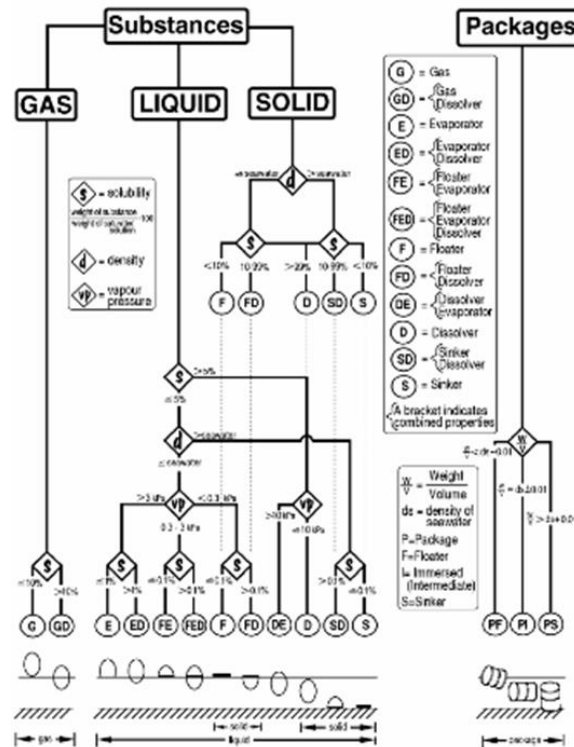


Figure 39: Characterization of substances behaviour discharged into seawater according to the Standard European Behaviour Code (SEBC) (Bonn Agreement 1994)

The objectives of the present document are to propose a general droplet distribution law for underwater massive release of chemical and, for various products, a validation of the velocity correlation for droplet rising in seawater and an estimation of mass transfer coefficients.

5.1.2 Droplet size distribution at breach level

When a ship sinks with a breach both in the hull and in a cargo tank containing floating chemicals, leakage causes an ascending plume of substances toward the surface. The release of a floating liquid from a vessel aground on the seabed generally corresponds to a release without injection speed and depends only on the fluid properties⁴. The released liquid leads to the formation of droplets directly at the orifice or at the end of a cylindrical jet. The knowledge of the droplets size distribution is then necessary to determine their fate in the water column (rising velocity and dissolution kinetic). Droplet diameters depend on their mode of formation, which directly depends on the liquid ejection velocity of the liquid at the breach level. The release rate, hydrodynamics and dissolution rate of the chemicals are issues which should be considered to assess the volume of product reaching the surface.

⁴ L. Aprin, Modelisation of draining mechanism for submerged vessel filled with chemical, *HNS-MS-TaskD-Report on draining model_20160723*.

The released liquid in other fluids leads to the formation of drops directly at the orifice or at the end of a cylindrical jet. The knowledge of the droplets size distribution is necessary to determine their fate in the water column (rising and solubilisation velocity). Drops diameters depend on their mode of formation, which directly depends on the liquid ejection velocity of the liquid at the breach level. Grant (Grant and Middleman 1966) observed three different modes of droplets rupture which depend on flow rate and system properties (Figure 40):

- Dripping mode (1): For very low ejection speeds, the drops are formed at the orifice, they have homogeneous size proportional to the size of the orifice;
- Jetting mode (2): As velocity increases, a jet is formed. Surface tension forces are dominant and the surface of the jet undergoes disturbances that form drops of different sizes;
- Atomization (3): For very high ejection speed, the influence of the surface tension forces decreases, the hydrodynamic forces become dominant: the jet disintegrates into droplets directly at the orifice.

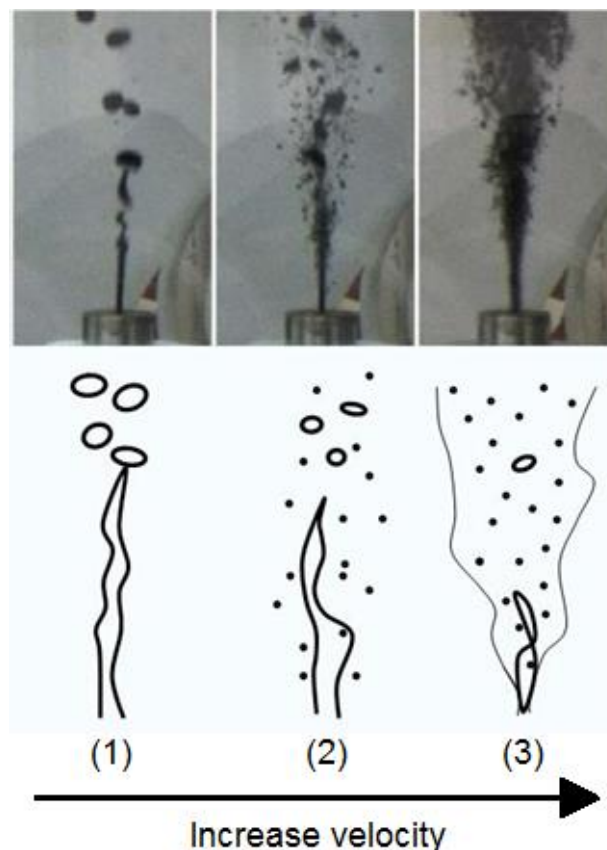


Figure 40: Illustration of the different modes of droplets formations at orifice level

In the present document, studies were performed on chemical releases without or with very low injection speed, which leads to the dripping or the jetting mode.

5.1.3 Dripping mode

For a single droplet formed directly at the injection nozzle level, the droplet volume is defined by the following relationship of Horvath et al. 1978.

$$V = \frac{\Psi \pi \sigma d_{or}}{g \Delta \rho} \quad (1)$$

$$\Psi = 0,6 + 0,4 \exp \left(-2 d_{or} \left(\frac{g \Delta \rho}{\pi \sigma d_{or}} \right)^{\frac{1}{3}} \right) \quad (2)$$

With V the droplet volume (m^3), σ the interfacial tension ($N.m^{-1}$), g the gravitational acceleration ($m.s^{-2}$), ρ de chemical density ($kg.m^{-3}$) and d_{or} , the orifice diameter (m)

5.1.4 Jetting mode

In case of jetting mode, no model exists to characterize the droplet size distributions. However, (Clift, Grace et al. 1978) give a definition to estimate the maximum diameter of a droplet according to its physicochemical properties (4).

$$\text{For } k = \frac{\mu_d}{\mu_c} > 0.5 \quad (3)$$

$$d_{frag} \approx 4 \sqrt{\frac{\sigma}{g \Delta \rho}} \quad (4)$$

5.1.5 Rising velocity of chemical droplet in seawater

One of the most important parameter for liquid droplets rising in a water column is the slip velocity U_s . It represents the velocity difference between rising droplets and the surrounding liquid. The most commonly used law to calculate U_s is based on the Stokes law. The smallest single isolated droplets are approximately perfect spheres due to the dominant effect of surface tension on their shape. This law remains validate as the particles keep small, spherical, rigid and for Reynolds number smaller than unity, i.e. laminar terminal velocity. Strictly speaking this assumption is not available for larger and more turbulent particles. The velocities are then representative for small and large fluid particles where the viscosity of ambient fluid is a

fundamental factor for the smallest, whereas the largest are governed by the equilibrium between the drag and buoyancy forces.

5.1.6 Spherical shape

Clift et al. (1978) have shown that the shape of fluid particles could be approximated by a sphere for the small size range (smaller than 1 mm). In this case; terminal velocity is influenced by the viscosity of the ambient fluid and the slip velocity is calculated by the following equation:

$$V_s = \frac{\mu_w Re}{\rho_w d_e} \quad (5)$$

5.1.7 Ellipsoid shape

For ellipsoid particles varying in the intermediate size range (1 mm to 15 mm), the interfacial tension is the key factor and the droplet velocity can be derived from:

$$V_s = \frac{\mu_c}{\rho_c d} Mo^{-0,149} (J - 0,857) \quad (6)$$

Where

$$J = 0,94H^{0,757} \quad 2 < H \leq 59,3 \quad (7)$$

$$J = 3,42H^{0,441} \quad H > 59,3 \quad (8)$$

$$H = \frac{4}{3} Eo Mo^{-0,149} \left(\frac{\mu_c}{\mu_w} \right)^{-0,14} \quad (9)$$

Where, d is the droplet diameter (m), μ_c is the dynamic viscosity of continue phase (Pa.s); μ_w is the dynamic viscosity of water phase ($\mu_w=9 \cdot 10^{-4}$ Pa.s) ρ_c is the density of continue phase ($\text{kg}\cdot\text{m}^{-3}$). Eo is the Eötvös number measures the importance of surface tension forces compared to body forces. This dimensionless number is used to characterize the shape of bubbles or drops moving in a surrounding fluid.

$$Eo = \frac{g(\rho_l - \rho_d)d_p^2}{\sigma} \quad (10)$$

σ is the interfacial tension ($\text{N}\cdot\text{m}^{-1}$) and ρ_d the droplet density ($\text{kg}\cdot\text{m}^{-3}$).

Mo is a dimensionless number called Morton number and it is used with the Eötvös number to

characterize the shape of bubbles or drops moving in a surrounding fluid.

$$Mo = \frac{g\mu^4\Delta\rho}{\rho^2\sigma^3} \quad (11)$$

5.1.8 Spherical cap

The spherical-cap regime corresponds to the larger size range of droplet.

$$V_s = 0.711 \sqrt{\frac{gd_e^2(\rho_w - \rho_d)}{\rho_w}} \quad (12)$$

The following figure (Figure 41) is a flow map to identify the bubbles or droplets regimes with respect to the Reynolds number based on the Eötvös number for different Morton numbers. It is possible to determine the Reynolds number and therefore the terminal rise velocity of a droplet, from the fluid physicochemical properties analysed through Eötvös and Morton numbers. However, this correlation has a triple logarithmic scale, which can lead to inaccuracies in the obtained velocity.

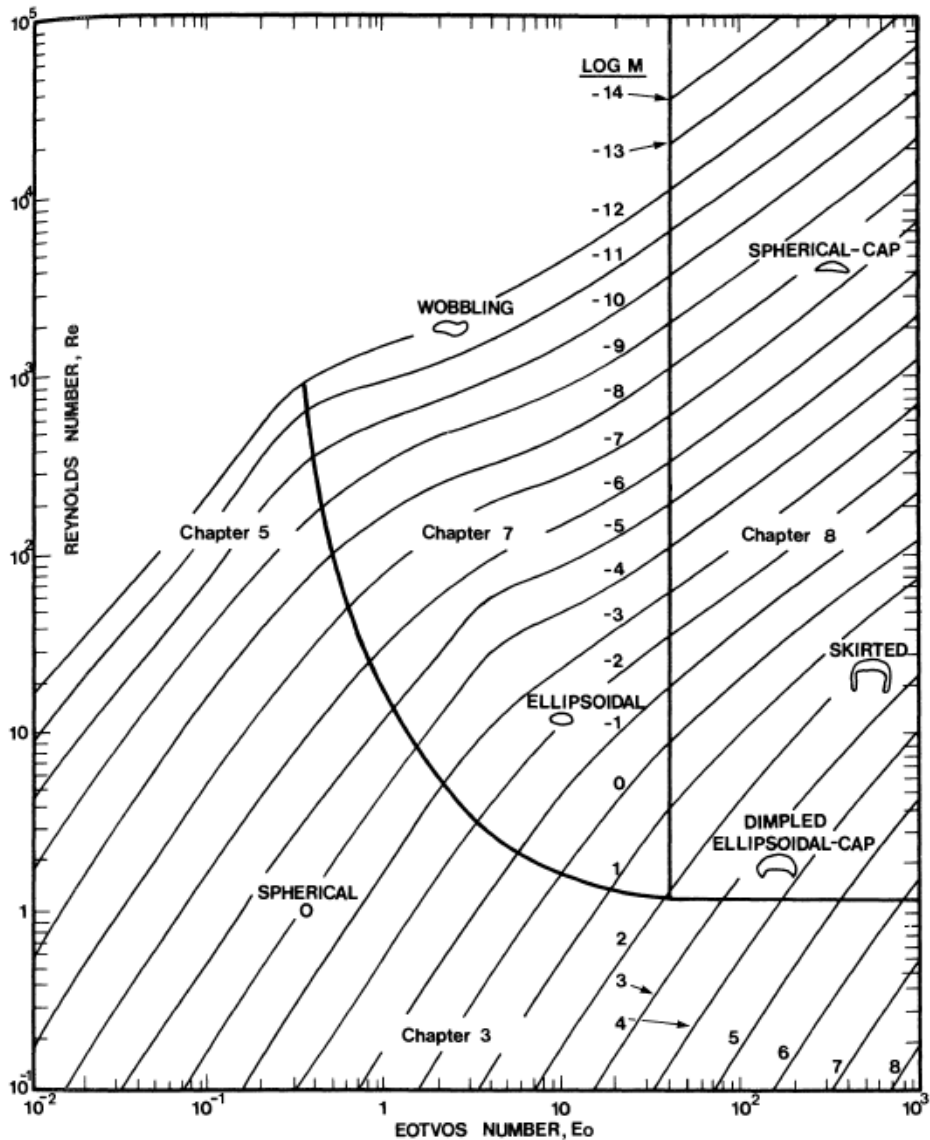


Figure 41: Shape regimes for bubbles and droplets in gravitational motion through liquids (Clift, 1978)

5.1.9 Solubilisation of chemicals droplets rising in seawater

The variations of miscible droplet rising in the water column have been mainly studied in the gas-liquid transfer (absorption or desorption) and the liquid-liquid transfer (liquid-liquid extraction) for chemical process. The mass transfer between a droplet of pure component and the surrounding water can be positive, negative or even zero if two species are transferred with same mass quantity. The mass transfer is governed by two mechanisms: molecular diffusion and convective transfer (generated by the movement of drops) which is dominant and faster. Several models have been performed about this mass transfer. The double film theory proposed by Whitman (Lewis & Whitman 1924) assumes that the resistance to mass transfer is for each phase in a thin layer on both sides of the interface. The theory of Higbie's penetration (Higbie 1935) suggests that the mass transfer is due to the regeneration of the fluid interface by

turbulence. Danckwerts (Danckwerts 1951) modified this approach by introducing a concept of residence time distribution of the fluid layer at the interface. In 1958, Toor and Marchello (Toor & Marchello 1958) proposed a more general expression called penetration films theory, showing the two previous relations are limiting cases of their general theory.

The double film theory is the most widely used despite the rudeness of the concept. The mathematical formulation is simple and the results are consistent with those of more complex theory. This model assumes that the resistance to mass transfer is for each phase in a thin layer on either side of the interface. It considers that there is, in each phase in the surrounding of the interface, a stationary film in which lies a resistance to mass transfer. The transfer material in these films is assumed to be diffusive. Concentrations outside films are assumed to be homogeneous and equal to a reference value (e.g. zero). The double film theory assumes that the material transfer coefficient k in one phase is inversely proportional to the film thickness δ ($k = D/\delta$ with D the diffusion coefficient).

At the interface, the mass transfer flux J can be written

$$J = K_c \cdot \Delta C \quad (13)$$

Where K_c is the mass transfer coefficient ($\text{m}\cdot\text{s}^{-1}$), ΔC is the difference between the concentration upstream and downstream of the interface. Then in the case of mass transfer from droplet to water, the mass transfer flux can be written as:

$$J = K_c \cdot (C_i - C_0) \quad (14)$$

Where C_i is the concentration of the migratory species at the interface, on the dispersed phase side and C_0 is the minimum concentration in the continuous phase (i.e 0 in the present study)

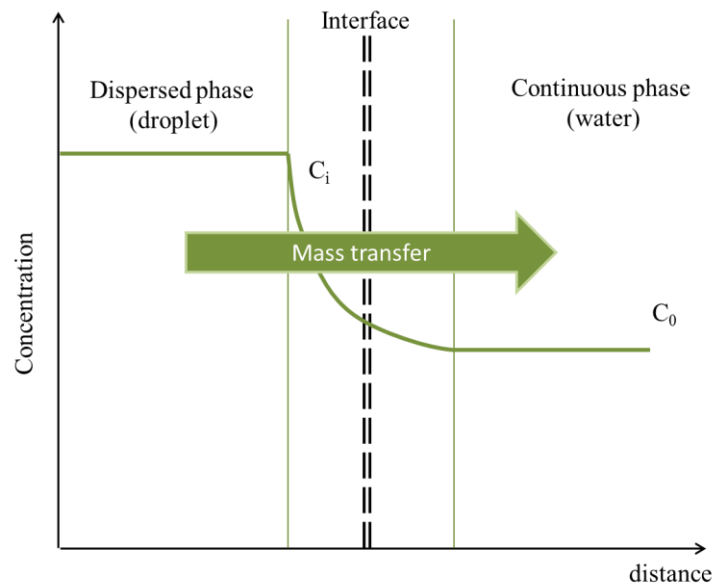


Figure 42: Illustration of the mass transfer between two liquid phases with the two film theory

5.2 Materials and methods

The experimental tests presented in this document have been performed in the Cedre Experimental Column (CEC). This device is filled with sea water in order to study the behaviour of bubbles, drops or object rising up or falling in the water column. It is a 4 meter high hexagonal column with a diameter of 0.8 m and a total capacity of 2,770 L (Figure 43). CEC is equipped with four full length glass windows to perform observation. Injection nozzles are also present at different levels from bottom to top.



Figure 43: Illustration of the Cedre Experimental Column

5.2.1 Droplet distribution measurements

5.2.1.1 Chemical characteristics

The experiments performed in HNS-MS project to characterize the droplets distributions at the orifice level, consisted in gravity releases (from the bottom) in a water column. The tests were designed to analyse the hydrodynamics release and the droplets size characterization for different configurations and various orifice diameters. A floating and non-soluble chemical, the di (2-ethylhexyl) adipate (DEHA) was used to achieve these tests. Physico-chemical properties are listed on Table 13.

Table 13: Physico-chemical properties of DEHA

Chemical	DEHA
SEBC Behaviour	Fp
CAS number	103-23-1
Density [kg.m⁻³]	930
Hydrosolubility at 20°C [mg/L]	1
Dynamic viscosity at 20°C [Pa.s]	14.2 10 ⁻³

5.2.1.2 Release system

The ejection device leads to a gravity release. In order to represent this discharge into the water column, a transparent vessel was immersed in the CEC. This container has a volume of 36L (0.4m * 0.3m * 0.3m) and was equipped with a system allowing instantaneous and passive release of product (Figure 44).

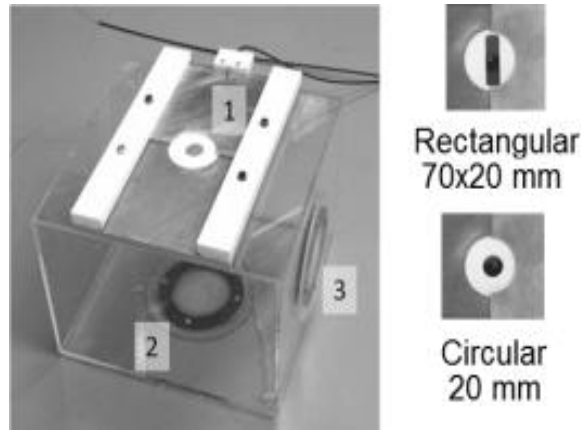
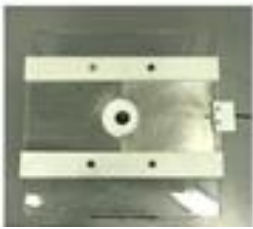
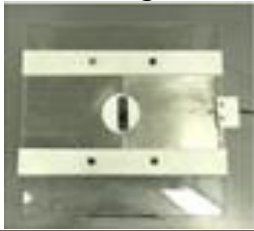


Figure 44: Box to experiment gravity release in the water column

This box allowed checking the influence of the configuration (horizontally or vertically). This tank presents three openings (1, 2 and 3 in Figure 44). The first opening is provided with a guillotine valve which was actuated by a cable system. The two other openings allowed testing different scenarios of tank release with several orifices. In this work two configurations were used: a single orifice located in position 1 and a double orifice system with orifices 1 and 2 opened. Different orifice shapes and sizes were investigated (Table 14): seven circular orifices (6, 13, 20, 30, 40, 50, 60 mm diameter) and two rectangular holes (70x10, 70x20). The released flow rate was deduced from weighting the immersed tank and considering fluid statics theory. Weight measurements were performed with a mass scale with an accuracy of 5 gram and a data sampling rate of 5 Hz.

Table 14: Summary of tested orifices

Orifice diameter (mm)	Shape
6	Round 
13	
20	
30	
40	
50	
60	
10x70	Rectangular 
20x70	

5.2.1.3 Optical set-up

DEHA is a transparent liquid with a refractive index close to that of water. Direct visualization with a single video camera is therefore not sufficient to see the DEHA flow in water. Thus an optical technique, the retro-reflective shadowscopy (Edgerton 1958; Settles, Grumstrup et al. 2005), based on the visualization of refractive index changes was set-in to contrast and highlight drops in water.

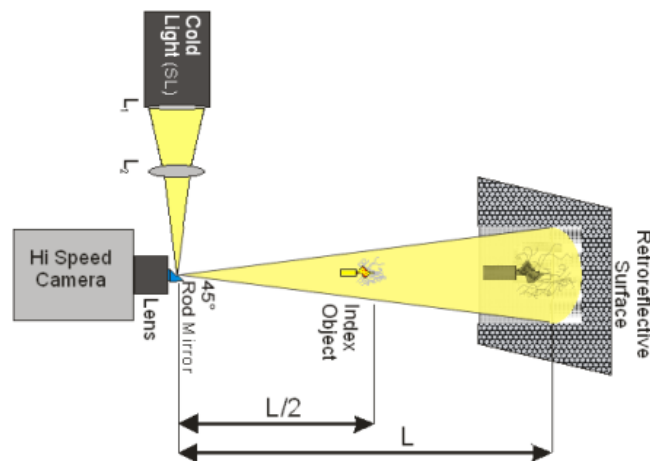


Figure 45: Retro-reflective shadowscopy principle

Figure 45 shows the experimental setup for the retro-reflective shadowscopy. This technique requires a powerful light source because it is usually used for large fields of view and outdoors. The light source (superluminescent diodes with a white light intensity of 18,000 mcd and a viewing angle of 15 °) focused on a mirror placed at the optical center of the camera. This mirror is a cylindrical rod cut at 45°. The light beam was aligned with the system axis and illuminated the retro-reflective panel but the source (usually bulky) was outside the axis. The screen reflected light in the center of the camera lens. With a small mirror in the center of the lens and the camera focused at the screen location. The presence of the mirror does not significantly affect the final image (Hargather 2008). This technique allowed viewing the superposition of the object and its shadow. Two high speed cameras (Photon Focus) were put in place during the experiments according to the graph in Figure 46.

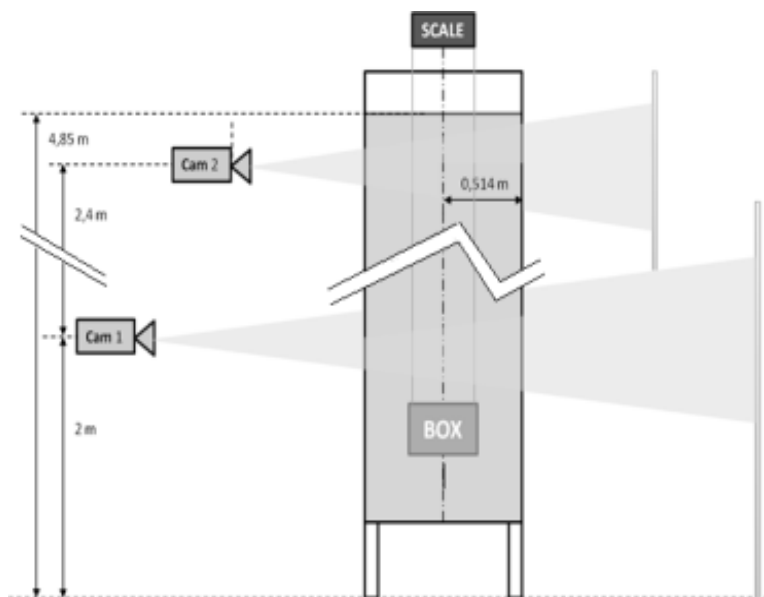


Figure 46: Experimental set-up on the CEC (retro-reflective shadowscopy)

5.2.2 Droplets velocity and solubilization measurements

5.2.2.1 Chemicals characteristics

To perform this study, chemicals with different solubility in seawater and densities lower than seawater were used. These products have been selected according to the frequency of transportation, accidents and its hazardous nature (Task C1). The typical physico-chemical properties are listed on Table 15.

Table 15: Physico-chemical properties of n-butanol

Chemical	n-butanol	Ethyl acetate	Methyl Metacrylate	Methyl Isobutyl Ketone	Methyl Ter Butyl Ether
SEBC Behaviour	Soluble	Soluble	Soluble	Soluble	Soluble
CAS number	71-36-3	141-78-6	80-62-6	108-10-1	1634-04-4
Density [kg.m⁻³]	810	902	940	800	940
Chemical Formula	C ₄ H ₁₀ O	C ₄ H ₈ O	C ₅ H ₈ O	C ₆ H ₁₂ O	C ₅ H ₁₂ O
Hydrosolubility at 20°C [mg/L]	77	86	16	18	48
Interfaciale tension at 25°C [mN/m]	56	6.79	14.3	15.7	nd

5.2.2.2 Release system

The injection system is composed of a gear pump Ismatec-IP 65 MCP-Z process equipped with a head pump (Micro pump series 125) injecting chemicals at a regular and accurate flow rate. In order to obtain a drip flow, the flow rates varied in a range between 0.25 mL/min to 2.15 mL/min. The pump is connected to the injection nozzle which is located at the bottom and at the centre of the column with a circular nozzle of 5 mm of internal diameter.

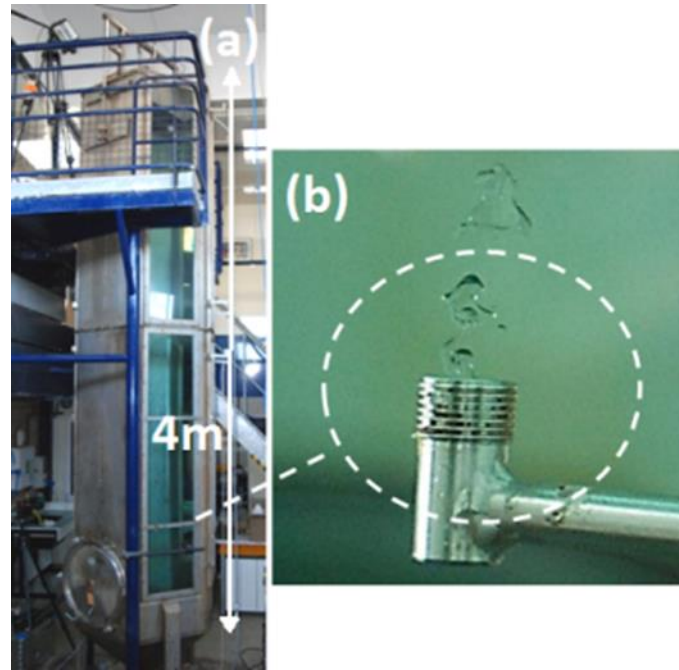


Figure 47: Picture of the Cedre Experimental Column (a) and the injection nozzle (b)

5.2.2.3 *Optical set-up*

In order to understand the different mechanisms governing the behaviour of a chemical in the marine environment, previous tests were performed in the Cedre Experimental Column (CEC) to visualize transparent chemicals in seawater (Le Floch et al. 2009). These preliminary experimentations consist in the comparison of diffuse lighting technique (Fuhrer et al. 2011) and shadowgraphy (Fuhrer et al. 2012) for rising droplet of n-butanol in seawater. Comparison of these optical techniques is presented on Figure 48. It clearly shows the relevance of shadowgraphy which highlights the "cloud" of solubilization and the recirculation cells in the droplet wake. This phenomenon was absolutely indistinguishable in the previous tests with diffuse lighting technique.

In addition, shadowgraphy has been successfully performed by Ehara et al. (1993) to visualize the evaporation of single n-pentane droplets in water. A laser shadowgraph system was used to observe a rising droplet of n-pentane in a vertical column filled with stagnant water. This system was initially developed to measure droplet evaporation floating on an immiscible liquid surface (Nosoko et al. 1987). Tests were performed with n-pentane droplets of diameter ranged between 2.2-2.6 mm. Ehara observes the main droplet evaporation is governed by heat transfers mechanisms in the droplet wake. This remark is relevant because heat transfer and mass transfer are similar and suggest that solubilisation processes will be established in the droplet wake.

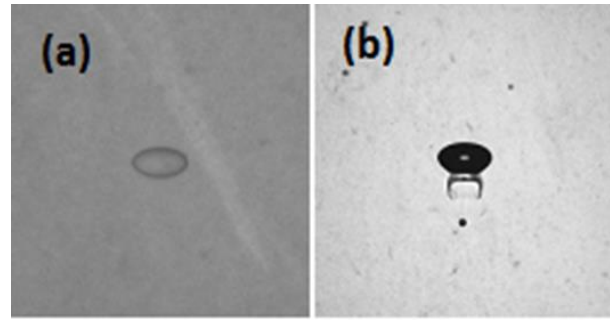


Figure 48: Comparison of light diffuser technique (a) and shadowgraphy (b) for n-butanol droplets rising in seawater (Fuhrer et al. 2011).

For droplet velocity and solubility measurements, shadowgraph technique was used. A telecentric light Vicolux TZB95 provides continuous red light illumination and a Nikkor lens 105mm coupled to SVS340 Muge (CAM0 and CAM1) records the event. The video cameras record at 20 images.s⁻¹ with a resolution of 640 x 840 pixels. Each test was recorded during about 1 min, and the results are in a sequence of images of the droplets in the seawater. Figure 50a illustrates the rise of n-butanol droplets at the bottom of the CEC. Table 16 resumes the characteristics of the optical techniques used in the present investigation.

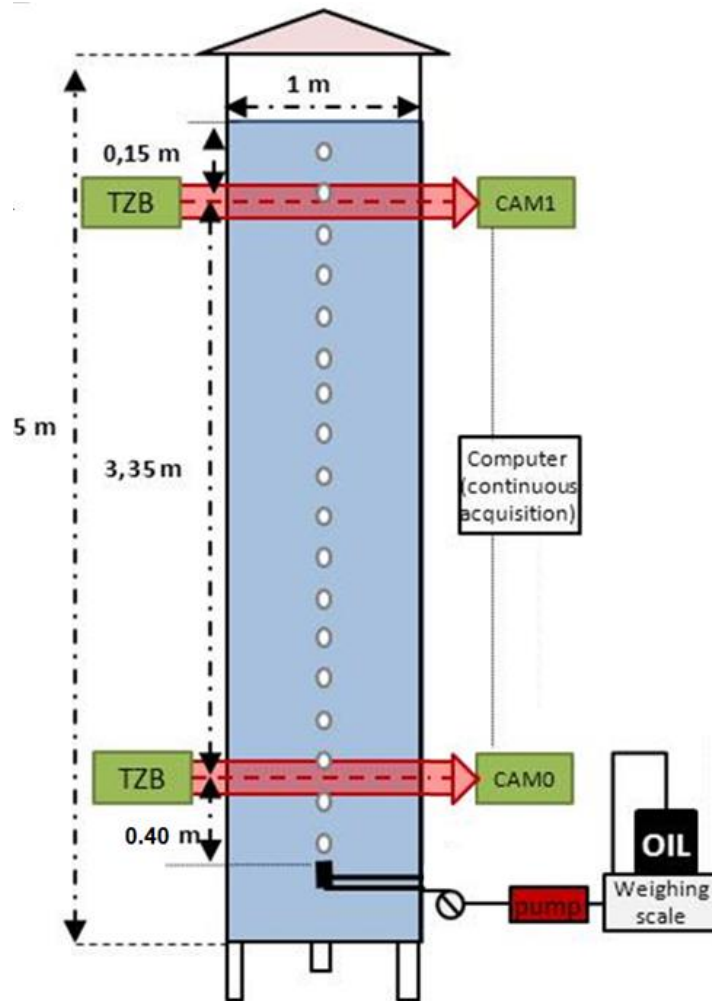


Figure 49: Position of the optical set-up (Direct Shadowgraphy Imaging)

Table 16: Optical set-up configuration

	Cam 0	Cam 1
Video camera	Photon focus	
Frame rate	20 fr/s	
Sensor area	640 pixels * 480 pixels	
Region of interest	40.9 mm * 30.7 mm	36.7 mm * 27.5 mm
Magnification	63.9 $\mu\text{m}/\text{pixel}$	57.4 $\mu\text{m}/\text{pixel}$

Each sequence of image was processed to locate and track the droplet with the support of the NI-vision software. Analysis is based on the detection of differences of gray level for each pixel on the images, isolate the droplet from the background. The resulting binary images are introduced in Figure 50b. This figure illustrates the detection of n-butanol droplets recorded at the bottom of the CEC (Figure 50a) by shadowgraphy.

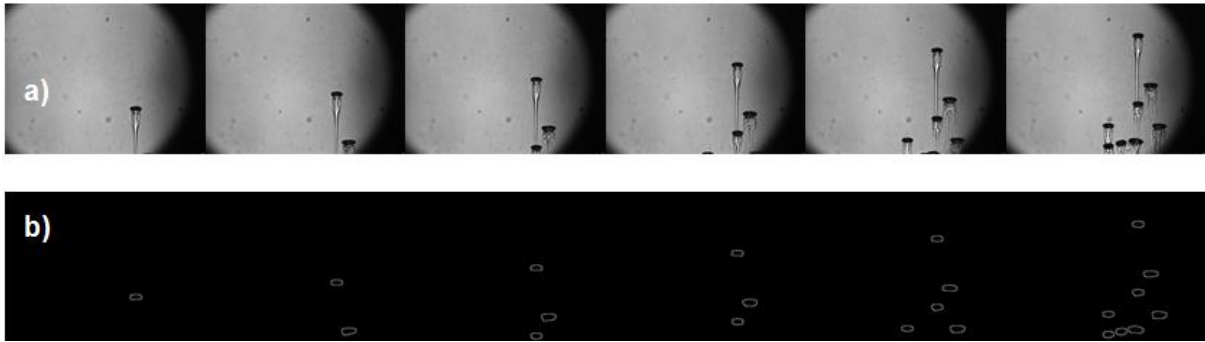


Figure 50: illustration of a n-butanol rising droplet in seawater, a) at 3.85m of depth, b) near the surface at 0.15m of depth

Analysis of the solubility of the products is obtained by measuring the variation of the Waddel disk diameter between images recorded at bottom and top of the column (a minimum sample of 100 droplets was used to provide a statistical analysis). The Waddel disk diameter d_w , is defined as the diameter of the disk with the same area as the particle and conducts in the calculation of the droplet volume and the dissolution kinetics between bottom to top of the water column.

$$d_w = 2 \cdot \sqrt{\frac{\text{droplet area}}{\pi}} \quad (15)$$

5.3 Results

5.3.1 Release flow rate

Analysis of the massive release experiments performed with submerged vessel and DEHA clearly shows two behaviours (Figure 51):

- The first configuration (case a) corresponds to a double orifice case (diameters top=20 mm, bottom=13 mm). Each orifice is crossed by a single flow;
- The second configuration (case b and c) corresponds to a single orifice case (top diameter 40 mm). The unique top orifice is crossed by a counter-current flow.

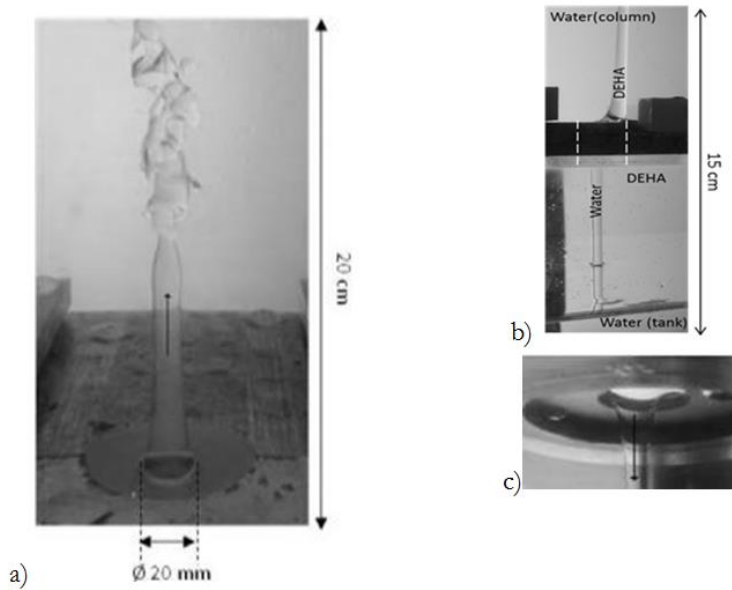


Figure 51: a) DEHA outflow at the upper orifice, b) DEHA outflow and water inflow at the upper orifice and c) Water inflow in the vessel at the top orifice

Considering experimental data, the two different flows (single and counter-current) can be distinguished on the flow rate measurements. Counter-current tests present a constant flow rate (linear volume loss) while single flow tests present a linear flow rate (Figure 52).

This is a major finding which is contrary to what one might think. Most cases of ship sinking involve a single hole and therefore a counter-current flow. The release flow rate will be constant during most time of tank draining, excepted at the final period where the Bernoulli assumptions are no more valid and the flow rate will decrease until last drops.

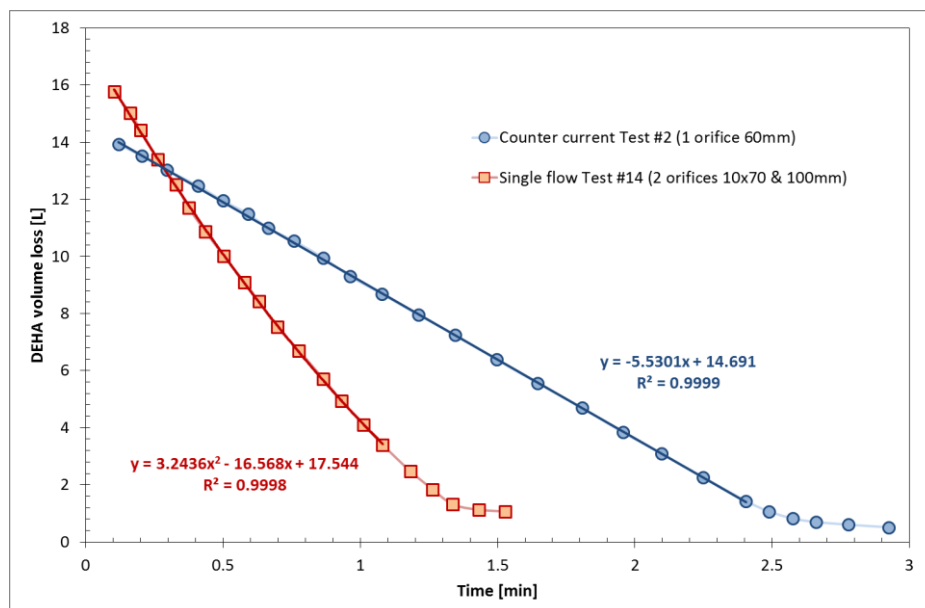


Figure 52: Experimental DEHA volume loss measurement for 2 configurations

Data about measured flow rates and flow typology are reported in Table 17. In case of one orifice, all flows were obviously counter-current. In case of two orifices, it is interesting to notice that the two behaviours can be expected according to the size of both orifices. Tests #7 and #8 are interesting to compare. The bottom orifice is very small (13mm) which creates a loss of energy for ingoing water. If the top orifice is small too, each orifice is crossed by a single flow. But if the top orifice is significantly greater than the other one (here a factor 4 in surface), a counter-current flow appears at the top orifice. The energy balance for both fluids reaches a new equilibrium with this new situation.

Table 17: Experimental flow rates

Test #	Top orifice diameter (mm)	Down orifice diameter (mm)	Release flow rate (m ³ .s ⁻¹)
1	40	/	2,5 10 ⁻⁵
2	60	/	9 10 ⁻⁵
3	10x70	/	5,9 10 ⁻⁵
4	20x70	/	3,5 10 ⁻⁵
5	30x70	/	5 10 ⁻⁵
6	20	13	2,9 10 ⁻⁵
7	30	13	2,9 10 ⁻⁵
8	60	13	1 10 ⁻⁴
9	13	30	3,5 10 ⁻⁵
10	40	30	1,7 10 ⁻⁴
11	60	30	1,6 10 ⁻⁴
12	6	100	7,1 10 ⁻⁴
13	20	100	8,6 10 ⁻⁵
14	30	100	2,1 10 ⁻⁴

5.3.2 Dispersion in the water column

The dispersion of a non-soluble chemical from a breach begins with the formation of a jet and its fragmentation into drops. Figure 11 presents comparison between top and bottom of the column for a DEHA release. The release orifice is a rectangle of 70x10 mm located at the top of the box and an orifice of 100 mm diameter at the bottom. We can notice that 25 cm above the orifice, the chemical jet is visible for about 80 seconds. This jet is disturbed, its surface is unstable and small droplets break away from it. From 85 seconds, the length of the jet decreases and large drops are formed. These latter are unstable and are very quickly fragmented. After hundred seconds, drops are much more dispersed and to 120 seconds, the dripping mode begins (Figure 53).

At the top of CEC, the delay of flowing droplets is evaluated at about 15 seconds after start of release. The drops cluster is very dense up to 100 seconds and the drip appears at the top of the column after 140 s.

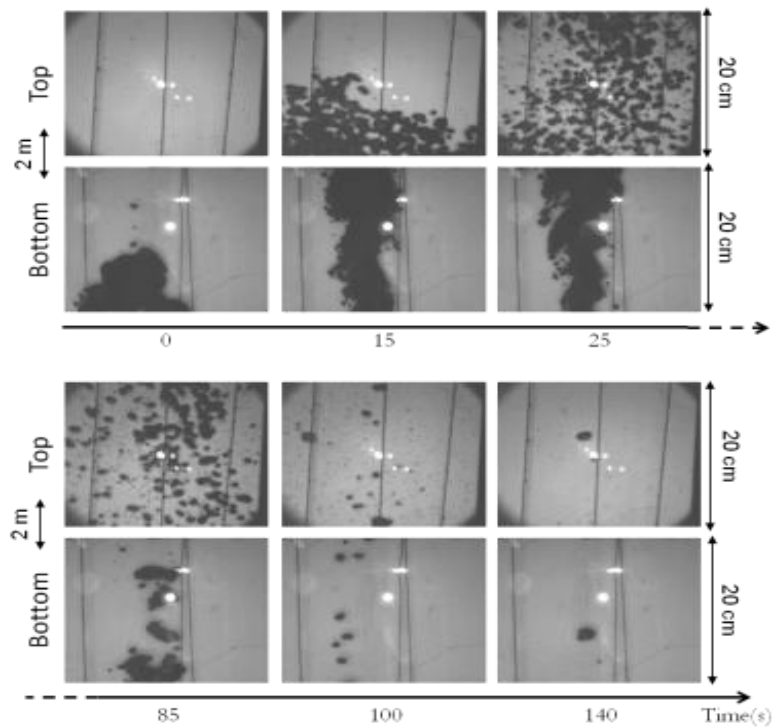


Figure 53: Evolution over time of a release of DEHA in the top and bottom of column

5.3.2.1 Droplet velocities

The flow map performed by Grace et al. (1976) provides a Reynolds number based on the number of Eötvös for different Morton numbers of drops. The experimental results of drain tests in CEC were plotted on this chart. The Morton is independent of droplets diameters and velocities, it only depends on the physicochemical properties of the fluid. The number of Morton for DEHA is $9,6 \cdot 10^{-11}$. According to the chart, these numbers are between 10^{-10} and 10^{-11} for DEHA and corresponds to wobbling droplets. The graph is logarithmic, these numbers cannot be more precise, but they are consistent with the theory.

Figure 55 shows that a gap of about 30% is found between prediction and experimental data Clift. This is not surprising given that the observed drops have a form of irregular ovoid (wobbling) and not ellipsoidal, thus changing their hydrodynamic lift.

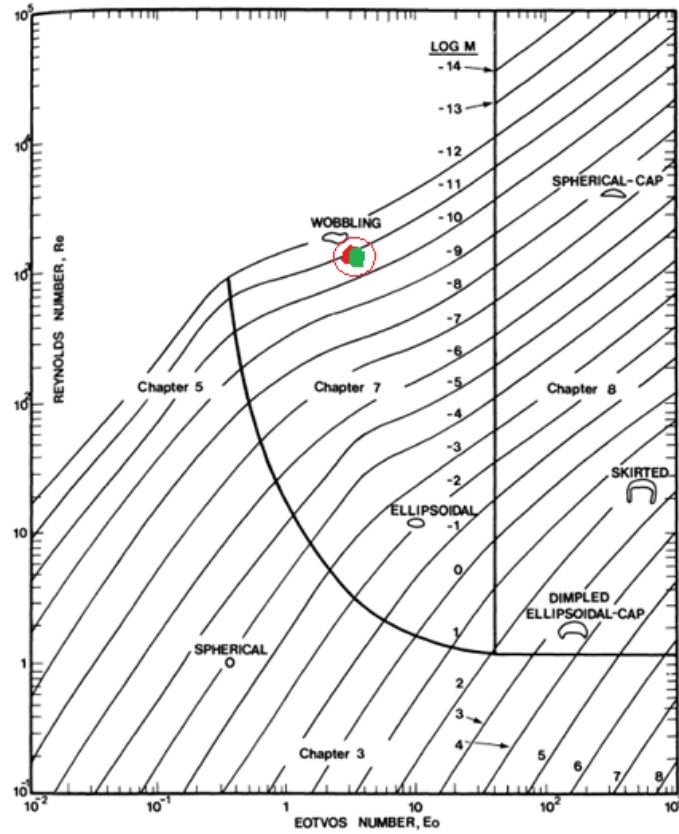


Figure 54: Comparison of experimental tests performed with DEHA and Clift map

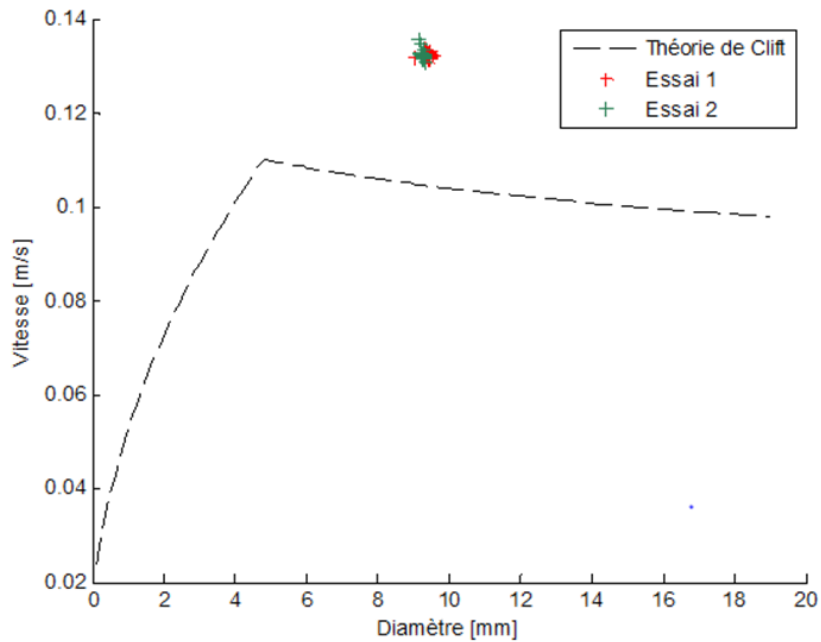


Figure 55: Droplet velocity vs. droplet diameters for DEHA tests

5.3.2.2 Droplets distribution

The analysis of the droplet size was performed on images recorded at the top of column. Manual processing has been performed on the drops of clusters images. It does not provide the same characterization of drops that the automated processing. Indeed, determining the position of the mass center of the section and the perimeter of the drop is difficult to obtain. However, the height and width of the bounding box and the small and the major axis of the droplet are measurable.

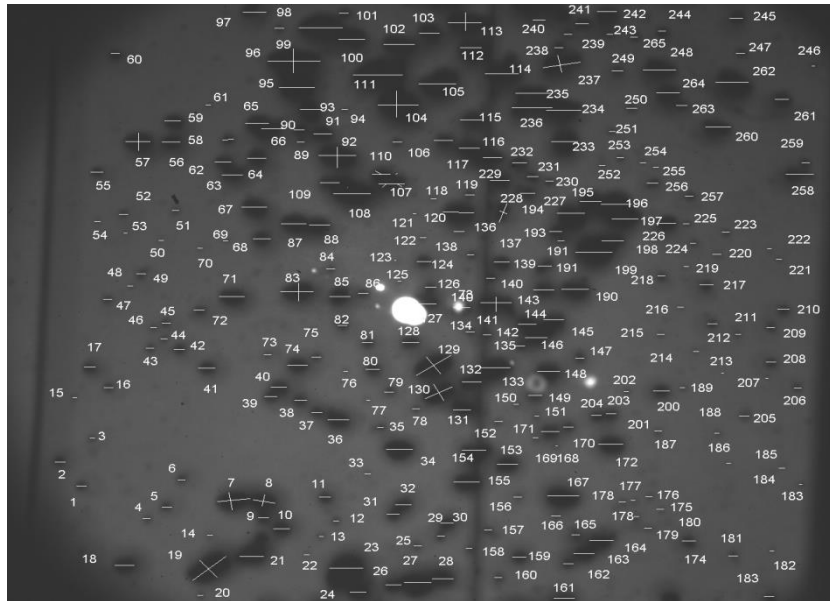


Figure 56: Image analysis of DEHA release in water

Droplet size distributions showed that there is little change over time. All data for each test, has been concatenated and one or two log-normal distributions could be calculated by regression on these measurements. Figure 57 shows two examples of droplet size distributions and log-normal distributions associated. Thus, this law seems appropriate to represent the system.

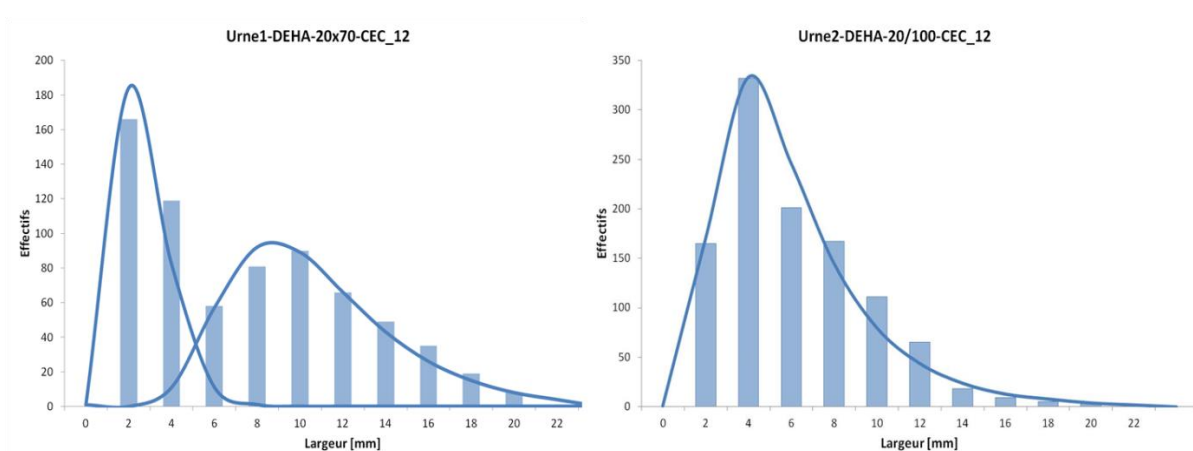


Figure 57: Drop size distribution and fitted log-normal laws

These histograms comparison highlights some points:

- The maximum size of the droplets is 22 mm, which agrees with the maximum size before fragmentation from equation (4), (Clift, Grace et al. 1978) (19.1 mm);
- For all results, the proportion of small droplets (<5 mm) is about 50% in number;
- Distributions do not appear to change significantly over time.

Data for each test has been concatenated and one or two log-normal distributions fitted on these measurements. These distributions appear to be independent of time and orifice size and can be represented as one log normal laws depending on the rate of ejection (16).

$$f(D) = \frac{e^{-\frac{1}{2}\left(\frac{\ln D - \mu}{\sigma}\right)^2}}{D\sigma\sqrt{2\pi}} \tag{16}$$

Where μ and σ respectively the mean and standard deviation of the logarithm of the variable (diameter D).

The parameters of the log-normal distributions adapted to the experimental distributions are summarized in Table 18. For rates below $10^{-4} \text{ m}^3.\text{s}^{-1}$, two pairs of μ and σ settings match the two laws of distributions, the final bimodal distribution being the sum of the two distributions.

Table 18: Summary of parameters of log-normal distributions

	$Q < 10^{-4} \text{ m}^3.\text{s}^{-1}$		$Q > 10^{-4} \text{ m}^3.\text{s}^{-1}$
μ	-5.69	-4.51	-5.3
σ	0.561	0.364	0.635

Future works have to focus on the new experiments with other fluids to validate le modelling law

5.3.3 Droplet solubilisation

5.3.3.1 Droplet diameter

Pictures of n-butanol, at the bottom and top of the column are presented on Figure 58. At the column bottom, groups of droplets have varied sizes with particularly large structures. At the top, these large structures have completely disappeared by solubilisation and fragmentation, and small drops were entirely solubilized. It noticed on both images that the cloud of solubilisation is visible after the passage of drops. Turbulences and recirculation cells behind the drops present coherent structure such as vortex. These mechanisms of solubilisation in the droplet wake can be compared to those observed by Ehara et al. (1993), and Bäumlér et al. (2011) who performed experimental and numerical simulation to determine the droplet

terminal velocity for chemicals/water system in liquid-liquid extraction process and in particular for n-butanol/water system. The solubilisation process is illustrated by Figure 59 showing droplet rise of soluble chemical. Mass transfer occurs in the boundary layer at the droplet surface which is enhanced by friction and droplet velocity. This solubilisation layer detaches from the droplet and generates a persistent cloud of solubilisation. From an optical point of view, clouds left by the previous droplets degrade the sharpness of drops, rendering analysis more difficult.

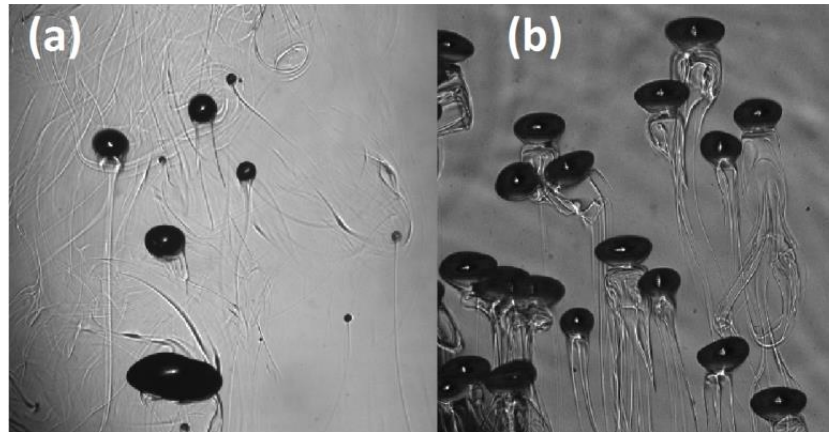


Figure 58: DSI images of n-butanol rising droplet in seawater, (a) picture obtained by the bottom camera, (b) picture obtained by the top camera.

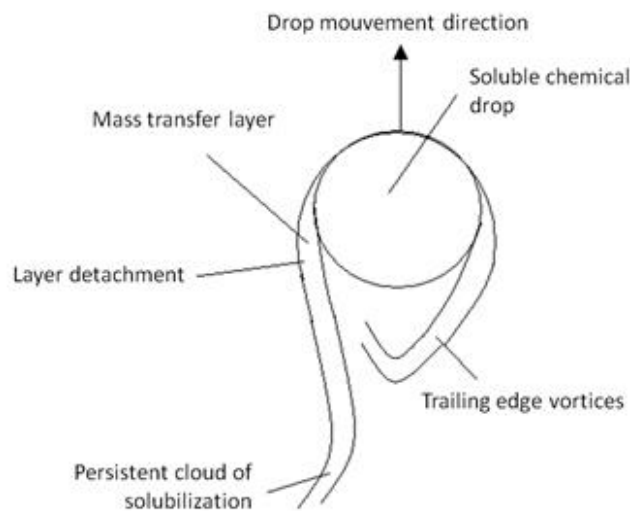


Figure 59: Illustration of solubilisation process for n-butanol droplet rising in seawater

The characterization of the solubilisation rate is obtained from the measurements of Waddel disk diameters between bottom to top of the column and assuming the droplet volume as a sphere. Figures 60, 61, 62, 63, 64 represent the variation of the probability density function of Waddel diameter respectively for n-butanol, ethyl acetate, methyl ter butyl ether, methyl

methacrylate and methyl isobutyl ketone tests. Each figure includes two types of distribution corresponding to bottom and top measurements. The comparison of the figures shows differences:

- Waddel diameters are varied and are between 0.8 mm for n-butanol to 6.3 mm for the methyl methacrylate
- Except for n-butanol and ethyl acetate for which notice a decrease of Waddel diameter between bottom and top, other chemicals do not clearly show significant difference along the column height.

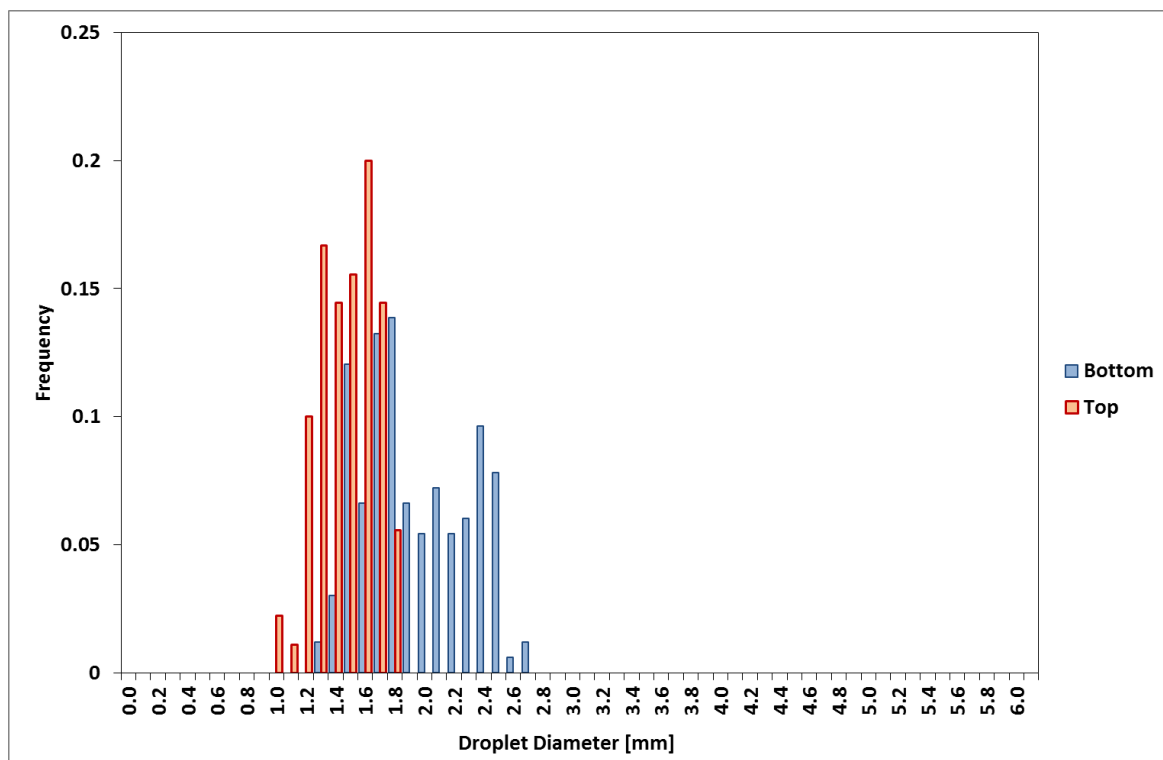


Figure 60: Histogram of distribution of equivalent droplet diameter for n-butanol

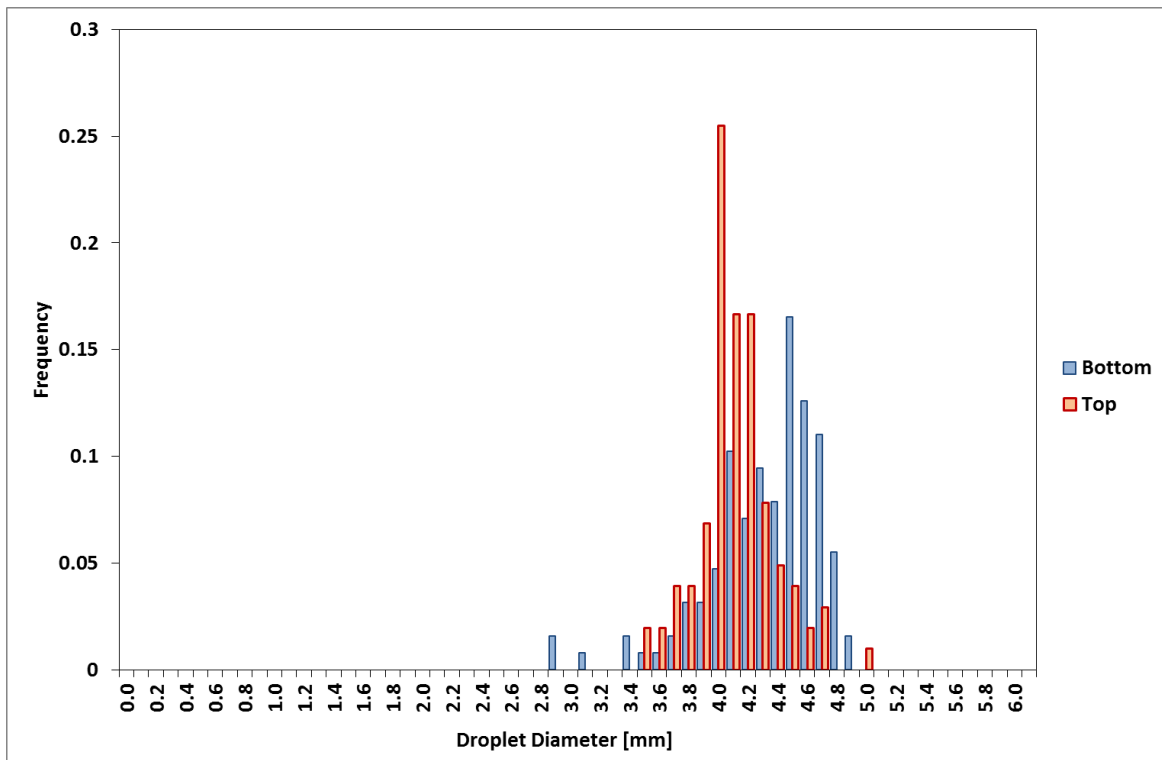


Figure 61: Histogram of distribution of equivalent droplet diameter for ethyl acetate

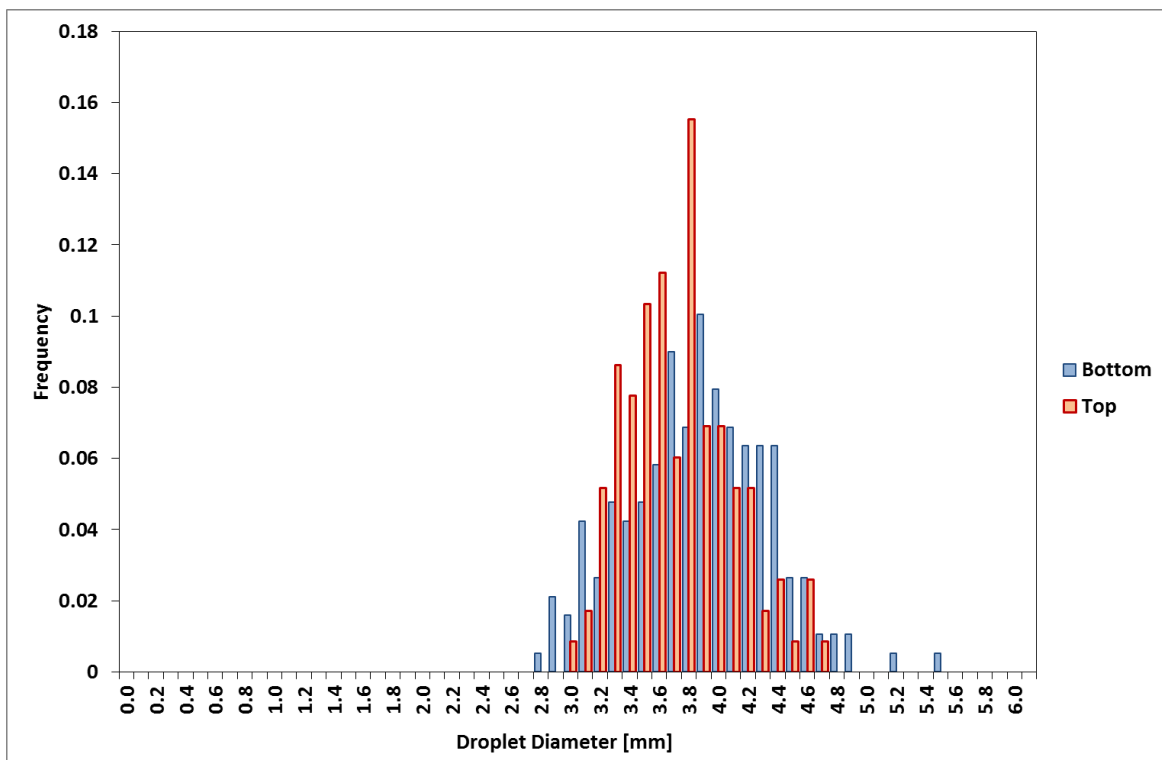


Figure 62: Histogram of distribution of equivalent droplet diameter for methyl ter butyl ether (MTBE)

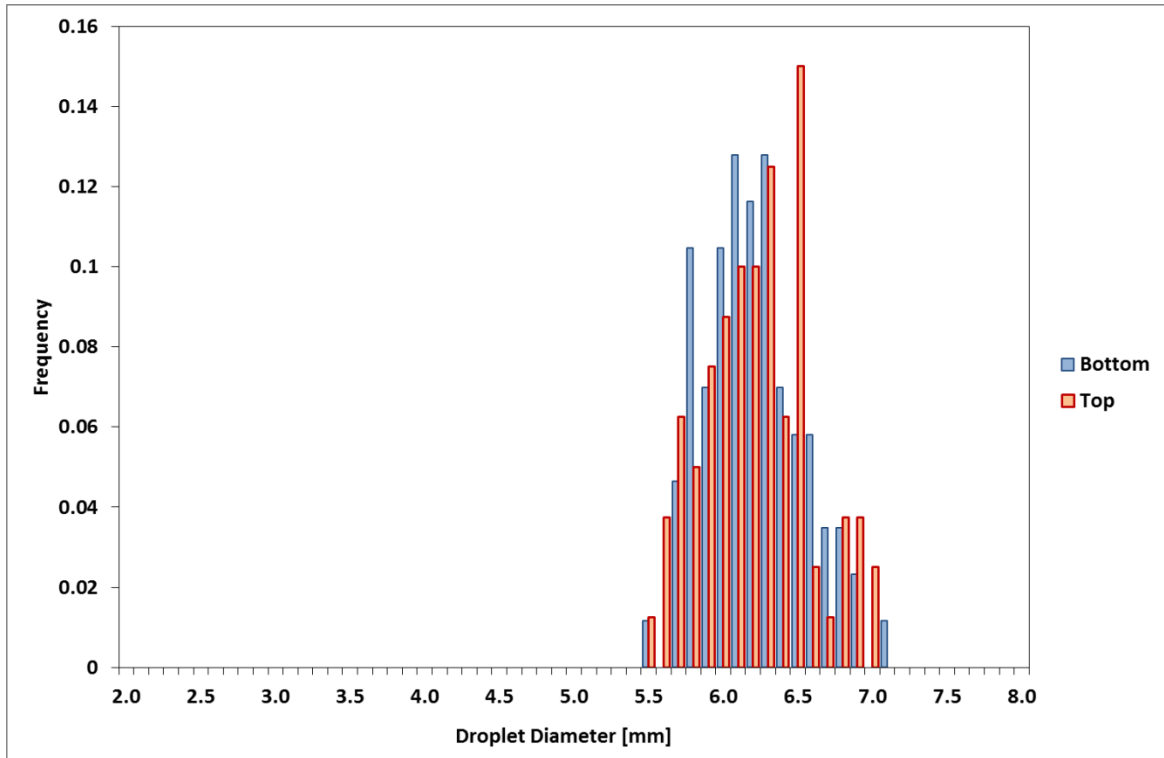


Figure 63: Histogram of distribution of equivalent droplet diameter for methyl methacrylate

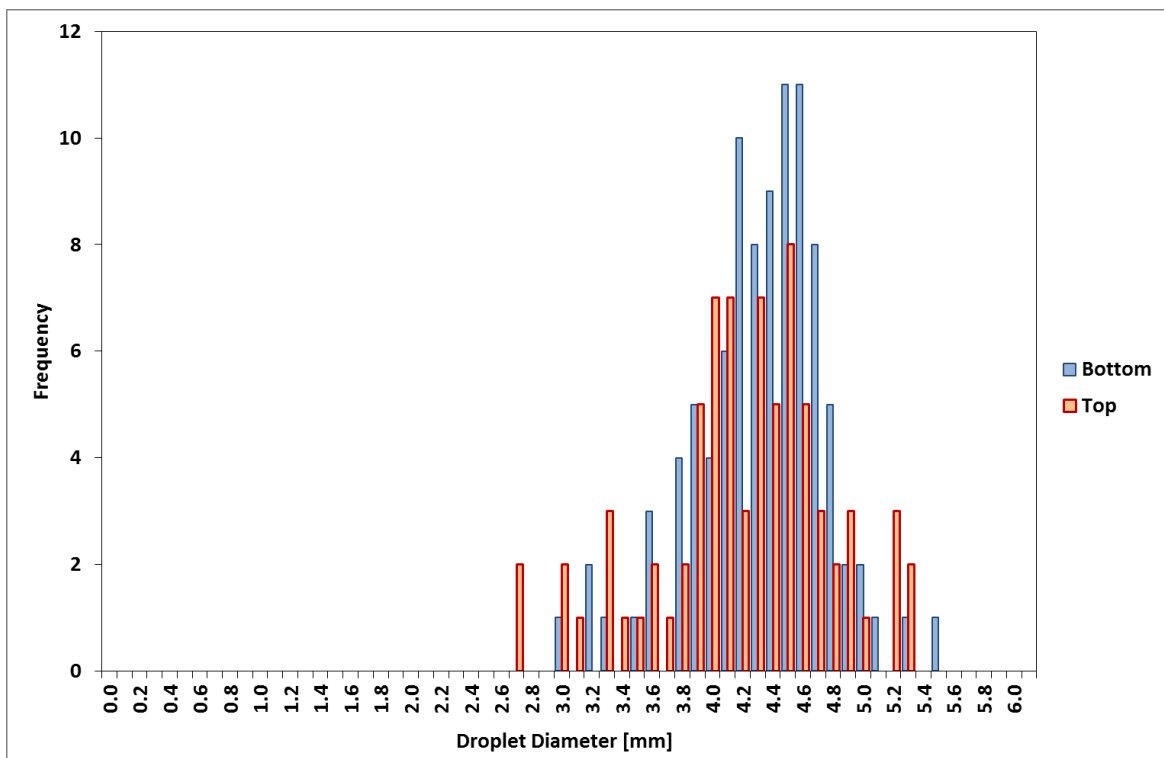


Figure 64: Histogram of distribution of equivalent droplet diameter for methyl isobutyl ketone (MIK)

To highlight the effects of solubilisation during ascent drops of chemicals, the mean Waddel diameter was drawn between the bottom and the top of the water column (Figures 65, 66, 67, 68 and 69). These figures not only confirm the variation of droplets diameters for n-butanol and ethyl acetate but it reveals variations of methyl ter butyl ether and methyl methacrylate. The last product (methyl isobutyl ketone) does not show significant changes of diameters.

Table 19 presents a first estimation of the variation of droplets diameters and volumes along the water column for the five tested fluids. The volume variation is calculated assuming the droplet as a spherical particle. The comparison between the different fluids highlights no logical trend of the variation of diameter and volume compared to the hydrosolubility values. N-butanol is the most soluble fluids with an equivalent diameter divided by a factor of 1.21 between bottom and top, linked to droplet volume decrease of about 46%. The direct comparison with the hydrosolubility value clearly shows no logical link with this parameter. However, it is assumed that the values of the solubility measurements from freshwater are not representative of the behavior of chemical in seawater. Indeed in some cases the salt in water tends to decrease or increase the solubility of the chemicals in sea water. Finally, it is important to note that all the diameter measurements should be weighted by the uncertainty and variability measurements of the droplet diameters.

Table 19: comparison of the variation of droplets diameters and volumes along the water column

Chemical	n-butanol	Ethyl acetate	Methyl Metacrylate	Methyl Isobutyl Ketone	Methyl Ter Butyl Ether
Hydrosolubility at 20°C [g.L⁻¹]	77	86	16	18	48
Variation of Waddel diameter along the water column	17.1%	5.1%	0%	2.9%	3.6%
Variation of mean droplet volume along the water column	46%	16%	0%	6%	12%

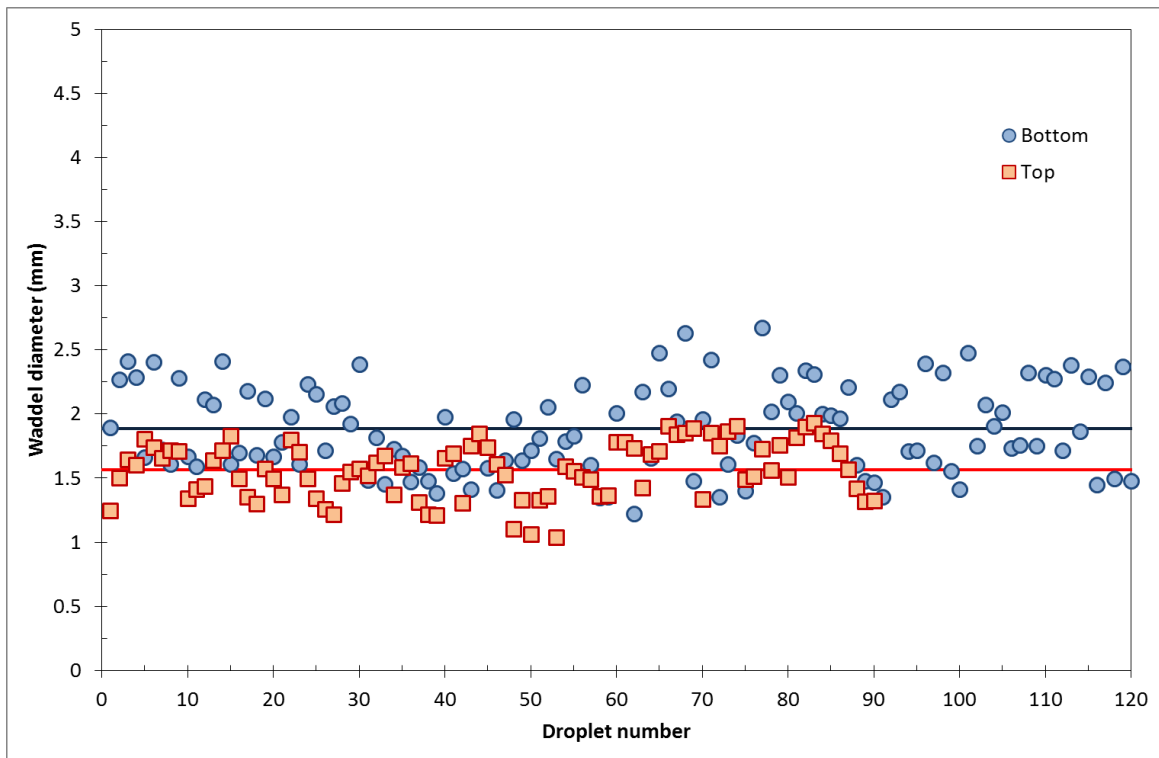


Figure 65: Variation of equivalent diameter for n-butanol/seawater system between bottom to top of CEC

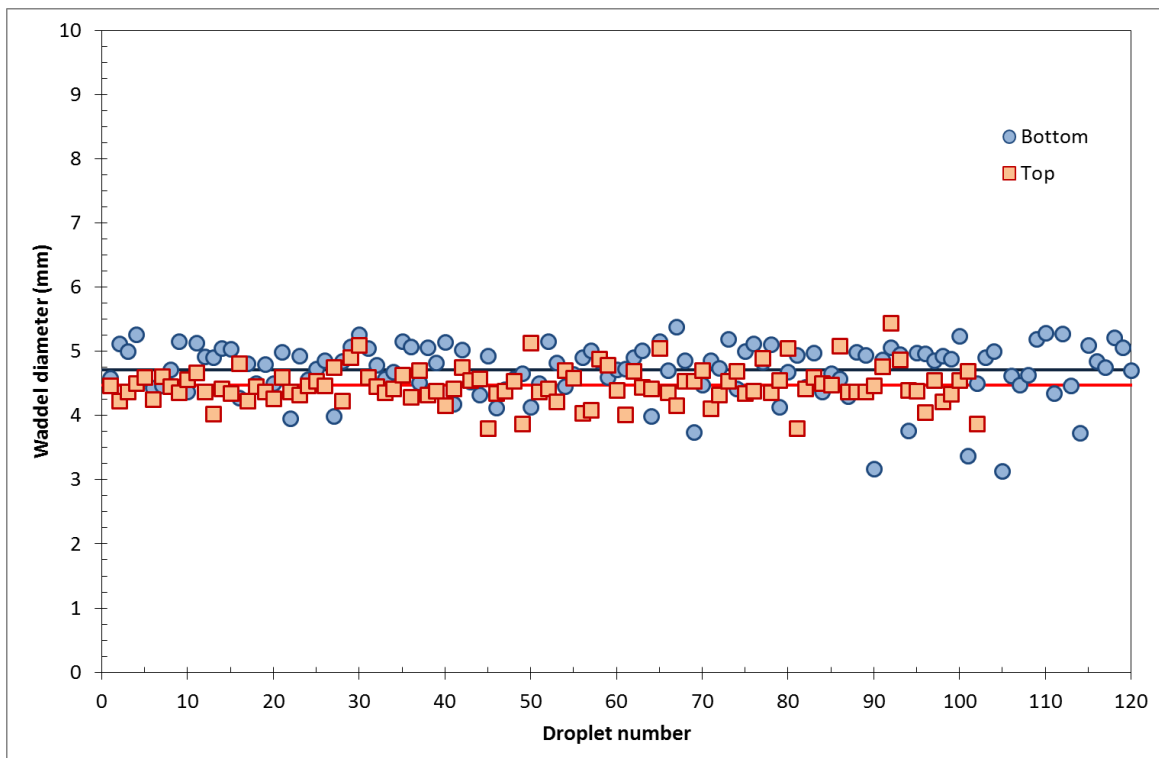


Figure 66: Variation of equivalent diameter for Ethyl acetate/seawater system between bottom to top of CEC

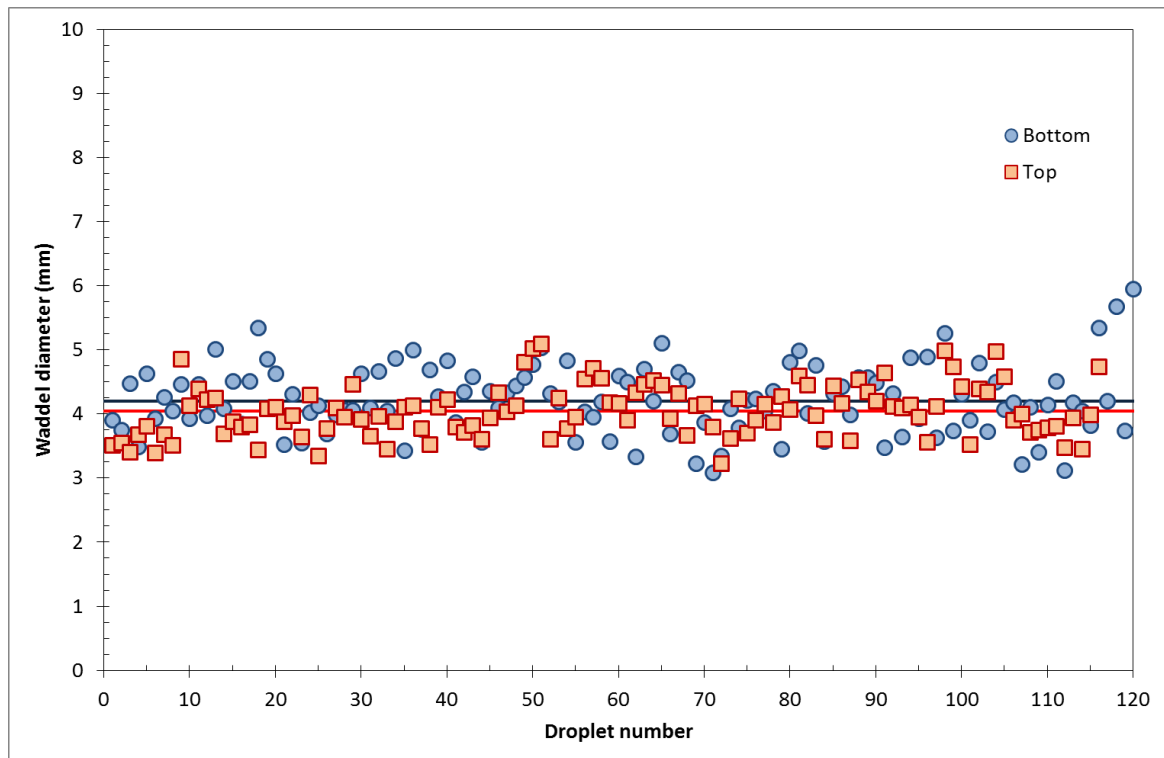


Figure 67: Variation of equivalent diameter for methyl MTBE/seawater system between bottom to top of CEC

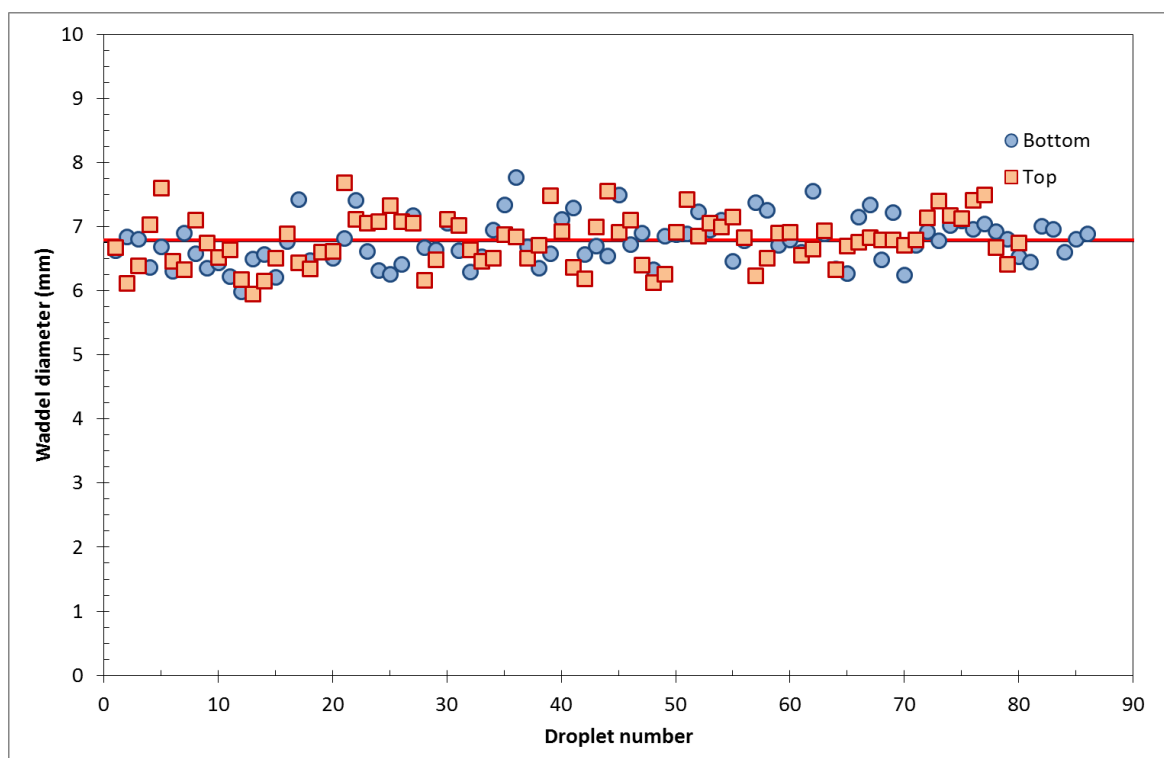


Figure 68: Variation of equivalent diameter for methyl metacrylate/seawater system between bottom to top of CEC

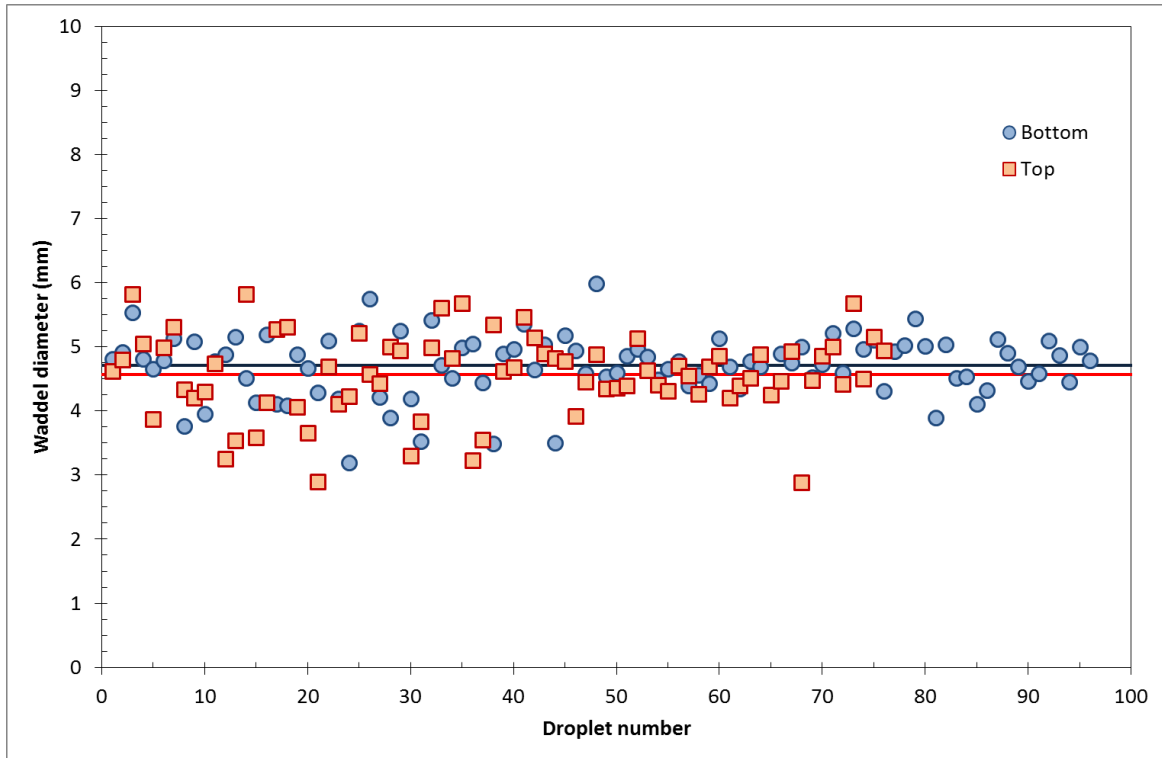


Figure 69: Variation of equivalent diameter for MIK/seawater system between bottom to top of CEC

5.3.3.2 Droplet velocities

This last analysis consists to compare the Clift's model with the experimental measurements of mean velocity of droplet rising in the water column. To obtain this value, the droplets appearing on bottom camera are identified on the top camera after a few seconds and times variation are noted. Mean velocity is then calculated by dividing the distance between the two cams by the time variation. The mean droplet diameter is an average of the diameter between bottom and top measurements.

Figures 70, 71, 72, 73 and 74 represent the variation of droplet rising velocity between bottom to top of the column and the comparison with Clift's theory for all the tested fluids. Clift has shown the shape of fluid particles could be approximated by a sphere for small size range (smaller than 1mm), an ellipsoid in the intermediate size range (1mm to 15mm), and a spherical-cap in the larger size range. Clift proposed several correlations depending on the different regimes of droplet shape (5.1.5). For the present study, the regime of ellipsoidal shape is retains because droplets diameters varied in the range of 2 to 8 mm.

The comparison with Clift's correlation with experimental data presents a good agreement with a deviation between 5% for n-butanol to 20% for methyl isobutyl ketone.

Table 20 presents an estimation of the variation of the mean droplet mass with time variation (dm/dt) for all the tested fluids, assuming a mean droplet diameter between bottom and top of the column and a droplet velocity following the Clift's theory.

Table 20: Variation of the mean droplet mass loss vs. time

Chemical	n-butanol	Ethyl acetate	Methyl Metacrylate	Methyl Isobutyl Ketone	Methyl Ter Butyl Ether
Hydrosolubility at 20°C [g.L⁻¹]	77	86	16	18	48
Mean mass variation vs. time (dm/dt) [g.s⁻¹]	$1.05 \cdot 10^{-5}$	$1.17 \cdot 10^{-4}$	0	$5.52 \cdot 10^{-5}$	$8.02 \cdot 10^{-5}$

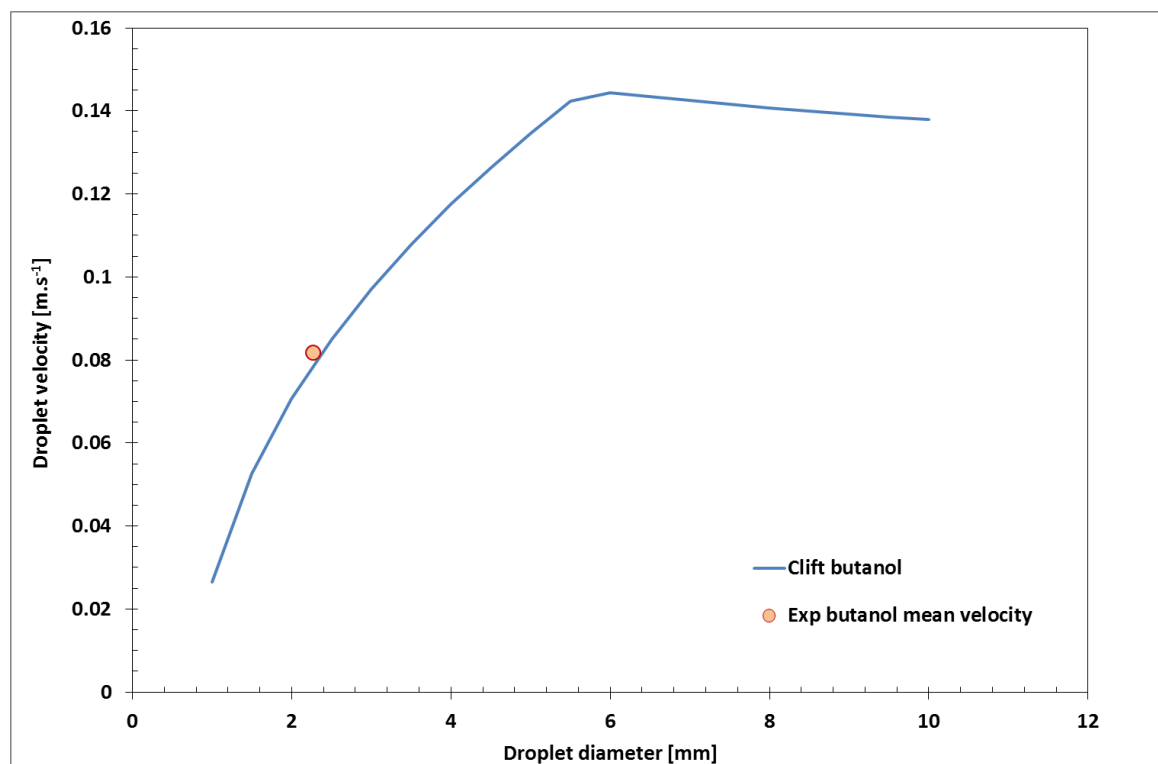


Figure 70: Variation of rising velocity vs. mean equivalent diameter and comparison with Clift's theory for n-butanol

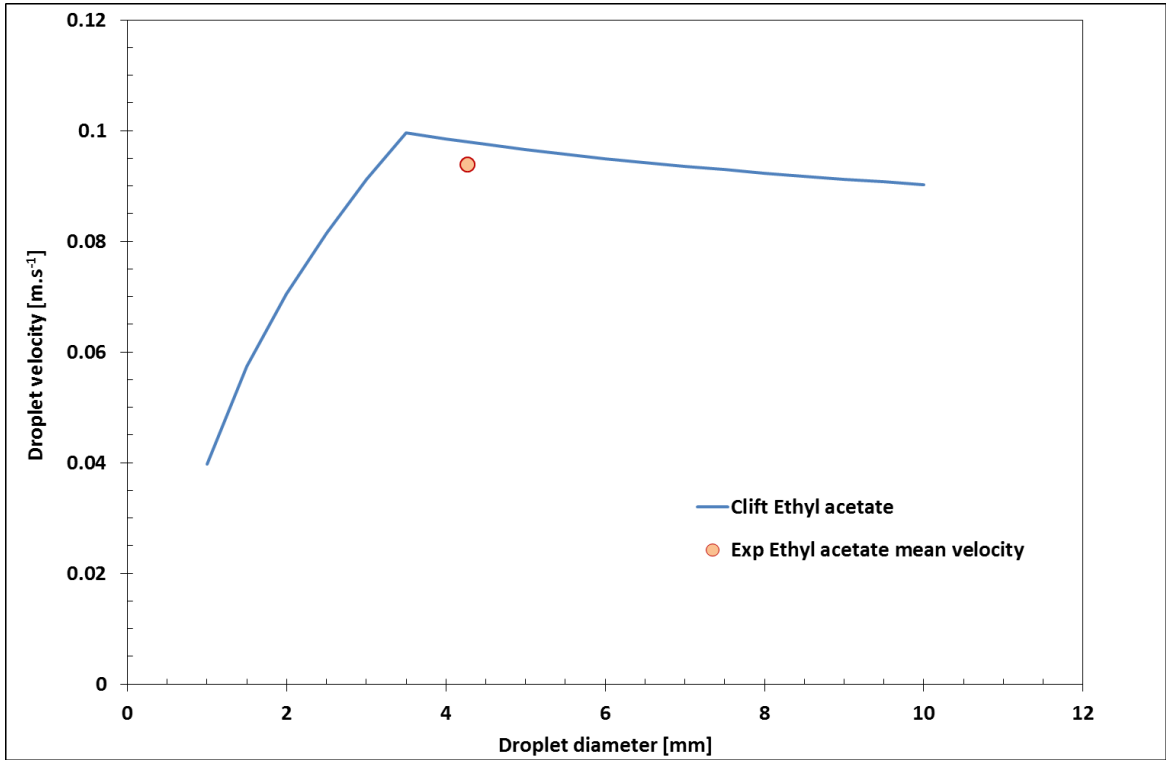


Figure 71: Variation of rising velocity vs. mean equivalent diameter and comparison with Clift's theory for ethyl acetate

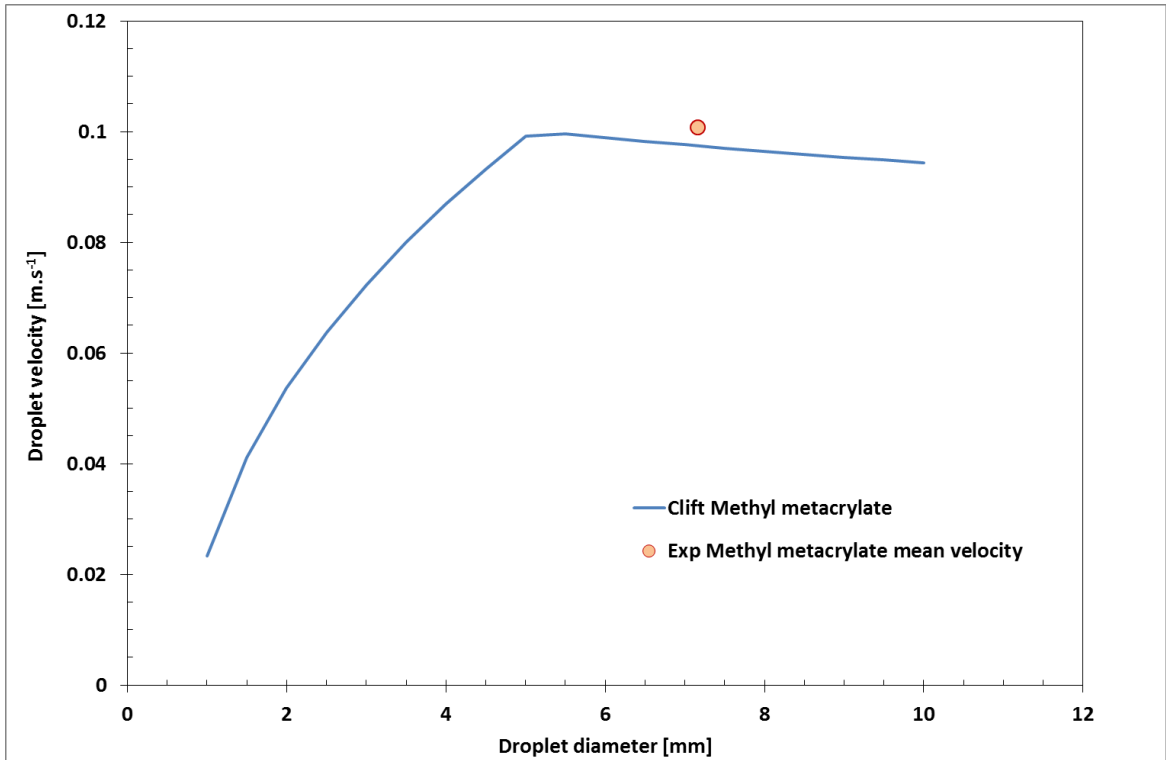


Figure 72: Variation of rising velocity vs. mean equivalent diameter and comparison with Clift's theory for methyl methacrylate

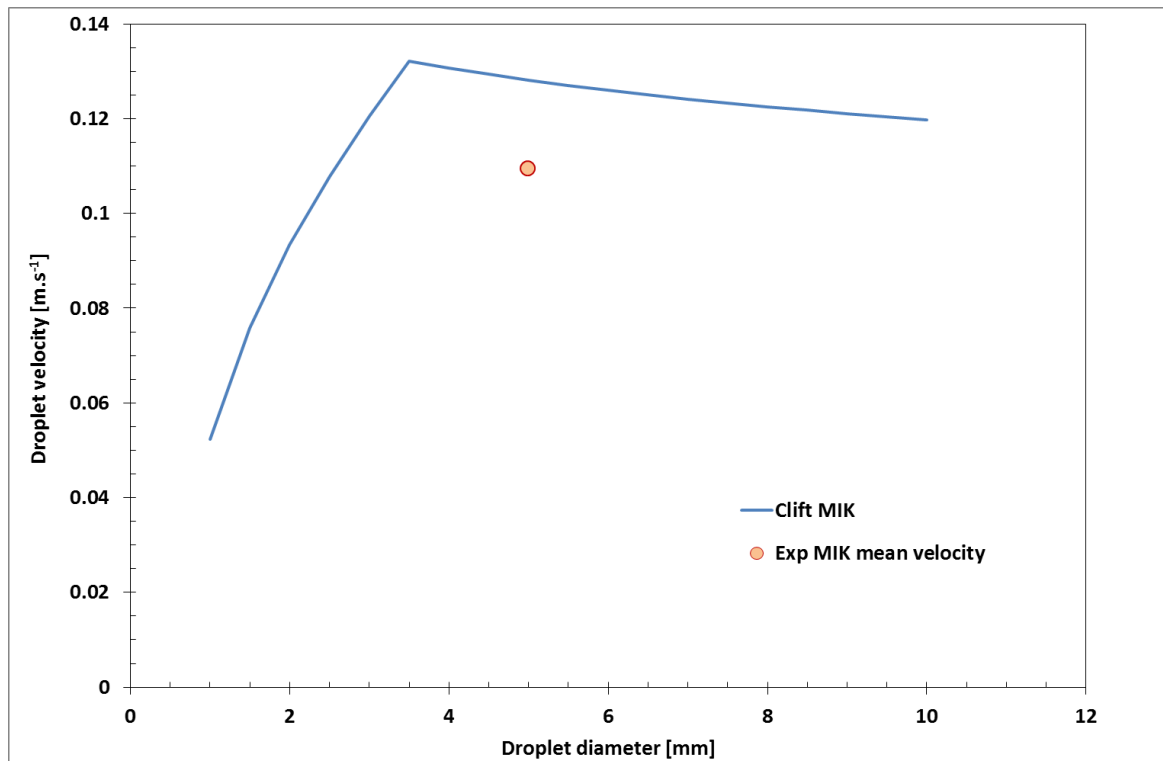


Figure 73: Variation of rising velocity vs. mean equivalent diameter and comparison with Clift's theory for methyl isobutyl ketone

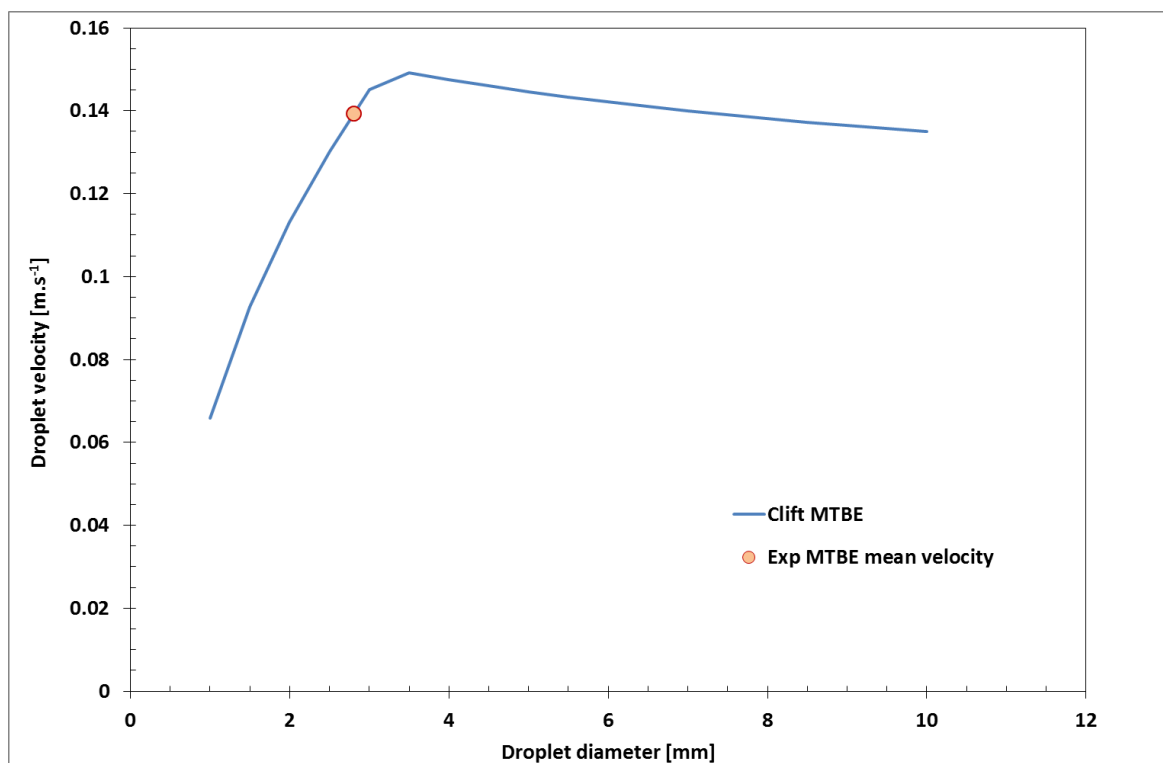


Figure 74: Variation of rising velocity vs. mean equivalent diameter and comparison with Clift's theory for methyl tert butyl ether

5.4 Conclusion

This chapter presents a global analysis to characterize the chemicals behaviours in seawater due to marine accident. This study focuses on laboratory scale experiments in the Cedre seawater column (CEC). The first part presents the drain of a chemical tank immersed in the CEC and filled with Di ethyl exyl adipate (DEHA). Two different behaviours were observed corresponding to different scenarios (one or two break in the vessel) and average volumic flow rates were estimated.

The second part of the project focuses on the characterization of the mass transfer process for n-butanol, ethyl acetate, methyl ter butyl ether, methyl methacrylate and methyl isobutyl ketone release in seawater. This experimental study gave information on the solubilisation processes of chemicals in sea water. In comparison with the SEBC method that is performed at laboratory scale with small quantity of chemicals and fresh water, this study is more representative of in-situ release and tends to better estimate the chemical mass reaching the surface. From a global scale, droplets diameters were measured and clearly show a decrease for the majority of the chemical tested (n-butanol, ethyl acetate, methyl ter butyl ether and methyl isobutyl ketone). The comparison of measurements with Clift's correlation for droplet rising velocity shows a good agreement for average data. Assuming the Clift's model; an estimation of average mass variation with time was calculated for the tested fluids.

Future works will focused on new experiments with other chemicals to sharply determine the rising velocity and mass transfer rate for massive release, in order to propose adapted mass transfer coefficient for numerical modelling.

PAGE INTENTIONALLY LEFT BLANK

Strength and weakness of the SEBC classification

PAGE INTENTIONALLY LEFT BLANK

6 Strength and weakness of the SEBC classification

The Standard European Behaviour Classification (SEBC), which is currently used by response authorities, is designed to define the short term fate of chemicals in the marine environment. This classification is based on the physical and chemical characteristics of HNS, *i.e.* the specific gravity, the vapour pressure and the solubility. Four main behaviours are identified (floaters F, evaporator E, dissolver D or sinker S) and are sub-divided in 12 classes.

However, as this classification is based on parameters determined independently of each other and usually in standard conditions (fresh water, 20 °C), gaps between the categorisation and the field reality can be observed.

For most HNS tested on the Cedre Chemical Bench (butyl acetate, 2-ethylhexanoic acid, 2-ethylhexyl acrylate, heptane, pentane, nonanol, Texanol® and xylene), the SEBC categorization is in accordance with the experimental results obtained at 20 °C with no winds. Hence, **SEBC categorization is a good tool to quickly get the short term fates of HNS in calm environmental conditions.**

Some reservations have to be made considering toluene and butyl acrylate. At 20 °C without wind, the slick of toluene persists at the surface for more than one hour. Even if this period of time can be considered as negligible in real case accident, this result warns on the possibility of presence of a slick despite the E classification of toluene. For butyl acrylate, classified as FED in the SEBC categorization, the three behaviours (floating, evaporating and dissolving) are actually occurring for 20 °C and no wind conditions. However, dissolution is rather limited (maximum of 12%) and the relevance of indicating D can be considered.

In deteriorated weather conditions, SEBC categorization cannot be used in a straightforward way.

In fact, as SEBC is based on independently determined properties measured in standard conditions, the emergence of an element (wind velocity, temperature for example) modifying the kinetic of the processes involved (evaporation and dissolution) may imply changes in the overall fate of the product. For examples:

- The presence in the water column of HNS is enhanced by the wind which impacts the surface agitation and thus the transfer (droplets in suspension) and/or dissolution of HNS.
- The velocity of wind directly promotes the kinetic of evaporation.
- The temperature regulates the maximum amount of HNS evaporated (higher with increasing temperature).

Moreover, the maximal wind velocity reached with the tool is $7 \text{ m}\cdot\text{s}^{-1}$ (*i.e.* $25.2 \text{ km}\cdot\text{h}^{-1}$ or 13.6 knots or force 4 on Beaufort scale), which is far from being exceptional in natural environmental conditions. As bad weather conditions increase the risk of an accident at sea, it is likely that stronger wind conditions could be expected during a spill accident. The gap between the SEBC categorization and the real fate of the HNS would probably be even greater in such weather conditions.

The experimental pilot-scale tool used in this project brings new information about HNS fate in the marine environment (measurement of concomitant dissolution and evaporation kinetics, evaluation of the impact of environmental conditions) and so is of major-importance for taking accurate decisions in the event of HNS spills.

Conclusion

PAGE INTENTIONALLY LEFT BLANK

7 Conclusion

When dealing with a HNS pollution incident, one of the priority requirements is the identification of the hazard and an assessment of the risk posed to the public and responder safety, the environment and socioeconomic assets upon which a state or coastal community depend. The primary factors which determine the safety, environmental and socioeconomic impact of the released substance(s) relate to their physicochemical properties and physical fate in the environment.

Available information on HNS fate in the environment is generally scarce or obtained for standard conditions (freshwater, 20°C for example). Hence, determining impacts in case of HNS accident can either be hardly possible or punctuated by errors or inaccuracies. To counteract these existing limits, HNS-MS project aimed at producing experimental data in order to:

- Get hardly available or inexistent information in the literature (physicochemical properties at different temperatures, solubility limits for different salinities, simultaneous evaluation of the dissolution and evaporation processes, characterization of HNS droplets distribution...);
- Improve the understanding on HNS behaviour both in the water column and at the sea surface under different controlled environmental parameters;
- Compare these data with the results obtained by the HNS drift and fate model developed in the framework of the project;
- Implement the database created during the project with these original experimental data.

The experimental data obtained in the framework of HNS-MS project enabled us to achieve the following conclusions:

- Concerning the physicochemical properties tested: unlike specific gravity, viscosity and surface tension are significantly impacted by a temperature shift. At 20°C, experimental data are in accordance with literature data which indirectly validate the protocols used in the project.
- Concerning the evaluation of evaporation kinetics: globally, experimental HNS evaporation rates are positively correlated with their vapour pressure. This result is not valid when evaporation is monitored after HNS have been spilled at the surface of seawater. This clearly illustrates the competition between evaporation and dissolution processes.
- Concerning the evaluation of dissolution kinetics: experimental solubility limits in freshwater are higher than in 5‰ and 35‰ water. This result is in accordance with the

“salting out effect”. Solubility limits in seawater are usually unavailable in the literature; hence these experiments enabled to gain new data.

- Concerning the evaluation of the competition between evaporation and dissolution kinetics: an original and unprecedented tool was used to simultaneously evaluate these two major processes affecting the fate of HNS in the environment. The overall fates of 10 HNS have been estimated under different environmental conditions (air and water temperature, wind velocity, surface agitation). Globally, during the first minutes or hours after HNS is spilled, temperature regulates the maximum amount of product evaporated, higher for the highest tested temperature, while the velocity of wind promotes directly the kinetic of evaporation.
- Concerning the HNS behaviour in the water column: the experimental tests performed in the Cedre Experimental Column are more representative of in-situ release than SEBC method that is performed at laboratory scale with small quantity of chemicals and fresh water. From a global scale, chemicals droplets diameters were measured during their rise to the surface and clearly show a decrease for the majority of the tested fluids (n-butanol, ethyl acetate, methyl ter butyl ether and methyl isobutyl ketone). The comparison of measurements with Clift’s correlation for droplet rising velocity shows a good agreement for average data. Assuming the Clift’s model; an estimation of average mass variation with time was calculated for the tested fluids.
- Concerning the SEBC classification strengths and weaknesses: the experimental HNS fates obtained at 20 °C with no winds are in accordance with SEBC categorization. Gaps have been observed between SEBC categorizations and experimental HNS overall fates in the case of deteriorated environmental conditions. Hence, SEBC categorization is a good tool to quickly get the short term fates of HNS in calm environmental conditions but must be used with precaution and nuanced when dealing with specific weather conditions.

References

PAGE INTENTIONALLY LEFT BLANK

References

- Bäumler, K., Wegener, M., Paschedag, A.R. & Bänsch, E. 2011. Drop rise velocities and fluid dynamic behavior in standard test systems for liquid/liquid extraction - experimental and numerical investigations, *Chemical Engineering Science* 66(3): 426-439.
- Bonn Agreement. Hazardous material spills. Counter pollution manual for incidents involving Hazardous and Noxious Substances (HNS). London., 1994.
- IMO. BC Code: International Code for the Construction and Equipment of Ships Carrying Dangerous Chemicals in Bulk. Edition. London, 2007.
- IMO. International Convention for the Prevention of Pollution from Ships, 1973, as Modified by the Protocol of 1978 Relating Thereto (MARPOL)". London, 2006.
- Le Floch, S., Fuhrer, M., Merlin, F., Aprin, L., Slangen, P. 2010. Fate of a Xylene Slick at Sea and Influence of Meteorological Conditions. Proc. of 33rd AMOP Technical Seminar on Environmental Contamination and Response, Halifax 8-10 June 2010, Nova-Scotia, Canada.
- Xie, W.-H., W.-Y. Shiu & D. Mackay. 1997. A review of the effect of salts on the solubility of organic compounds in seawater. *Marine Environmental Research* 44(4): 429-444.
- Grant, R. P. et S. Middleman (1966). Newtonian jet stability. *AIChE Journal* 12,(4) 669-678.
- Horvath, M., L. Steiner et S. Hartland (1978). Prediction of drop diameter, hold-up and backmixing coefficients in liquid-liquid spray columns. *The Canadian Journal of Chemical Engineering* 56,(1) 9-18.
- Clift, R., Grace, J.R. & Weber, M.E. 1978. *Bubbles, Drops, and Particles*. New York, Academic Press
- Lewis, W. K. et W. G. Whitman (1924). Principles of Gas Absorption. *Industrial & Engineering Chemistry* 16,(12) 1215-1220
- Higbie, R. (1935). The rate of absorption of a pure gas into still liquid during short periods of exposure. *Transactions of the American Institute of Chemical Engineers* 31, 365-389.
- Danckwerts, P. V. (1951). Significance of liquid-film coefficients in gas absorption. *Industrial & Engineering Chemistry* 43,(6) 1460-1467.

Toor, H. L. et J. M. Marchello (1958). Film-penetration model for mass and heat transfer. *AIChE Journal* 4,(1) 97-101.

Edgerton, H. E. 1958. Shock Wave Photography of Large Subjects in Daylight. *Review of Scientific Instruments* 29(2): 171-172.

Settles, G. S., Grumstrup, T. P., Miller, J. D., Hargather, M. J., Dodson, L. J. & Gatto, J. A. 2005. Full-scale high-speed "Edgerton" retroreflective shadowgraphy of explosions and gunshots. *Proc. of 5th Pacific Symp. on Flow Visualisation and Image Processing, Australia*.

Hargather, M. J. (2008). Scaling, characterization, and application of gram-range explosive charges to blast testing of materials PhD thesis in Mechanical Engineering, The Pennsylvania State University.

Le Floch, S., Benbouzid, H. & Olier, R. 2009. Operational device and procedure to test the initial dissolution rate of chemicals after ship accidents: the Cedre Experimental Column. *The Open Environmental Pollution & Toxicology Journal* 1: 1-10.

Fuhrer, M., Slangen, P., Aprin, L., Dusserre, G. & Le Floch, S. 2011. A New Approach to Analyze Chemical Releases Behavior in Water Column: High Speed Imaging, *Proc. Intern. Oil Spill Conf., Portland 23-26 May 2011, Oregon, United States*.

Fuhrer, M., Aprin, L., Le Floch, S., Slangen, P. & Dusserre, G. 2012. Behavior of chemicals in seawater column by shadowscopy. *Proc. SPIE 8413, Speckle 2012: V International Conference on Speckle Metrology*, doi:10.1117/12.981670. Vigo 10-12 September 2012. Spain.

Ehara, N., Kojima K., Mori Y.H. 1993. Visualization study of evaporation of single n-pentane drops in water. *Experiments in Fluids* 14: 97-103.

Nosoko, T., Endo S. & Mori Y.H. 1987. Laser shadowgraphy and holographic interferometry for visualizing thermal convection induced by direct-contact evaporation of liquid lenses. *Flow Visualization IV* (ed. Véret, C.) Washington, D.C.: Hemisphere, 67-72.

Grace, J. R., T. Wairegi et T. H. Nguyen (1976). Shapes and velocities of single drops and bubbles moving freely through immiscible liquids. *Transactions of the Institution of Chemical Engineers* 54,(3) 167-173.

Annexes

PAGE INTENTIONALLY LEFT BLANK

Annex 1: Experimental data for 2-ethylhexanoic acid

The concentrations in 2-ethylhexanoic acid in the water are given in the two following tables regrouping the 6 environmental conditions tested.

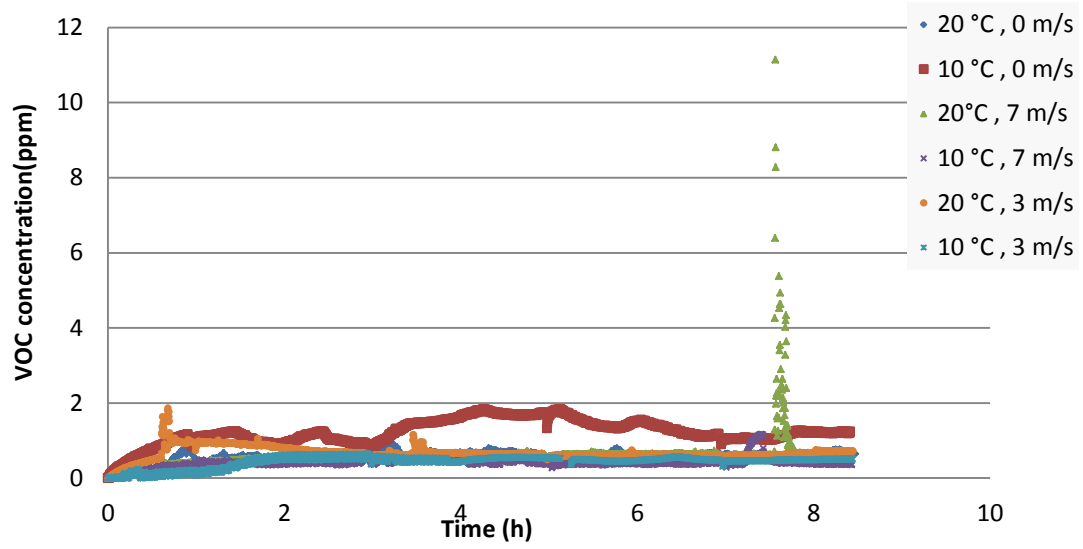
Temperature	20 °C					
Wind velocity	0 m.s ⁻¹		3 m.s ⁻¹		7 m.s ⁻¹	
Time (h)	Concentration (g.L ⁻¹)	Deviation (g.L ⁻¹)	Concentration (g.L ⁻¹)	Deviation (g.L ⁻¹)	Concentration (g.L ⁻¹)	Deviation (g.L ⁻¹)
1	0.0580	0.002	0.074	0.001	1.079	-
3	0.167	0.009	0.167	0.006	1.354	0.014
5	0.261	0.011	0.256	0.0004	1.339	0.002
7	0.352	0.009	0.346	0.021	1.332	0.057
8,5	0.394	0.018	0.393	0.039	1.327	0.026

Temperature	10 °C					
Wind velocity	0 m.s ⁻¹		3 m.s ⁻¹		7 m.s ⁻¹	
Time (h)	Concentration (g.L ⁻¹)	Deviation (g.L ⁻¹)	Concentration (g.L ⁻¹)	Deviation (g.L ⁻¹)	Concentration (g.L ⁻¹)	Deviation (g.L ⁻¹)
1	0.0612	0.002	0.106	0.001	0.912	0.0005
3	0.150	0.006	0.215	0.024	1.400	0.005
5	0.223	0.009	0.316	0.009	1.426	0.020
7	0.295	0.004	0.375	0.005	1.412	0.033
8,5	0.354	0.0004	0.477	0.007	1.441	0.020

A slick was still visible at the end of the test allowing the evaluation of the persistence of the HNS.

Temperature	20°C		10°C	
Wind velocity	0 m.s ⁻¹	3 m.s ⁻¹	0 m.s ⁻¹	3 m.s ⁻¹
Slick persistence at 8.5 h (%)	71.1	76.9	81.6	80.6

The atmospheric concentrations of 2-ethylhexanoic acid registered during the test are presented in the next graph. The evaporation can be considered as negligible (concentrations below 2 ppm most of the time).



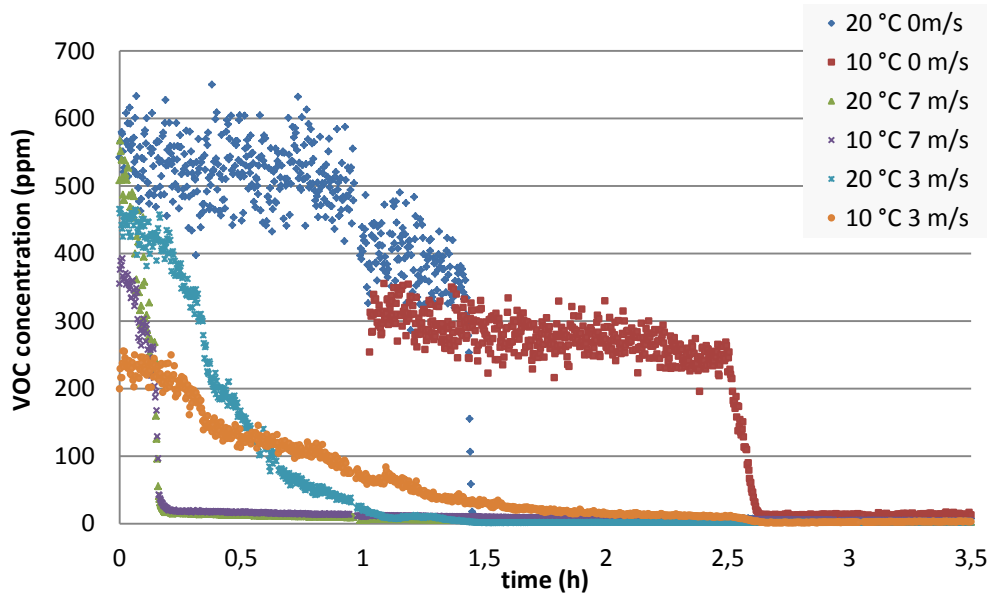
Annex 2: Experimental data for n-butyl acetate

The concentrations in butyl acetate in the water are given in the two following tables regrouping the 6 environmental conditions tested.

Temperature	20 °C					
Wind velocity	0 m.s ⁻¹		3 m.s ⁻¹		7 m.s ⁻¹	
Time (h)	Concentration (g.L ⁻¹)	Deviation (g.L ⁻¹)	Concentration (g.L ⁻¹)	Deviation (g.L ⁻¹)	Concentration (g.L ⁻¹)	Deviation (g.L ⁻¹)
1	0.294	0.001	0.198	0.005	0.309	0.021
3	0.308	0.0003	0.174	0.004	0.099	0.003
5	0.274	0.009	0.0159	0.001	0.047	0.002
7	0.245	0.008	0.134	0.013	0.033	0.001
8,5	0.227	0.013	0.108	0.002	0.029	0.00003

Temperature	10 °C					
Wind velocity	0 m.s ⁻¹		3 m.s ⁻¹		7 m.s ⁻¹	
Time (h)	Concentration (g.L ⁻¹)	Deviation (g.L ⁻¹)	Concentration (g.L ⁻¹)	Deviation (g.L ⁻¹)	Concentration (g.L ⁻¹)	Deviation (g.L ⁻¹)
1	0.260	0.017	0.297	0.012	0.518	0.002
3	0.474	0.017	0.352	0.011	0.220	0.019
5	0.429	0.013	0.303	0.016	0.105	0.004
7	0.380	0.005	0.279	0.011	0.066	0.001
8,5	0.357	0.012	0.253	0.006	0.049	0.001

There was no slick left after 8.5 h. The atmospheric concentrations of butyl acetate registered during the test are presented in the next graph. The PID did not record the first hour for the conditions 10°C and no wind.



Annex 3: Experimental data for Butyl acrylate

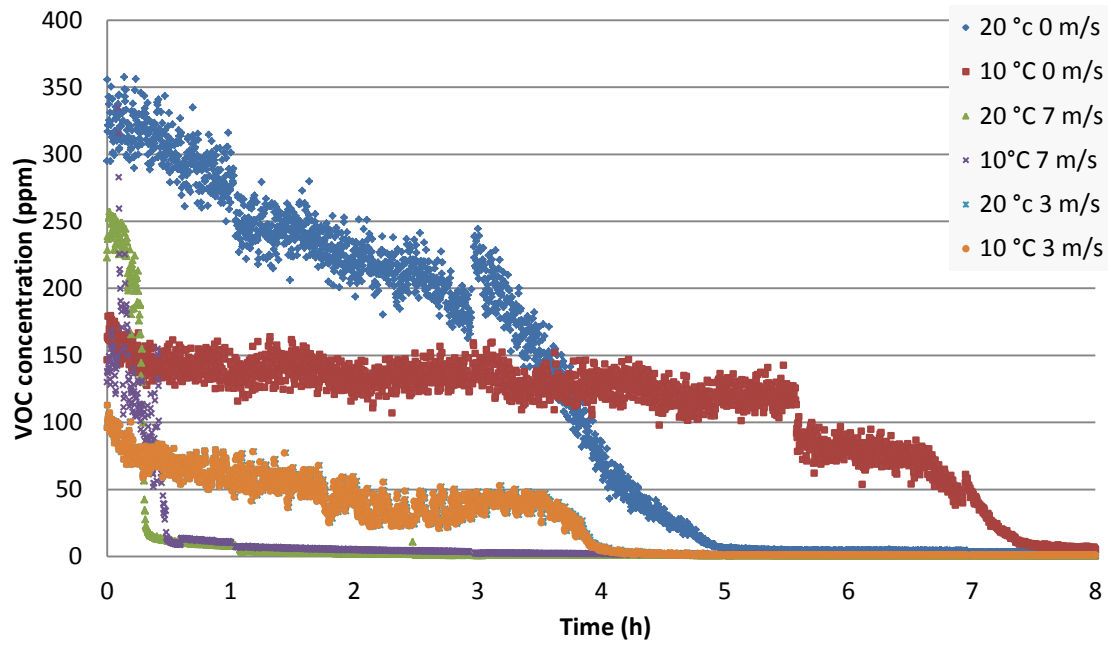
The concentrations in butyl acrylate in the water are given in the two following tables

Temperature	20 °C					
Wind velocity	0 m.s ⁻¹		3 m.s ⁻¹		7 m.s ⁻¹	
Time (h)	Concentration (g.L ⁻¹)	Deviation (g.L ⁻¹)	Concentration (g.L ⁻¹)	Deviation (g.L ⁻¹)	Concentration (g.L ⁻¹)	Deviation (g.L ⁻¹)
1	0.080	0.024	0.047	0.001	0.237	
3	0.188	0.012	0.096	0.004	0.072	
5	0.232	0.003	0.092	0.001	0.012	
7	0.182	0.012	0.084	0.004	0.006	
8,5	0.150	0.011	0.076	0.0003	0	-

Temperature	10 °C					
Wind velocity	0 m.s ⁻¹		3 m.s ⁻¹		7 m.s ⁻¹	
Time (h)	Concentration (g.L ⁻¹)	Deviation (g.L ⁻¹)	Concentration (g.L ⁻¹)	Deviation (g.L ⁻¹)	Concentration (g.L ⁻¹)	Deviation (g.L ⁻¹)
1	0.067	0.001	0.061	0.007	0.440	0.042
3	0.166	0.002	0.152	0.008	0.208	0.027
5	0.229	0.005	0.137	0.00008	0.093	0.004
7	0.261	0.022	0.152	0.004	0.048	0.001
8,5	0.257	0.030	0.125	0.012	0.026	0.002

regrouping the 6 environmental conditions tested.

There was no slick left after 8.5 h. The atmospheric concentrations of butyl acrylate registered during the test are presented in the next graph.



Annex 4: Experimental data for 2-ethylhexyl acrylate

The concentrations in 2-ethylhexyl acrylate in the water are given in the two following tables regrouping the 6 environmental conditions tested.

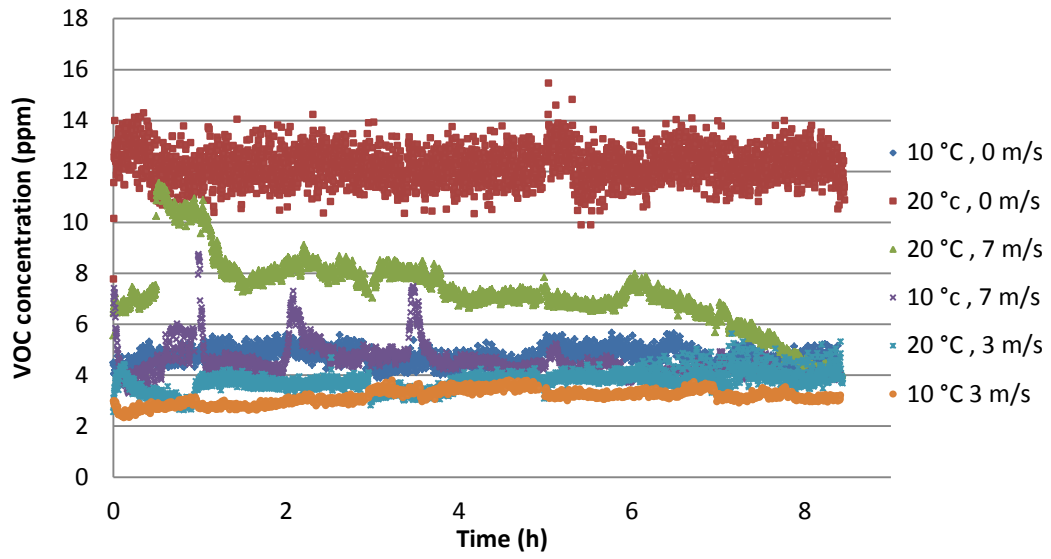
Temperature	20 °C					
Wind velocity	0 m.s ⁻¹		3 m.s ⁻¹		7 m.s ⁻¹	
Time (h)	Concentration (g.L ⁻¹)	Deviation (g.L ⁻¹)	Concentration (g.L ⁻¹)	Deviation (g.L ⁻¹)	Concentration (g.L ⁻¹)	Deviation (g.L ⁻¹)
1	0	-	0.0015	0.00002	0.102	0.035
3	0	-	0.0017	0.00005	0.231	0.058
5	0	-	0.0019	0.00001	0.328	0.028
7	0	-	0.0020	0.00004	0.339	0.078
8,5	0.027	0.002	0.0021	0.00007	0.215	0.027

Temperature	10 °C					
Wind velocity	0 m.s ⁻¹		3 m.s ⁻¹		7 m.s ⁻¹	
Time (h)	Concentration (g.L ⁻¹)	Deviation (g.L ⁻¹)	Concentration (g.L ⁻¹)	Deviation (g.L ⁻¹)	Concentration (g.L ⁻¹)	Deviation (g.L ⁻¹)
1	0	-	0.0018	0.0002	0.063	0.076
3	0	-	0.0019	0.00007	0.012	0.012
5	0	-	0.0021	0.00004	0.091	0.092
7	0.0008	0.00001	0.0022	0.00006	0.047	0.047
8,5	0.001	0.0002	0.0025	0.0001	0.043	0.043

It was possible to sample the slick when the wind velocity was 0 and 3 m.s⁻¹.

Temperature	20°C		10°C	
Wind velocity	0 m.s ⁻¹	3 m.s ⁻¹	0 m.s ⁻¹	3 m.s ⁻¹
Slick persistence at 8.5 h (%)	94.1	80.8	77.4	87.4

The atmospheric concentrations of 2-ethylhexyl acrylate registered during the test are presented in the next graph.

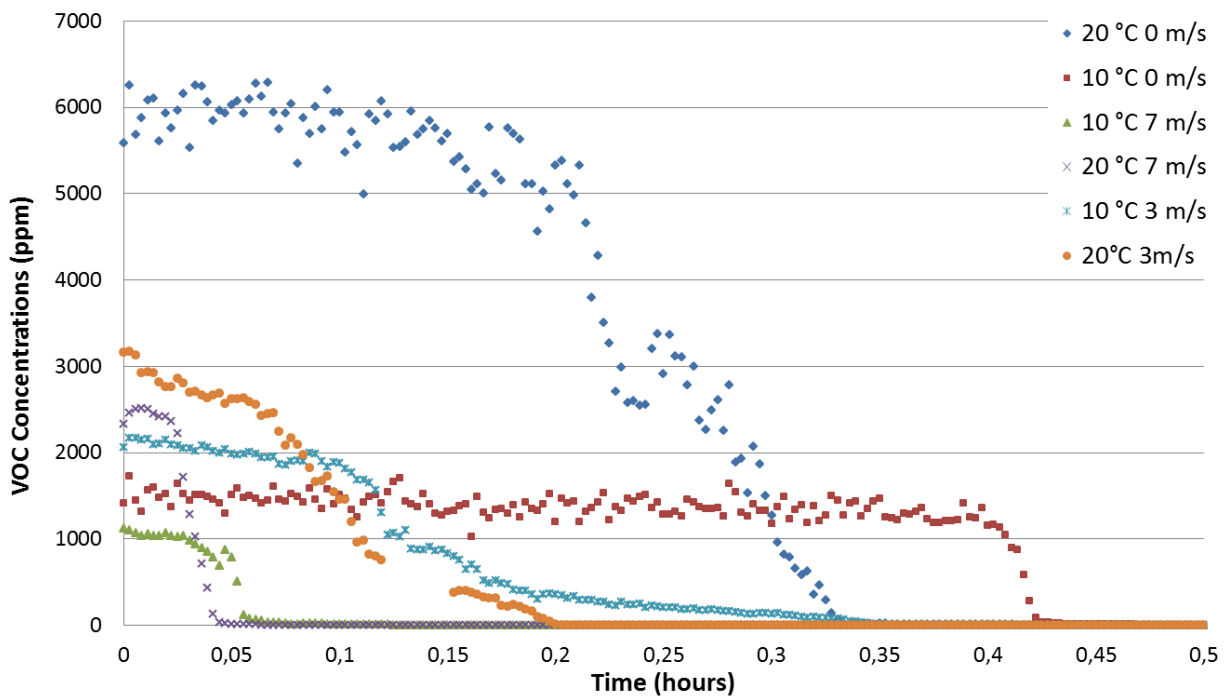


Annex 5: Experimental data for Heptane

The concentrations in heptane in the water are below the analytical limits of detection for the 6 environmental conditions tested.

No slick was remaining at the end on the test.

The atmospheric concentrations of heptane registered during the test are presented in the next graph.



The overall fate of heptane is represented through the normalized material balance given underneath. The percentages of HNS dissolved in seawater, remaining at the surface as a slick or evaporated are detailed for each tested environmental conditions: wind velocities of 0; 3 and 7 m.s-1 and 10°C (a, b, c) and 20°C (d, e, f).

Annex 6: Experimental data for n-nonanol

The concentrations in n-nonanol in the water are given in the two following tables regrouping the 6 environmental conditions tested.

Temperature	20 °C					
Wind velocity	0 m.s ⁻¹		3 m.s ⁻¹		7 m.s ⁻¹	
Time (h)	Concentration (g.L ⁻¹)	Deviation (g.L ⁻¹)	Concentration (g.L ⁻¹)	Deviation (g.L ⁻¹)	Concentration (g.L ⁻¹)	Deviation (g.L ⁻¹)
1	0.0070	0	0.0406	0.0035	0.1613	0.0041
3	0.0137	0.0001	0.0457	0.0008	0.3264	0.0002
5	0.0185	0.0006	0.0495	0.0002	0.2312	0.0021
7	0.0231	0.0017	0.0512	0.0001	0.1882	0.0096
8,5	0.0256	0.0006	0.0531	0	0.3410	0.0050

Temperature	10 °C					
Wind velocity	0 m.s ⁻¹		3 m.s ⁻¹		7 m.s ⁻¹	
Time (h)	Concentration (g.L ⁻¹)	Deviation (g.L ⁻¹)	Concentration (g.L ⁻¹)	Deviation (g.L ⁻¹)	Concentration (g.L ⁻¹)	Deviation (g.L ⁻¹)
1	0.0067	0.00003	0.0173	0.0002	0.0982	0.0023
3	0.0119	0.00007	0.0263	0.0004	0.1671	0.0155
5	0.0167	0.00016	0.0305	0.0008	0.1853	0.0137
7	0.0207	0.00010	0.0426	0.0002	0.1979	0.0186
8,5	0.01234	0.00012	-	-	0.1570	0

It was possible to sample the slick for all wind velocities.

Temperature	20°C			10°C		
Wind velocity	0 m.s ⁻¹	3 m.s ⁻¹	7 m.s ⁻¹	0 m.s ⁻¹	3 m.s ⁻¹	7 m.s ⁻¹
Slick persistence at 8.5 h (%)	98.5	83.1	78	98.5	89.9	97.3

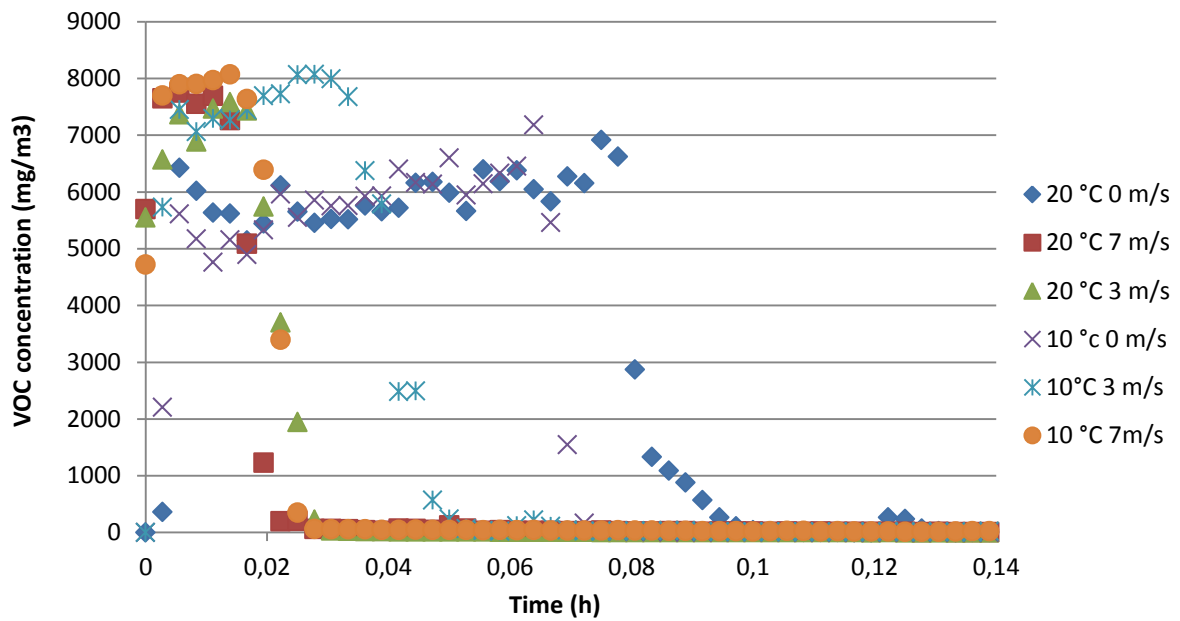
The atmospheric concentrations of n-nonanol registered during the test are always below 2 ppm.

Annex 7: Experimental data for Pentane

The concentrations in pentane in the water are below the analytical limits of detection for the 6 environmental conditions tested.

No slick was remaining at the end on the test.

The atmospheric concentrations of pentane registered during the test are presented in the next graph.



Annex 8: Experimental data for Texanol®

The concentrations in Texanol® (2,2,4-Trimethyl-1,3-Pentanediol-1-Isobutyrate) in the water are given in the two following tables regrouping the 6 environmental conditions tested.

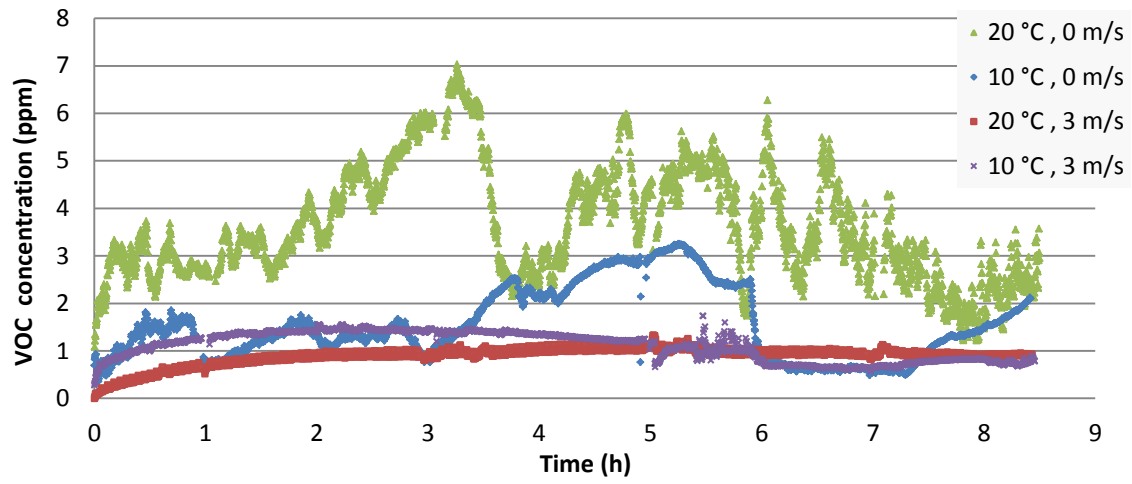
Temperature	20 °C					
Wind velocity	0 m.s ⁻¹		3 m.s ⁻¹		7 m.s ⁻¹	
Time (h)	Concentration (g.L ⁻¹)	Deviation (g.L ⁻¹)	Concentration (g.L ⁻¹)	Deviation (g.L ⁻¹)	Concentration (g.L ⁻¹)	Deviation (g.L ⁻¹)
1	0.038	0.001	0.181	0.006	0.761	0.003
3	0.094	0.001	0.229	0.001	0.908	0.012
5	0.141	0.002	0.273	0.011	0.955	0.039
7	0.184	0.006	0.299	0.005	0.926	0.003
8,5	0.225	0.009	0.327	0.007	0.835	0.029

Temperature	10 °C					
Wind velocity	0 m.s ⁻¹		3 m.s ⁻¹		7 m.s ⁻¹	
Time (h)	Concentration (g.L ⁻¹)	Deviation (g.L ⁻¹)	Concentration (g.L ⁻¹)	Deviation (g.L ⁻¹)	Concentration (g.L ⁻¹)	Deviation (g.L ⁻¹)
1	0.056	0.00002	0.088	0.0003	0.785	0.015
3	0.119	0.002	0.175	0.0002	1.127	0.053
5	0.171	0.003	0.243	0.001	1.102	0.049
7	0.223	0.001	0.301	0.0003	1.006	0.001
8,5	0.248	0.001	0.367	0.002	0.976	0.071

The slick has not been sampled for the conditions 10°C and 0 m.s⁻¹ and 10°C and 7 m.s⁻¹.

Temperature	20°C			10°C
Wind velocity	0 m.s ⁻¹	3 m.s ⁻¹	7 m.s ⁻¹	3 m.s ⁻¹
Slick persistence at 8.5 h (%)	98.4	90.2	50.4	76.2

The atmospheric concentrations of Texanol® registered during the test are presented in the next graph.



Annex 9: Experimental data for Toluene

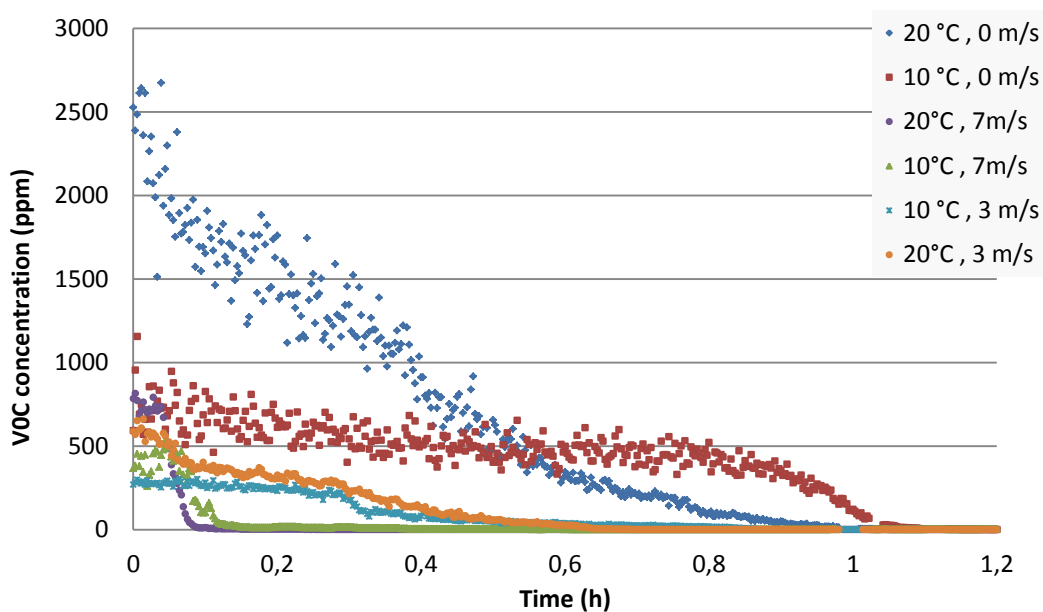
The concentrations in toluene in the water are given in the two following tables regrouping the 6 environmental conditions tested.

Temperature	20 °C					
Wind velocity	0 m.s ⁻¹		3 m.s ⁻¹		7 m.s ⁻¹	
Time (h)	Concentration (g.L ⁻¹)	Deviation (g.L ⁻¹)	Concentration (g.L ⁻¹)	Deviation (g.L ⁻¹)	Concentration (g.L ⁻¹)	Deviation (g.L ⁻¹)
1	0.0032	0.0002	0.0018	0.00005	0.0025	0.00012
3	0.0027	-	0.0015	0.00005	0.00096	0.00002
5	0.0023	0.0006	-	-	0.00035	0.00001
7	0.0014	0.0001	0.00088	0.0009	0	-
8,5	0	-	0.00081	0.0008	0	-

Temperature	10 °C					
Wind velocity	0 m.s ⁻¹		3 m.s ⁻¹		7 m.s ⁻¹	
Time (h)	Concentration (g.L ⁻¹)	Deviation (g.L ⁻¹)	Concentration (g.L ⁻¹)	Deviation (g.L ⁻¹)	Concentration (g.L ⁻¹)	Deviation (g.L ⁻¹)
1	0.0062	0.0001	0.0034	0.0001	0.0035	0.00009
3	0.0042	0.0002	0.0022	0.00006	0.0015	0.00005
5	0.0036	0.0001	0.0018	0.0001	0.00066	0.00002
7	0.0028	0.000004	0.0015	0.000009	0.00033	0.00004
8,5	0.0026	0.0001	0.0012	0.000008	0	-

No slick was remaining at the end of the test.

The atmospheric concentrations of toluene registered during the test are presented in the next graph.



Annex 10: Experimental data for Xylenes

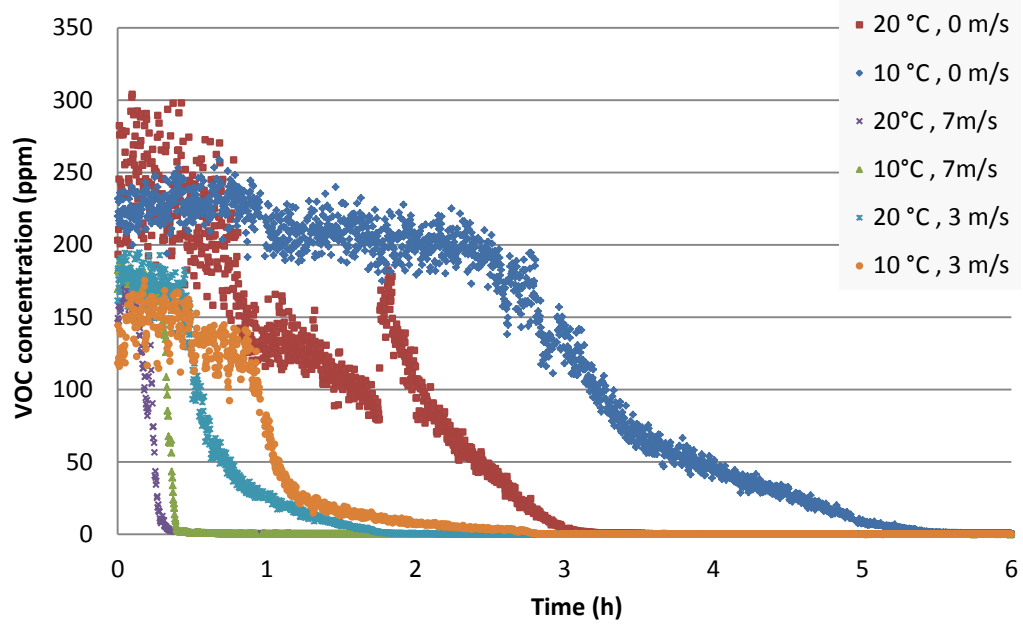
The concentrations in xylenes in the water are given in the two following tables regrouping the 6 environmental conditions tested.

Temperature	20 °C					
Wind velocity	0 m.s ⁻¹		3 m.s ⁻¹		7 m.s ⁻¹	
Time (h)	Concentration (g.L ⁻¹)	Deviation (g.L ⁻¹)	Concentration (g.L ⁻¹)	Deviation (g.L ⁻¹)	Concentration (g.L ⁻¹)	Deviation (g.L ⁻¹)
1	0.0086	-	0.0085	-	0.026	0.002
3	0.010	-	0.0037	-	0.010	0.0004
5	0.0093	-	0.0040	-	0.0034	0.0002
7	0.0070	-	0.0025	-	0.0015	0.0000003
8,5	0.0068	-	0.0018	-	0.0010	0.00004

Temperature	10 °C					
Wind velocity	0 m.s ⁻¹		3 m.s ⁻¹		7 m.s ⁻¹	
Time (h)	Concentration (g.L ⁻¹)	Deviation (g.L ⁻¹)	Concentration (g.L ⁻¹)	Deviation (g.L ⁻¹)	Concentration (g.L ⁻¹)	Deviation (g.L ⁻¹)
1	0.0020	0.00006	0.0025	0.00001	0.030	0.002
3	0.0043	0.0001	0.0026	0.00003	0.014	0.001
5	0.0045	0.00004	0.0020	0.00006	0.0060	0.0007
7	0.0043	0.0004	0.0012	0.00004	0.0030	0.00005
8,5	0.0045	0.0002	0.00080	0.00003	0.0017	0.00011

No slick was remaining at the end of the test.

The atmospheric concentrations of xylenes registered during the test are presented in the next graph.



PAGE INTENTIONALLY LEFT BLANK



Improving Member States preparedness
to face an HNS pollution of the Marine System